

ISTANBUL TECHNICAL UNIVERSITY ★ GRADUATE SCHOOL OF SCIENCE
ENGINEERING AND TECHNOLOGY

**EVALUATION OF CATIONIC POLYMER VECTORS FOR NON-VIRAL
GENE DELIVERY**

M.Sc. THESIS

Hatice İmran GÜNGÖRDÜ

Department of Chemistry

Chemistry Programme

JUNE 2012

ISTANBUL TECHNICAL UNIVERSITY ★ GRADUATE SCHOOL OF SCIENCE
ENGINEERING AND TECHNOLOGY

**EVALUATION OF CATIONIC POLYMER VECTORS FOR NON-VIRAL
GENE DELIVERY**

M.Sc. THESIS

Hatice İmran GÜNGÖRDÜ
(509101061)

Department of Chemistry

Chemistry Programme

Thesis Advisor: Prof. Dr. Gülaçtı TOPÇU

JUNE 2012

İSTANBUL TEKNİK ÜNİVERSİTESİ ★ FEN BİLİMLERİ ENSTİTÜSÜ

**KATYONİK POLİMERLERİN GEN TAŞIYICI SİSTEMLERİ OLARAK
DEĞERLENDİRİLMESİ**

YÜKSEK LİSANS TEZİ

**Hatice İmran GÜNGÖRDÜ
(509101061)**

Kimya Anabilim Dalı

Kimya Programı

Tez Danışmanı: Prof. Dr. Gülaçtı TOPÇU

HAZİRAN 2012

Hatice İmran GÜNGÖRDÜ, a **M.Sc.** student of **ITU Graduate School of Science Engineering and Technology** student ID **509101061**, successfully defended the thesis entitled **“EVALUATION OF CATIONIC POLYMER VECTORS FOR NON-VIRAL GENE DELIVERY”**, which she prepared after fulfilling the requirements specified in the associated legislations, before the jury whose signatures are below.

Thesis Advisor : **Prof. Dr. Gülaçtı TOPÇU**
İstanbul Technical University



Jury Members : **Prof. Dr. Bahire Filiz ŞENKAL**
İstanbul Technical University



Prof. Dr. Jülide AKBUGA
Marmara University



Date of Submission : 04 May 2012
Date of Defense : 08 June 2012

*Dedicated to my beloved family and
everyone in pursuit of his curiosity,*

FOREWORD

First of all, I am greatly indebted to my thesis advisor in Istanbul Technical University, Prof. Dr. Gülaçtı Topçu who has inspired me with her hard-working and enthusiastic personality as a scientist. She has always supported me about my area of interest and rendered the possibility for an international research experience for me.

I feel honored to express my gratitude to my thesis advisor in Ghent University, Prof. Dr. Kevin Braeckmans as well as his colleagues Prof. Dr. Stefaan De Smedt and Prof. Dr. Jo Demeester for giving me the opportunity to pursue my thesis study as a member of their interdisciplinary and extraordinary group.

My very sincere thanks to my supervisor Thomas Martens for his guidance, encouragements and teaching me all the skills that I needed to work on this project independently. As a chemist, gene therapy was a brand new research area for me. During my thesis studies, he has shared all his knowledge and experience with me and expedited my adaptation to this research.

Despite my short stay in Ghent, I had the chance to collaborate with two different groups. I would like to mention my thanks to Prof. Dr. Johan Engbersen and Dr. Marc Ankone from University of Twente and Prof. Dr. Peter Dubruel and Dr. Kehinde Adesanya from Ghent University for their kind collaborations and helps for polymer synthesis.

I am also thankful to everyone in “Laboratory of Biochemistry and Physical Pharmacy”, especially Dr. Joanna Rejman, Dr. Katrien Remaut and Dr. Bart Lucas, for their warmest welcome and sharing their experience whenever I needed.

I cannot forget to thank the dear people, both my lab-mates and home-mates, that beautiful city of Ghent brought to me during those unforgettable days of my Erasmus experience. I would also like to say my warmest thanks to my lab-mates and colleagues in İTÜ, Dr. Fatemeh Bahadori, Demet, Burcu, Tuba, Seda, Anıl, Tayyibe, and Mervenur for their moral support during my studies.

Finally, I owe the greatest gratitude to my beloved family who stands by me unconditionally with full support and advice all the time.

June 2012

Hatice İmran GÜNGÖRDÜ
(Chemist)

TABLE OF CONTENTS

	<u>Page</u>
FOREWORD	ix
TABLE OF CONTENTS	xi
ABBREVIATIONS	xv
LIST OF TABLES	xvii
LIST OF FIGURES	xix
SUMMARY	xxiii
ÖZET	xxv
1. INTRODUCTION	1
1.1 Purpose of The Thesis	1
1.2 Outline of The Thesis	2
2. BASICS OF CELL BIOLOGY	3
2.1 The Cell	3
2.2 Cell (Plasma) Membrane	3
2.3 Cellular Entry of Extracellular Material	5
2.3.1 Endocytosis and endosomes	5
2.3.2 Lysosome	7
2.4 Intracellular Environment	8
2.4.1 Cytoplasm and cytosol	8
2.4.2 Cytoskeleton	8
2.5 Cell Nucleus	9
2.5.1 Function	9
2.5.2 Nuclear envelope and pores	9
2.6 Gene Expression	10
2.6.1 Transcription	10
2.6.2 Translation	11
3. GENE THERAPY	13
3.1 A Brief History of Gene Therapy	13
3.2 Barriers for Gene Delivery	15
3.2.1 Stability in the extracellular environment	15
3.2.2 Cellular attachment and adhesion	16
3.2.3 Cellular uptake	17
3.2.4 Endosomal escape	18
3.2.5 Cellular translocation to the nucleus	19
3.2.6 Nuclear import	20
3.3 Methods for Gene Delivery	21
3.3.1 Physical methods	21
3.3.1.1 Gene gun	21
3.3.1.2 Electroporation	21
3.3.1.3 Gene transfer by ultrasound radiation	22
3.3.2 Viral vectors	23

3.3.2.1 Adeno-associated virus	23
3.3.3 Non-viral vectors.....	23
3.3.3.1 Lipid-based gene delivery systems	24
3.3.3.2 Polymer-based gene delivery systems.....	25
4. MATERIALS AND METHODS.....	29
4.1 Polymer Synthesis	29
4.1.1 Synthesis of pDMAEMA by radicalic polymerization	29
4.1.2 Synthesis of SS-PAA by Michael-type polyaddition	34
4.2 Cell Culture	37
4.2.1 Materials.....	37
4.2.2 Methods used in cell culture.....	37
4.3 Nucleic acids used in this study.....	38
4.3.1 pGL4.13 plasmid.....	38
4.3.2 gWiz™-GFP plasmid.....	39
4.3.3 YOYO®-1 iodide labelled pGL4.13 plasmid	40
4.4 Preparation and Physicochemical Characterization of Polyplexes	40
4.4.1 Dynamic light scattering	40
4.4.1.1 Theory and working principles	40
4.4.1.2 Particle size and surface charge measurements.....	43
4.4.2 Preparation of polyplexes.....	43
4.4.2.1 pDMAEMA polyplexes	44
4.4.2.2 SS-PAA polyplexes.....	46
4.4.3 Agarose gel electrophoresis	47
4.4.3.1 Principles.....	47
4.4.3.2 Experimental part	48
4.5 In vitro Biological Evaluation of Polyplexes	49
4.5.1 Flow cytometry	49
4.5.1.1 Principles.....	49
4.5.2 Uptake and transfection efficiency studies.....	50
4.5.3 Cell viability.....	51
4.5.3.1 MTT assay.....	51
4.5.3.2 Experimental	52
5. RESULTS AND DISCUSSION.....	53
5.1 Polymer Synthesis	53
5.1.1 Characterization of polymers	53
5.1.1.1 pDMAEMA.....	53
5.1.1.2 SS-PAA.....	53
5.2 pDMAEMA polyplexes.....	58
5.2.1 Physicochemical characterization	58
5.2.1.1 Particle size and surface charge measurements.....	58
5.2.1.2 pDNA complexation efficiency	59
5.2.2 In vitro biological evaluation	61
5.2.2.1 Uptake efficiency	61
5.2.2.2 Transfection efficiency.....	62
5.2.2.3 Cell viability.....	62
5.2.3 Discussion	63
5.3 SS-PAA Polyplexes.....	66
5.3.1 p(CBA-ABOL) polyplexes	67
5.3.1.1 Physicochemical characterization	67
5.3.1.2 In vitro biological evaluation	70

5.3.1.3 Discussion	72
5.3.2 p(CBA-ABOL/DMEDA/PEG) polyplexes	74
5.3.2.1 Physicochemical characterization	75
5.3.2.2 In vitro biological evaluation	76
5.3.2.3 Discussion	79
5.3.3 HA-coated p(CBA-ABOL) polyplexes.....	80
5.3.3.1 Physicochemical characterization	80
5.3.3.2 In vitro biological evaluation	83
5.3.3.3 Discussion	86
5.3.4 p(CBA-HIS) polyplexes.....	87
5.3.4.1 Physicochemical characterization	87
5.3.4.2 In vitro biological evaluation	90
5.3.4.3 Discussion	93
6. CONCLUSION.....	95
REFERENCES	97
APPENDICES	109
APPENDIX A.	111
CURRICULUM VITAE.....	113

ABBREVIATIONS

ABOL	: 4-aminobutan-1-ol
AIDS	: Acquired immunodeficiency syndrome
App	: Appendix
APS	: Ammonium persulfate
CBA	: N,N'-cystaminebisacrylamide
CF	: Cystic Fibrosis
DLS	: Dynamic Light Scattering
DMAEMA	: Dimethylaminoethyl methacrylate
DMEDA	: N, N'-dimethyl ethyl-1,2-diamine
DMEM	: Dulbecco's modified Eagle's medium
DNA	: Deoxyribonucleic acid
DTT	: Dithiothreitol
ECM	: Extracellular matrix
FC	: Flow Cytometry
GAG	: Glycosaminoglycan
GFP	: Green Fluorescent Protein
GPC	: Gel Permeation Chromatography
HA	: Hyaluronic acid (Hyaluronan)
HEPES	: 4-(2-hydroxyethyl)-1-piperazineethanesulfonic acid
HIS	: Histamine
HS	: Heparan Sulphate
HSPG	: Heparan sulphate proteoglycan
IF	: Integrated filament
kDa	: Kilodalton
LF	: Lipofectamine™ 2000 Reagent
MF	: Microfilament
mRNA	: Messenger Ribonucleic Acid
MT	: Microtubule
MTT	: 3-(4,5-dimethylthiazol-2-yl)-2,5-diphenyltetrazolium bromide
Mw	: Molecular weight
MWCO	: Molecular weight cut-off
NLS	: Nuclear localization signal
NMR	: Nuclear Magnetic Resonance
NPC	: Nuclear pore complex
OTC	: Ornithine transcarbamylase
P/S	: Penicillin-Streptomycin
PAA	: Poly(amidoamine)
PAMAM	: Poly(amidoamine)
PBS	: Phosphate buffer saline
pDI	: Polydispersity index
pDNA	: Plasmid DNA
PEG	: Poly(ethylene glycol)

PEI	: Poly(ethylene imine)
PG	: Proteoglycan
pHPMA	: Poly(hydroxypropyl methacrylate)
PLL	: Poly(L-lysine)
Pplx	: Polyplex
PS	: Polystyrene
RGD	: Arginine-glycine-aspartate
RNA	: Ribonucleic acid
RPE	: Retinal Pigment Epithelium
RT	: Room Temperature
SCID	: Severe combined immunodeficiency
SS-PAA	: Linear, disulfide-containing poly(amidoamine)
TBE	: Tris-base boric acid EDTA
TMS	: Tetramethylsilane
US	: Ultrasound

LIST OF TABLES

	<u>Page</u>
Table 5.1 : The amounts of pDMAEMA polymer and pDNA which was used to obtained desired polymer/pDNA (w/w) ratios	59
Table 5.2 : Illustration of average size, pDI and charge values for pDMAEMA polyplexes.....	59
Table 5.3 : The amounts of p(CBA-ABOL) polymer and pDNA which was used to obtain desired polymer/pDNA (w/w) ratios. The polyplexes were prepared with increasing amount of polymer while the amount of plasmid was the same for each.....	67
Table 5.4 : Illustration of average size, pDI and charge values for p(CBA-ABOL) pplxes with different polymer/pDNA mass ratios	68
Table 5.5 : Illustration of average size, pDI and charge values for PEGylated p(CBA-ABOL) polyplexes with different polymer/pDNA mass ratios .	75
Table 5.6 : Illustration of the amount of HA and pDNA used to apply the coating in appropriate HA/pDNA molar ratio	81
Table 5.7 : The amounts of p(CBA-HIS) polymer and pDNA which was used to obtain desired polymer/pDNA (w/w) ratios. The polyplexes were prepared with increasing amount of polymer while the amount of plasmid was constant.	88
Table 5.8 : Illustration of average size, pDI and charge values for p(CBA-HIS) polyplexes with different polymer/pDNA mass ratios.....	88

LIST OF FIGURES

	<u>Page</u>
Figure 2.1 : Comparison of sizes of precellular organisms with an average cell in human body.	3
Figure 2.2 : A cross section from cell membrane (Bolsover, 2004)	4
Figure 2.3 : A general molecular formula of HSPGs where $R = SO_3^-$ (Gallagher et al, 1986).....	5
Figure 2.4 : a. Categorisation of different endocytotic pathways, adapted from (Mayor and Pagano, 2007). b. Multiple routes of endocytosis into mamallian cells (Conner and Schmid, 2003).	6
Figure 2.5 : The mechanism of endocytosis.	7
Figure 2.6 : Cytosolic transport and nuclear import of the cargo, adapted from (Wong et al, 2007).....	8
Figure 2.7 : The structure of cell nucleus [Url-1].	9
Figure 2.8 : Illustration of gene expression process [Url-2]	10
Figure 3.1 : a. Number of approved gene therapy clinical trials worldwide 1989-2011, b. Clinical phases of approved gene therapy trials, adapted from [Url-3].....	14
Figure 3.2 : Intracellular barriers for gene delivery, adapted from (De Smedt et al, 2005).....	15
Figure 3.3 : Schematic illustration of proton sponge hypothesis.....	19
Figure 3.4 : Chemical structure of cationic lipid (A) DOTMA, (B) DOTAP and (C) an illustration of liposome, adapted from (Remaut et al, 2007).....	24
Figure 3.5 : Chemical structures of selected polymers , adapted from (Wong et al, 2007).....	26
Figure 4.1 : Chemical structures of a. DMAEMA monomer, b. pDMAEMA polymer.....	30
Figure 4.2 : Illustration of radicalic polymerization reaction mechanism	31
Figure 4.3 : Illustration of Michael type polyaddition of a primary amine to bisacryl amide monomer, adapted from (Lin et al, 2007a).....	35
Figure 4.4 : Illustration of Michael type addition polymerization of a. p(CBA-ABOL), b. p(CBA-HIS), adapted from(Coue and Engbersen, 2011)	35
Figure 4.5 : Illustration of Michael type addition polymerization of a p(CBA-ABOL/DMEDA/PEG) copolymer, adapted from (Vader et al, 2012)....	36
Figure 4.6 : Schematic representation of pGL4.13 plasmid. The plasmid encodes for luc2 gene under the control of SV40 promoter. Amp ^r : ampicilline resistance marker [Url-4]	39
Figure 4.7 : Schematic representation of gWiz TM -GFP plasmid. kan ^r : kanamycin resistance [Url-5].....	40
Figure 4.8 : Schematic illustration of zeta potential [Url-6]	42
Figure 4.9 : Main components and optical configurations of a Nano Zeta-sizer instrument for DLS measurements [Url-7]	44

Figure 4.10 : Formation of polymer/DNA nanocomplex (polyplex) by self-assembly, adapted from (Coue and Engbersen, 2011)	45
Figure 4.11 : The scattering of laser in flow cytometer [Url-8]	50
Figure 4.12 : Reduction of MTT reagent to formazan	52
Figure 5.1 : Illustration of ¹ H-NMR spectrum of DMAEMA monomer	54
Figure 5.2 : The ¹ H-NMR spectrum relative to TMS (CDCl ₃ , 300 MHz and expressed in ppm) of pDMAEMA	55
Figure 5.3 : ¹ H-NMR spectrum relative to D ₂ O (D ₂ O, 300 MHz and expressed in ppm) of p(CBA-ABOL)	56
Figure 5.4 : The ¹ H-NMR spectrum relative to D ₂ O (D ₂ O, 300 MHz and expressed in ppm) of p(CBA-HIS)	56
Figure 5.5 : Illustration of the Mw distribution of p(CBA-ABOL) obtained by gel permeation chromatography	57
Figure 5.6 : Illustration of the Mw distribution of p(CBA-HIS) obtained by gel permeation chromatography	57
Figure 5.7 : Illustration of a. particle size and polydispersity, b. Z-potential of polyplexes formed by pDMAEMA with different Mw and mass ratios	60
Figure 5.8 : Agarose gel electrophoresis of pDMAEMA polyplexes Mw 50 kDa and 600 kDa with different mass ratios. The lanes with the polyplexes contain 20 µL of sample (corresponding to 200 ng of pDNA per well). As a negative control, 20 µL of heparin (7 µg/µL) was added to last 4 samples to simulate pDNA displacement.....	61
Figure 5.9 : Comparison of cellular internalization of p(DMAEMA) polyplexes with different Mw and mass ratios.	62
Figure 5.10 : Comparison of transfection efficiency of pDMAEMA polyplexes with different Mw and mass ratios and LF as a positive control.....	63
Figure 5.11 : Cell viability results of pDMAEMA polyplexes with different Mw and polymer ratios.....	64
Figure 5.12 : Illustration of a. particle size and polydispersity, b. ζ-potential of p(CBA-ABOL) polyplexes with different mass ratios.....	68
Figure 5.13 : Agarose gel electrophoresis of p(CBA-ABOL) pplxes with different mass ratios. Each sample was colored with 5 µL loading buffer. The polyplex samples contain 0.2 µg of pDNA. As a negative control, 10 µL of Heparin (7 µg/µL) was added to last sample	69
Figure 5.14 : Comparison of cellular internalization of p(CBA-ABOL) polyplexes with different mass ratios	70
Figure 5.15 : Comparison of transfection efficiencies of p(CBA-ABOL) polyplexes with various mass ratios compared to LF.....	71
Figure 5.16 : Cell viability results of p(CBA-ABOL)/pDNA polyplexes with different mass ratios	72
Figure 5.17 : Illustration of the effect of PEGylation on a. particle size and polydispersity, b. ζ-potential	75
Figure 5.18 : Agarose gel electrophoresis for p(CBA-ABOL/DMEDA/PEG) complexes. The lanes with the polyplexes contain 20 µL of sample (corresponding to 200 ng of pDNA per well). As a negative control, 5 µL of Heparin (7 µg/µL) was added to last 3 samples to simulate pDNA displacement.....	77
Figure 5.19 : The effect of PEGylation on cellular internalization of p(CBA-ABOL) polyplexes with different mass ratios in ARPE-19 cells.	78

Figure 5.20 : Comparison of the effect of PEGylation on transfection efficiency of p(CBA-ABOL) polyplexes with various mass ratios in ARPE-19 cells.	78
Figure 5.21 : Illustration of the effect of HA-coating on a. particle size and polydispersity, b. ζ -potential of p(CBA-ABOL) polyplexes with different HA/pDNA molar ratios	81
Figure 5.22 : Agarose gel electrophoresis of HA-coated p(CBA-ABOL) polyplexes with different HA/pDNA molar ratios. The lanes with the polyplexes contain 20 μ L of sample (corresponding to 200 ng of pDNA per well). As a negative control, 5 μ L of Heparin (7 μ g/ μ L) was added to last 4 samples to simulate pDNA displacement.....	83
Figure 5.23 : The effect of HA-coating on cellular internalization of p(CBA-ABOL) polyplexes with different HA/pDNA molar ratios in ARPE-19 cells.....	84
Figure 5.24 : Comparison of transfection efficiencies of different gene carriers HA-coated p(CBA-ABOL) with different HA/pDNA molar ratios, non-coated p(CBA-ABOL) and LF complexes.....	84
Figure 5.25 : Effect of HA-coating on the viability of ARPE-19 cells.....	85
Figure 5.26 : Illustration of a. particle size and polydispersity, b. ζ -potential of pDMAEMA polyplexes with different Mw and mass ratios	89
Figure 5.27 : Agarose gel electrophoresis of p(CBA-HIS) polyplexes with different mass ratios. The lanes with polyplexes contain 20 μ L of sample (corresponding to 200 ng of pDNA per well). As a negative control, 3 μ L of Heparin (7 μ g/ μ L) was added to last 5 samples to simulate pDNA displacement. 48/1 p(CBA-ABOL) polyplexes were applied as a comparative reference.	90
Figure 5.28 : Comparison of internalization of different gene carriers p(CBA-HIS) with different mass ratios, p(CBA-ABOL) and LF in ARPE-19 cells....	91
Figure 5.29 : Comparison of transfection efficiencies of different gene carriers p(CBA-HIS) with different mass ratios, p(CBA-ABOL) and LF in ARPE-19 cells.....	91
Figure 5.30 : Cell viability results of p(CBA-HIS)/pDNA pplexes with different mass ratios	92
Figure A.1 : Preliminary study for HA-coating	111

EVALUATION OF CATIONIC POLYMER VECTORS FOR NON-VIRAL GENE DELIVERY

SUMMARY

Gene therapy has been a promising way to treat human genetic disorders. The major goal of gene therapy is to repair the genetic cause underlying the disorder by transferring the therapeutic nucleic acid with a safe and efficient carrier. For this purpose, two main classes of vectors are explained: viral and non-viral vectors. Even though, viral vectors are the most efficient carriers known, they have restrictions about their safety and production process. Cationic polymers have been the mostly investigated non-viral vector systems as a safe and easy-to-produce alternative to viral carriers. Moreover, numerous research have been done to increase their transfection efficiency.

In this thesis study, two different types of cationic polymers were synthesized and investigated for their non-viral gene carrier potentials. One of them is a cationic, non-biodegradable poly(2-(dimethylamino)ethyl methacrylate) (pDMAEMA). The second type of carriers is cationic and biodegradable linear, disulfide linkage containing poly(amidoamine)s (SS-PAA) that include four different polymers with different side groups and coating strategies. The SS-PAA family consists of p(CBA-ABOL), p(CBA-ABOL/DMEDA/PEG) with PEGylation strategy, p(CBA-ABOL) with HA-coating and lastly, p(CBA-HIS).

The main objectives of this study were first of all, physicochemical characterization of the polymer/pDNA complexes with different polymer Mw and polymer/pDNA ratio in terms of size, polydispersity and surface charge which were measured by DLS. Secondly, the pDNA complexation ability of polyplexes was investigated by performing agarose gel electrophoresis. Thirdly, *in vitro* biological evaluation of polymers on ARPE-19 cells were performed. For this purpose, uptake and transfection efficiencies of the polymers and the effect of different polymer Mw's and different polymer/pDNA ratios on uptake and transfection efficiency of polyplexes were evaluated by Flow Cytometry. Finally, the effect of polyplexes on the viability of ARPE-19 cells was analyzed with MTT Assay.

While evaluating the pDMAEMA complexes, they showed the ability to form stable complexes in HEPES buffer and were able to efficiently complex pDNA. Nevertheless, the cationic nanoparticles formed with these polymers only exhibited signs of transfection in concentrations already toxic for the cells. This is why a new family of biodegradable polymers- the disulfide-containing PAAs, were investigated. p(CBA-ABOL) particles were also able to form stable polyplexes with efficiently complexed pDNA and also showed very high transfection efficiency, without significant effect on cell viability. Unfortunately, these nanoparticles were not stable in mimicked physiological conditions, which is why the same polymer was investigated with a PEG-chain as a universal coating strategy. Even though these particles were stable under physiological conditions, their uptake was drastically

hindered. A different coating strategy with hyaluronic acid showed promising preliminary results, but the same results could not be observed with the research grade purity low Mw HA. Subsequently, another member of SS-PAA family with a different side chain and buffering capacity was evaluated. p(CBA-HIS) polymer was able to condense the pDNA in HEPES buffer and transfected the cells with almost no cytotoxic effect. However, the colloidal stability of p(CBA-HIS) polyplexes in physiological conditions should be further increased.

KATYONİK POLİMERLERİN GEN TAŞIYICI SİSTEMLERİ OLARAK DEĞERLENDİRİLMESİ

ÖZET

Gen tedavisi, genetik kaynaklı birçok hastalığa çözüm sunma potansiyeli açısından son yıllarda oldukça rağbet gören bir çalışma alanı olmuştur. Gen tedavisinin ana amacı hastalıkların ortaya çıkardığı semptomları iyileştirmeye çalışmak yerine, hastalığa sebep olan genetik bozuklukları ortadan kaldırmaktır. Bu tedavide, tedavi edici özelliği olan genler, en güvenli ve verimli bir taşıyıcı ile hedef dokuya ya da hücreye transfer edilmektedir. Bu amaçla kullanılan taşıyıcılar viral ve viral olmayan taşıyıcılar olmak üzere ikiye ayrılır. Viral taşıyıcılar, hedefe ulaşma verimliliği açısından bilinen en verimli taşıyıcılar olmakla birlikte güvenilirlik ve üretim aşamaları açısından uygulamaları çok kısıtlıdır. Bu sebeple, güvenli ve üretimi kolay alternatif bir metod olarak katyonik polimerler araştırılmaktadır. Literatürde, katyonik polimerlerin transfeksiyon verimliliklerini artırmak için yapılmış pek çok çalışmaya ulaşılabilir.

Bu tez çalışmasında, gen tedavisi potansiyelleri açısından iki farklı polimer türü sentezlendi ve çeşitli özellikleri bakımından incelendi. Bu polimerlerin ilki, katyonik fakat biyobozunur olmayan poli(2-(dimetilamino)etil metakrilat) (pDMAEMA) polimeridir. İkinci tür taşıyıcı sistem ise katyonik ve biyobozunur disülfür bağı içeren, lineer poli(amidoamin) (SS-PAA) polimer türevleridir. SS-PAA ailesine ait farklı yan grup ve kaplama stratejileri ile sentezlenen 4 farklı polimer bu çalışmada incelendi. Bunlar poli-(*N,N'*-sistamin bisakrilamit-4-amino bütanol) p(CBA-ABOL), PEG'leme stratejisi ile geliştirilen p(CBA-ABOL/DMEDA/PEG), hiyaluronik asit (HA) kaplanmış p(CBA-ABOL) ve son olarak da poli-(*N,N'*-sistamin bisakrilamit-histamin) (p(CBA-HIS))'dir. Bu çalışmanın ilk aşaması olarak farklı molekül ağırlıklı ve farklı polimer oranlarına sahip polimer/pDNA (plazmit DNA) kompleksleri (polipleks) fizikokimyasal özellikleri açısından incelendi.

Bu amaçla boyut, polidispersite ve yüzey yükü ölçümleri DLS cihazı ile yapıldı. İkinci olarak poliplekslerin pDNA'yı kaplayarak kararlı kompleksler oluşturma etkinlikleri agaroz jel elektroforez ile belirlendi. Bu karakterizasyonları takiben, polimer/pDNA komplekslerinin ARPE-19 hücreleri ile *in vitro* biyolojik değerlendirmeleri amaçlandı. Farklı molekül ağırlığına (M_A) ve farklı polimer oranlarına sahip polipleksler hazırlanarak hücrelere transfer edildi ve hücre içine alınma ve genetik materyali hedefe ulaştırma verimlilikleri Hücre Sitometresi (Flow Cytometry) cihazı ile ölçüldü. Son olarak, poliplekslerin hücreler üzerindeki sitotoksik etkisi MTT Testi ile analiz edildi.

pDMAEMA polimeri ile oluşturulan 2 farklı M_A ve farklı polimer oranına sahip poliplekslerin HEPES tamponu ortamında yapılan boyut ve yük tayini sonuçlarına göre bu ortamda pDNA ile kararlı kompleksler yapabildiği görüldü. Yapılan ölçümlerin fizyolojik ortama uygunluğunun denenmesi için aynı seri ölçümler bir de serum içermeyen transfeksiyon ortamı olan OptiMEM ortamında gerçekleştirildi.

OptiMEM ortamında kompleks kararlılığının azaldığı ve agregasyon oluşumu gözlemlendi. Bu ölçümleri takiben pDMAEMA polimerinin pDNA'yı kondanse edebilme özelliğinin analizi için pDMAEMA polipeksleri agaroz jel elektroforeze uygulandı. Her iki M_A ve polimer oranındaki kompleksler pDNA kaplamaya muktedir. Polimer M_A ve oranının polipeks kararlılığına bariz bir etkisinin olmadığı gözlemlendi fakat yüksek polimer oranına sahip kompleksler daha küçük parçacık boyutu gösterdiler. pDMAEMA polipekslerinin *in vitro* biyolojik değerlendirilmesi sonuçlarına göre pDMAEMA/pDNA komplekslerinin hücre içine alınma verimlilikleri oldukça tatmin ediciydi. Fakat hücre içine alınan polipekslerin çekirdeğe ulaşma potansiyelleri oldukça düşük ve ancak hücreler için toksik olan polimer miktarlarında ilgi çekici sonuçlar verdi.

SS-PAA polimerleri içerdikleri tekrarlanan sülfür köprüleri sayesinde biyobozunur polimerler olduklarından gen salımı konusunda iyi bir potansiyele sahiptirler. Bu ailenin ilk üyesi olarak p(CBA-ABOL) polimeri gen taşıyıcısı olarak değerlendirildi. pDMAEMA polipeksleri için yapılan tüm işlemler p(CBA-ABOL)/pDNA kompleksleri için de denendi. Farklı polimer oranlarıyla oluşturulan p(CBA-ABOL) komplekslerinin yüzey yükü ve boyut tayini HEPES ve OptiMEM ortamlarında gerçekleştirildi. HEPES ortamında artan polimer miktarının daha kararlı kompleksler oluşturmaya karşılık, aynı komplekslerde OptiMEM ortamında agregasyon gözlemlendi. Agaroz jel elektroforez sonuçlarına göre yüksek polimer oranları 48/1 ve 96/1 ile oluşturulan kompleksler pDNA'yı kaplama açısından daha elverişli idiler. p(CBA-ABOL) polipekslerinin *in vitro* biyolojik değerlendirilmelerinin sonucunda ise p(CBA-ABOL) polipekslerinin genetik materyalin hücre içine alınması ve ardından çekirdeğe ulaştırılması açısından pDMAEMA komplekslerine göre daha verimli olduğu ayrıca ARPE-19 hücreleri için yalnızca ihmal edilebilir düzeyde bir toksisiteye sebep olduğu görüldü.

p(CBA-ABOL) komplekslerinin fizyolojik ortamdaki agregasyonunu engellemek amacıyla evrensel bir strateji olan PEG'leme stratejisi kullanıldı. PEG'lenen p(CBA-ABOL) polimeri ile oluşturulan kompleksler de daha önceki ölçümlere tabi tutuldu. PEG'leme sonucunda komplekslerin OptiMEM ortamındaki koloidal kararlılığında artış gözlenirken *in vitro* biyolojik değerlendirme açısından PEG'lenen p(CBA-ABOL) polimeri ile yapılan ölçümler istenilen verimi göstermedi. Hücre içine alınma verimliliği açısından PEG'lenmiş komplekslerin yok denecek kadar az bir potansiyellerinin olduğu gözlemlendi. Kompleksler hücre içine alınmadığından sitotoksite analizine gerek duyulmadı.

p(CBA-ABOL) komplekslerinin hücre içine alınma kapasitelerinin artırılması için kompleksler bir hücre zarı proteini olan HA ile elektrostatik olarak farklı HA/pDNA oranlarında kaplanarak önceki polimerler ile aynı şekilde fizikokimyasal ve biyolojik değerlendirmelere tabi tutuldu. Komplekslerin dış kabuğu anyonik HA ile kaplandığından yüzey yükünün pozitiften negatife döndüğü gözlemlendi. Parçacık boyutu ve koloidal stabilite açısından ise kaplanmamış p(CBA-ABOL) komplekslerine göre OptiMEM ortamında daha kararlı kompleksler elde edildi. Biyolojik değerlendirme sonuçlarında, polipekslerin hücre içine alınmada HA kaplama ile elde edilmek istenen artış gözlenmedi.

En son taşıyıcı sistem olarak SS-PAA polimerlerinin bir türevi olan p(CBA-HIS) polimeri ile oluşturulan kompleksler gen taşıma kapasiteleri açısından değerlendirildi.

HIS yan grubu, ABOL yan grubuna göre daha asidik olduğundan komplekslerin hücre içine endozomlar vasıtasıyla alınmasını takiben endozomlardan çıkışı artıracak ve buna bağlı olarak çekirdeğe ulaşan kompleks miktarının artacağı amaçlandı. p(CBA-HIS) kompleksleri koloidal karalılık ve pDNA kondenzasyonu açısından p(CBA-ABOL) kompleksleri ile benzer özellikler gösterdiler. Aynı şekilde *in vitro* ölçümler sonucunda p(CBA-HIS) komplekslerinin hücre içine alınma kapasitelerinin daha yüksek olmasına rağmen genetik materyalin çekirdeğe ulaşma verimliliği açısından amaçlanan artış gözlenmedi.

Sonuç olarak pDMAEMA polimer/pDNA komplekslerinin artan moleköl ağırlıkları ve polimer miktarları hücreler üzerinde toksik etki yaparken, SS-PAA polimerlerinin transfeksiyon açısından iyi bir potansiyellerinin olduğu tespit edildi. Bu gruptan son olarak incelenen p(CBA-HIS) poliplekslerinin HEPES tamponu ortamında pDNA'yı kondanse etmesi ve transfekte ettiği hücreler üzerinde sitotoksik aktivite göstermemesine rağmen agregasyon oluşumu tamamen engellenemedi. Bu nedenle bu poliplekslerin fizyolojik şartlardaki davranışlarının daha ileri araştırmalarla incelenmesi gerekmektedir.

1. INTRODUCTION

Gene therapy has been a promising way to treat human genetic disorders during the last two decades. The major goal of gene therapy is to repair the genetic cause underlying the disorder by transferring therapeutic nucleic acids with a safe and efficient carrier to the target cells. For this purpose, two main classes of vectors are explained: viral and non-viral vectors. Even though viral vectors are the most efficient carriers known, they have restrictions about their safety and production process and they are reported to have immune response after repeated administrations (Thomas et al, 2003). Synthetic non-viral vectors such as cationic polymers have been the mostly investigated gene delivery systems as a safer and easy-to-produce alternative to viral carriers (De Smedt et al, 2000).

The most recently studied examples of cationic polymer vectors include polyethylenimine (PEI), poly(L-lysine) (PLL), poly(amidoamine) (PAA) and poly(2-(dimethylamino)ethyl methacrylate) (pDMAEMA). In this project pDMAEMA, and a new class of PAAs with repetitive disulfide linkages in the polymer backbone (SS-PAAs) were chosen to be synthesized and evaluated as potential gene delivery systems.

pDMAEMA has attracted the attentions by being readily synthesized via radicalic polymerization and having relatively high transfection efficiency (van de Wetering et al, 1997). Moreover, PAAs are widely investigated since they are highly biocompatible and biodegradable (Ferruti et al, 2002). SS-PAAs have been previously described as a new bio-reducible class of PAAs. They can be synthesized by Michael-type addition polymerization of amine compounds to disulfide containing bisacrylamides (Lin et al, 2007a).

1.1 Purpose of The Thesis

The main purpose of the study described in this thesis is first of all, synthesis of cationic polymer vectors for gene delivery applications. Secondly, physicochemical characterization of the polymer/pDNA complexes with different polymer Mw and

polymer/pDNA ratio was done in terms of size, polydispersity and surface charge. Thirdly, the ability of the polymers to condense and retain the plasmid DNA in an electrostatic complex was investigated. Subsequently, *in vitro* biological evaluations of polymers were aimed. For this purpose, the effect of different polymer Mw's and different polymer/pDNA ratios on uptake and transfection efficiencies was evaluated. Finally, the influence of polyplexes on the viability of cells was analyzed.

1.2 Outline of The Thesis

In the first following chapter, in order to give a background about general cell biology, the main components of an eukaryotic cell that are related to the journey of a gene carrier system are briefly explained.

In the “Gene Therapy” chapter, because the understanding of the efficiency of the polymers to transfer the therapeutic genetic material to its target depends on understanding the various gene delivery barriers that a carrier system has to overcome, the major barriers for gene delivery are explained in relation to the biological chapter. Subsequently, the most leading gene delivery methods including physical, viral and synthetic methods to overcome these barriers are introduced according to literature.

The other two chapters describe the materials and methods used in this study and the results obtained, respectively. Finally, the concluding remarks about the results of this project can be found in conclusion.

2. BASICS OF CELL BIOLOGY

2.1 The Cell

The cell is the smallest living unit of an organism. The term “cell” was defined for the first time by Robert Hooke (1635-1702), an English physicist (Mazzarello, 1999). Following the developments and technical improvements in microscopy science in late 18th century, scientists became interested in visualizing the living organisms. Then it was stated by a German physician and physiologist Theodore Schwann (1810-1882) that animal tissues are comprised of cells and each cell has a nucleus (Hajdu, 2002). Three centuries after the first discovery of the cell, today it is estimated that there are ± 10 trillion cells in a human body. Still, not all the cells have the same function in the body and are specialized to carry out different functions, such as epithelium, muscle and neuron cells. In general, cells have a size ranging from 10 μm to 50 μm , yet depending on its function this can vary (See Figure 2.1).

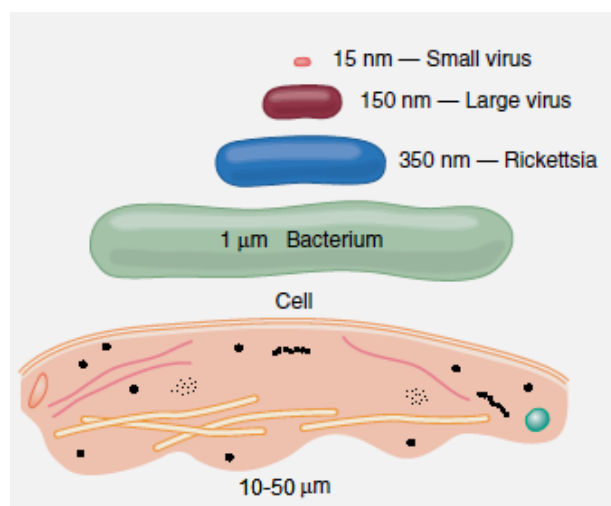


Figure 2.1 : Comparison of sizes of precellular organisms with an average cell in human body.

2.2 Cell (Plasma) Membrane

The cell membrane (or plasma membrane) is the protective boundary of a cell with a thickness of 3 nm (Chen and Moy, 2000). The semi-permeability of the cell membrane regulates what is being taken into cell and what is being given out of the

cell. Besides, this selectively permeable membrane controls the electrical and chemical signals between cells. Lipids form half of the mass of cell membrane, while the other half is made up of proteins, cholesterol and sugars (carbohydrates), (See Figure 2.2).

The lipid bilayer of the membrane is built up through self assembly of phospholipid molecules. These lipids contain a hydrophilic phosphate head, which is soluble in water, and a hydrophobic fatty acid tail, which is soluble in lipid. Because hydrophobic tails are repelled by the water molecules of intracellular and extracellular fluids, they are located in the inner part of the bilayer membrane while the hydrophilic heads are in contact with intracellular and extracellular fluids (Bolsover, 2004).

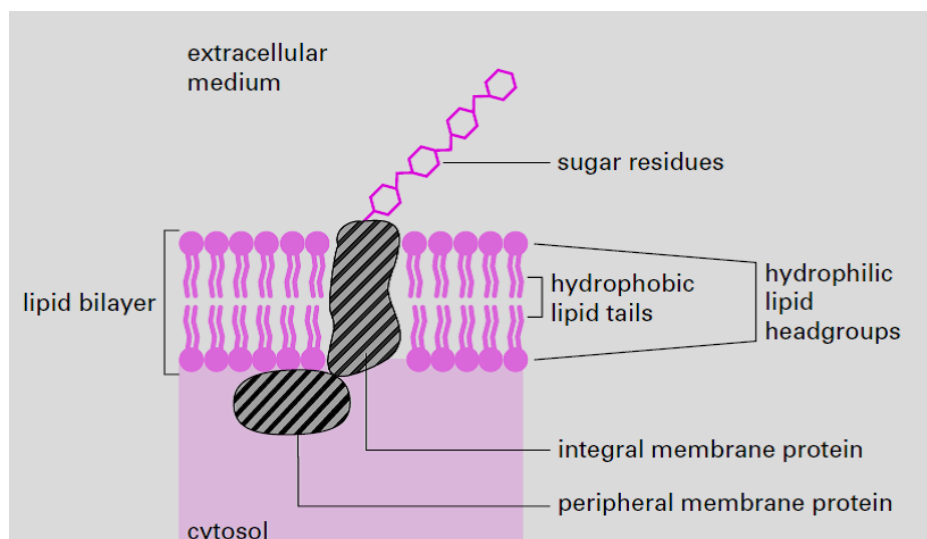


Figure 2.2 : A cross section from cell membrane (Bolsover, 2004).

The proteins in the cell membrane maintain the chemistry of the cell and the transfer of the chemical messages into the cell. The highly hydrophobic environment of the lipid bilayer makes it easier for the fat soluble molecules such as oxygen, carbon dioxide and alcohols to enter the cell. On the other hand, specific proteins form pores on the membrane and this way, also water soluble molecules such as ions, glucose, amino acids and urea can diffuse into the cell (Edidin, 2003), (Poo and Cone, 1974).

There are sugar chains which are called glycosaminoglycans (GAGs) attached via protein moieties to the outer surface of the membrane. These protein-carbohydrate complexes, called proteoglycans (PGs) play a crucial role in determining the charge characteristic of the cell membrane. The most abundant PG on the cell surface is the

polyanionic heparan sulphate proteoglycans (HSPGs), which makes the cell membrane negatively charged (Perrimon and Bernfield, 2000), (See Figure 2.3). Thus, any compound with negative electrical charge will be electrostatically repelled by the cell membrane, whereas positively charged particles will readily adhere to the cell surface.

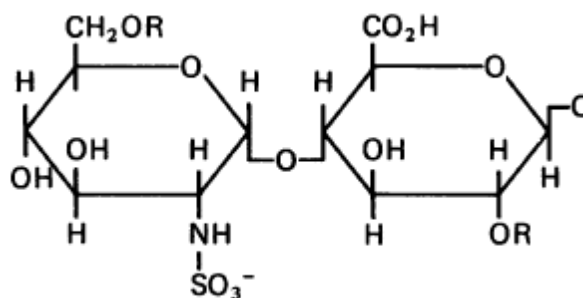


Figure 2.3 : A general molecular formula of HSPGs where $R = \text{SO}_3^-$ (Gallagher et al, 1986).

2.3 Cellular Entry of Extracellular Material

2.3.1 Endocytosis and endosomes

A cell internalizes the nutrients which are necessary to maintain its functions from the extracellular environment. Diffusion and active transport are the most common ways that small substances such as amino acids, sugars and certain ions use to pass through the cell membrane (Conner and Schmid, 2003). Diffusion is the simple and passive movement of a particle (atom, ion or molecule) according to concentration gradient. Particles are transported from a region in which they have higher concentration to a region of lower concentration. Active transport is an energy-demanding process that can occur when a particle needs to be passed against the concentration gradient, i.e., from lower concentration to higher concentration. It is assisted by special protein carriers.

However, very large molecules cannot enter through cell membrane neither via diffusion nor active transport. They use a specialized function of the cell membrane which is called endocytosis to be taken up by the cell. There are several routes described for endocytosis, but the main mechanism remains the same. In general, endocytotic pathways can be divided into two major categories: phagocytosis, which is the uptake of large particles, and pinocytosis, which entails the uptake of fluid and

solutes (See Figure 2.4). Phagocytosis can be seen only in specialized mammalian cells while pinocytosis occurs in all cell types (Conner and Schmid, 2003). Moreover, pinocytosis has 4 subcategories: macropinocytosis (Apodaca, 2001), clathrin-dependent endocytosis, caveolae-mediated endocytosis and clathrin- and caveolae- independent endocytosis (Gong et al, 2008) (Nichols and Lippincott-Schwartz, 2001). These routes differ from each other with regard to the size and formation mechanism of the vesicle and the nature of the cargo that is being taken up (Conner and Schmid, 2003).

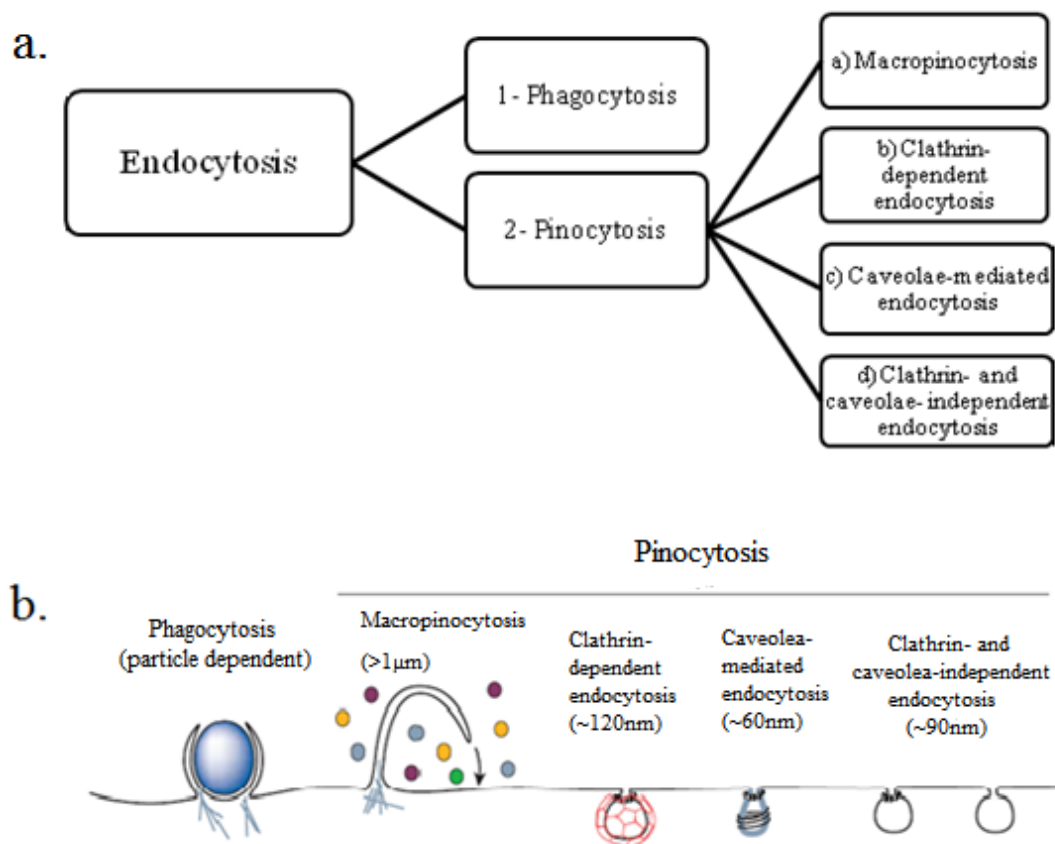


Figure 2.4 : a. Categorization of different endocytotic pathways, adapted from (Mayor and Pagano, 2007). b. Multiple routes of endocytosis into mammalian cells (Conner and Schmid, 2003).

During endocytosis, the plasma membrane invaginates and engulfs some of the extracellular fluid containing the foreign material (cargo). When two portions of the plasma membrane reencounter each other, a part of the membrane pinches off and forms an internal membrane-bounded vesicle named endosome (See Figure 2.5).

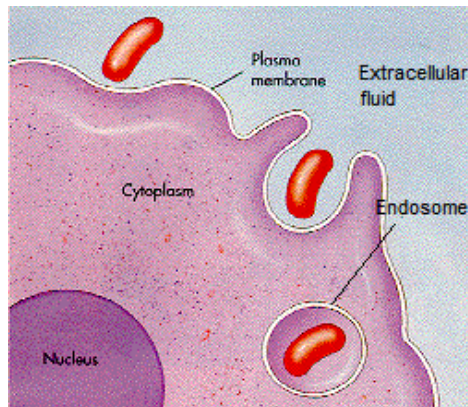


Figure 2.5 : The mechanism of endocytosis.

The pH of the endosomal compartment is around 6 when the vesicle is near the cell membrane. As the endosomal vesicles mature and get closer to a lysosomal state and then to the nucleus it becomes more acidified (pH ~5) by the proton pumps (H^+ -ATPase) of the endosome (Wong et al, 2007), (Luby-Phelps, 2000). The endocytotic transport pathway is followed by lysosomal digestion of the cargo material.

2.3.2 Lysosome

Lysosomes are the organelles containing hydrolytic enzymes which are specialized in the digestion of intra- and extracellular compounds (Ciftci and Levy, 2001). The enzymes are optimally active at pH 5 to digest damaged cellular structures, exogenous materials -the compounds that are not wanted inside the cell- and the food particles that have been taken into the cell (Rybak and Murphy, 1998).

Immediately after the cargo is taken up by endosomes, one or more lysosomes attach to the endosome and the vesicle becomes acidified by proton pumps. The vesicular hydrolytic enzymes of the lysosomes start to digest proteins, carbohydrates and lipids to their building blocks amino acids, glucose and phosphates respectively. These small digestion products can be delivered out of the vesicle to the cytosol. The indigestible substances (residual body) are excreted through the cell membrane by a process called exocytosis –the opposite mechanism of endocytosis.

2.4 Intracellular Environment

2.4.1 Cytoplasm and cytosol

Cytoplasm - the intracellular matrix - contains high volume of water while holding the organelles inside. The watery-liquid part of the cytoplasm without any organelles is defined as cytosol. It is a mixture of substances dissolved in water such as salts, nutrients and some macromolecules. Additionally, cytosol contains nucleolytic enzymes (nucleases), which are ready to degrade nucleic acids, distributed over the cytoskeleton (Lechardeur and Lukacs, 2006) and intracellular reduction agents that can cleave bio-reducible foreign materials (Saito et al, 2003). The pH of intracellular fluid ranges between 6.8 - 7.4 depending on the cell type and biological mechanism and viscosity of the cytosol is nearly the same as pure water (Bright et al, 1987). The major function of the cytosol is to help the transport of the metabolites and compounds, through cytoskeleton, from their place of production to the place that they will be used.

2.4.2 Cytoskeleton

The cytoskeleton is a dynamic structure, maintaining the cell shape, mechanical resistance of the cell and cytoplasmic transport of organelles and large molecules inside the cell (Luby-Phelps, 2000). It has a network of proteins which form the microtubules (MTs), actin filaments (microfilaments) (MFs) and integrated filaments (IFs), (See Figure 2.6).

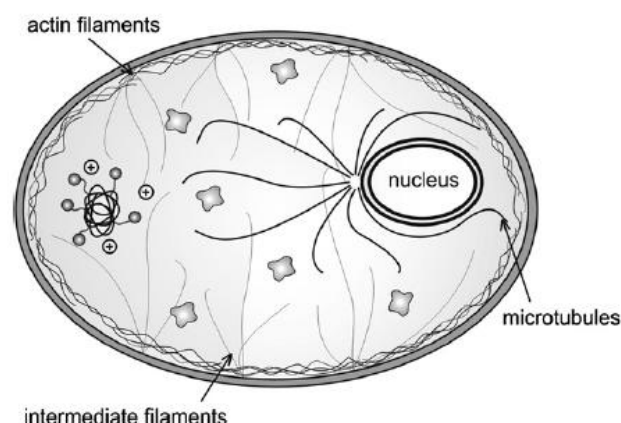


Figure 2.6 : Cytosolic transport and nuclear import of the cargo, adapted from (Wong et al, 2007).

The cytoplasmic MTs are responsible for intracellular trafficking of vesicles, proteins and organelles (Fuchs and Yang, 1999). The actin MFs gives the cell polarity and contractility for migratory processes (Apodaca, 2001). Finally, the IFs provides the need for mechanical integrators of cytoplasm (Fuchs and Yang, 1999).

2.5 Cell Nucleus

2.5.1 Function

The cell nucleus is the control center of the eukaryotic cells. It is the largest organelle in animals cells and can fill up to 10 % of the cell space with an average diameter of 6 μm (Lodish, 2004). Nuclear envelope, nuclear pores, nucleolus and genetic material (chromosomes and chromatin) form the main structure of a cell nucleus (See Figure 2.7). The nucleus coordinates essential cellular activities including growth, protein synthesis and cell division. The genetic material in the nucleus is very well protected by the nuclear envelope - the bilayer membrane of the nucleus.

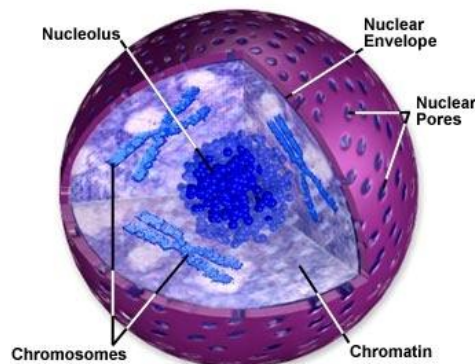


Figure 2.7 : The structure of cell nucleus [Url-1].

2.5.2 Nuclear envelope and pores

The nuclear envelope encloses the nucleus separating the nucleoplasm and genetic material from the cytoplasm by a double membrane (Gorlich and Mattaj, 1996). The inner membrane which is called nuclear lamina is made from proteins and gives extra rigidity to nucleus. The inner and outer membranes are penetrated with thousands of nuclear pores.

The transport of macromolecules, such as proteins, from cytoplasm to the interiors of nucleus, is controlled by highly selective membrane proteins through the formation

of an aqueous channel (Laskey et al, 1996). These proteins are termed as nuclear pore complexes (NPCs). The NPCs recognize the macromolecules which are forwarded to the nucleus and provide the energy for their translocation into nucleus. The recognition process is guided by nuclear localization signals (NLSs) (Pouton, 1998). NPCs allow passive diffusion of metal ions, small metabolites and molecules less than 40kDa in mass with diameters of 5 nm (Wente and Rout, 2010). Nevertheless, there are particles known with a diameter up to 26 nm that can pass the nuclear pores if a suitable NLS guides the particle (Dworetzky and Feldherr, 1988). Moreover, breakdown of the nuclear envelope during the cell division, gives a possibility for nuclear entry of some macromolecules like exogenous DNA (Wilke et al, 1996).

2.6 Gene Expression

Gene expression is the process of synthesis of a functional gene product by using the information from another gene (See Figure 2.8).

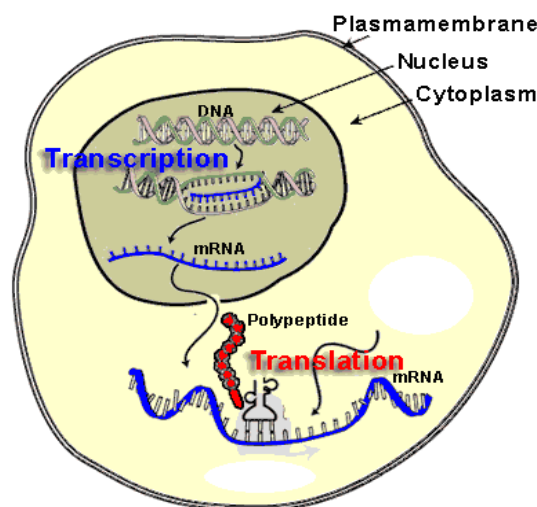


Figure 2.8 : Illustration of gene expression process [Url-2].

2.6.1 Transcription

Transcription is the first step of gene expression that takes place in the nucleus by means of enzymatic complexes that are produced by specific genes. In this step ribonucleic acid (RNA) copies of deoxyribonucleic acid (DNA) are produced. The three major classes of RNA are ribosomal RNA (rRNA), transfer RNA (tRNA), and messenger RNA (mRNA). All play crucial roles in protein synthesis. During

transcription, the double helix of DNA is opened, and one strand of DNA is used as a pattern for the production of an RNA molecule (Bolsover, 2004).

2.6.2 Translation

Genes encoding mRNAs are known as protein-coding genes. Translation follows the transcription process. In this step a single strand mRNA, which was transcribed from double stranded DNA in the nucleus, produces proteins (polypeptides) (Lodish, 2004).

3. GENE THERAPY

Gene therapy is the treatment of human diseases with an underlying genetic cause by delivering therapeutic genetic material (transgene) into the diseased cells of the patient. It has been a promising way to treat genetic diseases over the last decades because it offers a solution to treat the causes of diseases rather than curing the symptoms (Mountain, 2000). When a gene has a mutation, it becomes unable to express the proteins that it encodes for or the mutation can cause the production of inactive or toxic proteins. In both cases, the vital cell functions are affected and eventually induce symptoms. Consequently, gene therapy can be used to treat diseases caused by a defect in a particular gene such as cystic fibrosis (CF) (Russ and Wagner, 2007), or to treat acquired redoubtable diseases such as cancer and acquired immunodeficiency syndrome (AIDS) (Ledley, 1995). The efficiency of gene therapy depends on the delivery of DNA to target cells and long-term expression of the gene (Naik et al, 2009).

3.1 A Brief History of Gene Therapy

The first approved clinical trials of gene therapy took place in United States in 1990 (Scollay, 2001). One of those two *ex vivo* trials was employed to cure an enzyme deficiency that causes severe combined immunodeficiency (SCID) and the other as an immunotherapy for melanoma (Blaese, 1995). Both of them relied on viral vectors for the transfection of the therapeutics into cells, but neither of them were successful applications. Then scientists had an encouraging result in 1995, with the treatment of a four year old girl – an SCID patient. Although the disease was not treated, it was under a better control after the treatment (Blaese, 1995). Nearly a decade after the initial thoughts occurred about gene therapy, more than 175 clinical trials were done and 2000 patients were already treated (G. Ross et al, 1996). However, the first decade ended tragically with the death of a 18-year old patient who suffered from a hepatic metabolic disorder - ornithine transcarbamylase (OTC) deficiency (Edelstein et al, 2004). He was being treated with a viral vector but during the clinical safety

trial, he had an adverse patient reaction which affected his immune system and caused fatality in 1999 (Thomas et al, 2003).

Then the millennium brought the success together for gene therapy. In 2000, three children had been treated for SCID and the first actual healing with gene therapy was reported (Cavazzana-Calvo et al, 2000). Unfortunately the success lasted shortly, because three years after, two of these patients were diagnosed with leukemia (Thomas et al, 2003).

After all the trials with failure, there were some lessons to be learned. Scollay (2001) suggested that scientists had to base their studies more on the development of safer and feasible technologies rather than unrealistic expectations.

According to the survey of Journal of Gene Medicine Clinical Trial Database (See Figure 3.1), there have been 1786 approved clinical trials evidenced in worldwide since the year 1989. Although the idea of treating the causes of diseases is only three decades old and most of the clinical trials are still on phase I, with the acceleration and success gained, it is a candidate to revolutionize the treatment of genetic disorders.

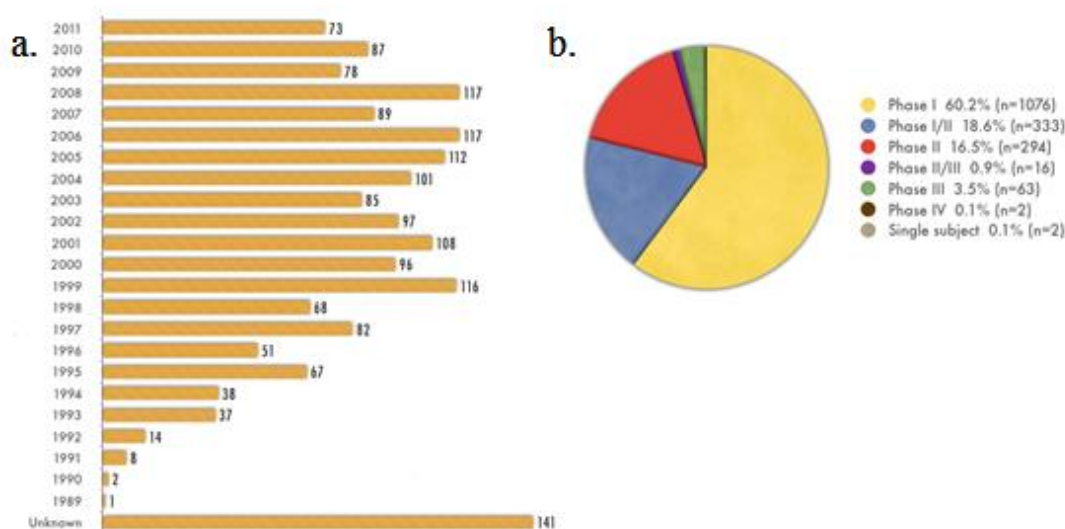


Figure 3.1 : a. Number of approved gene therapy clinical trials worldwide 1989- 2011, b. Clinical phases of approved gene therapy trials, adapted from [Url-3].

3.2 Barriers for Gene Delivery

In general, gene therapy involves the delivery of the transgene which is encoded to produce a specific protein, into the patient's somatic cells. In order for the therapeutic nucleic acid to be effective, it should overcome both extracellular and intracellular barriers. Delivering the pDNA has additional hurdles than delivering mRNA, since the pDNA has to be transferred into nucleus for mRNA transcription, whereas the translation of mRNA occurs in cytoplasm.

These barriers for pDNA delivery can be summarized into following steps as in Figure 3.2:

- I. stability in the extracellular environment,
- II. cellular attachment and adhesion,
- III. cellular uptake,
- IV. endosomal escape,
- V. cellular translocation and
- VI. nuclear import.

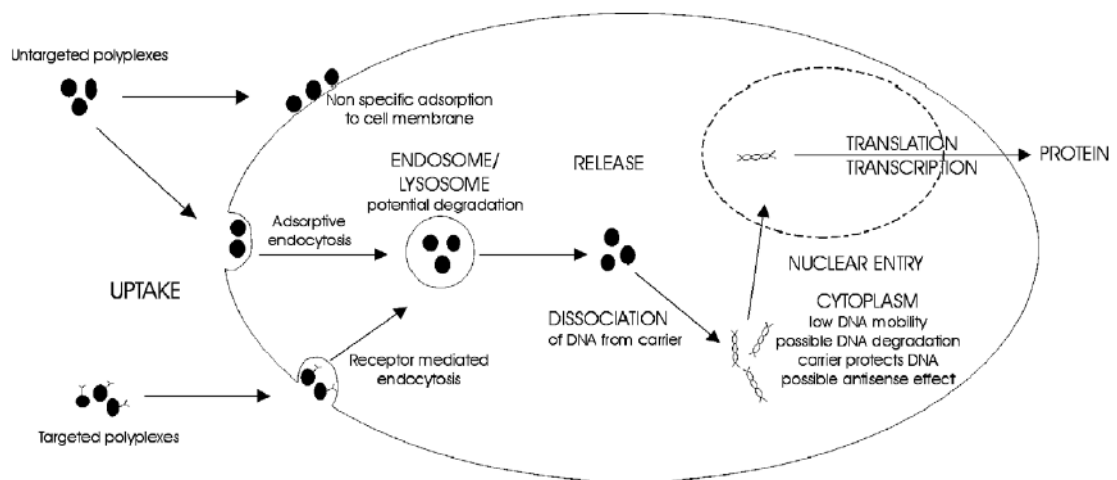


Figure 3.2 : Intracellular barriers for gene delivery, adapted from (De Smedt et al, 2005).

3.2.1 Stability in the extracellular environment

Due to the phosphate groups present in the DNA backbone, it is negatively charged. Also, DNA is not a small molecule that can easily be delivered. It has a bulky structure which has to be condensed in order to ensure cellular internalization. Moreover, the plasmid should be protected against the existence of degradation

enzymes (nucleases) both in the extracellular and intracellular environment (Abdelhady et al, 2003) (Lechardeur et al, 1999). The stability of the therapeutics in the extracellular environment such as intravascular spaces is highly related to the chemical stability of DNA. The exogenous negatively charged materials such as GAGs and serum albumin cause instability of non-viral cationic carriers. The potential carrier which will answer the requirements mentioned above has to provide colloidal stability for carrier/DNA complexes. It is observed for the systems, which require high concentration of cationic lipid or polymer particles to deliver the therapeutic DNA molecule, that in the presence of excess positive charge complexes readily aggregate (Davis, 2002).

There are different strategies which have been tried to avoid aggregation of the complex particles in heterogeneous extracellular milieu. One of them is the covalent attachment of biocompatible hydrophilic polymers such as polyethylene glycol (PEG) or polyhydroxypropyl methacrylate (pHPMA) to the cationic carrier, to provide a steric barrier against aggregation. Since PEG is the most favored polymer for this purpose, it has given the name to the strategy as PEGylation. Covalent coupling of PEG can be performed either before the polyplex formation (prePEGylation) (Kursa et al, 2003) or after the polyplex formation (postPEGylation) (Ogris et al, 1999). The effectiveness of PEGylation to form stable complexes both for cationic lipid and polymers has been proved (Hong et al, 1997) (Y. H. Choi et al, 1998). In addition to increased solubility (Ogris et al, 2003) and stability, PEGylation also provides lower toxicity and extended circulation time in blood, which can be perceived as a heterogeneous extracellular compartment with high ionic strength (Wagner and Kloeckner, 2006).

3.2.2 Cellular attachment and adhesion

When the stability of the complexes is ensured, the first obstacle is the attachment to the cell membrane. There are two main factors affecting the cellular association of cationic lipid or polymer carriers. First of all, the colloidal stability of the complexes has a major impact on the cellular attachment of the complexes. It has been shown that particles which form aggregates can better manifest the cellular attachment *in vitro* (P. C. Ross and Hui, 1999). Nevertheless, from a pharmaceutical point of view these aggregation events are dangerous and undesirable. Secondly, the cellular

attachment and adhesion of cationic particles is thought to be mediated by the interactions with anionic cell surface HSPGs (Wiethoff and Middaugh, 2003). These PGs are involved in various cellular processes as well as cellular attachment and adhesion (Bernfield et al, 1999). The interruption of HSPG expression on the cell surface results in a decrease in the amount of cellular associated-DNA and posterior transgene expression *in vitro* (Mislick and Baldeschwieler, 1996). Furthermore, for cationic lipid or polymer based gene delivery systems it is clearly shown that, the presence of HSPGs increases the efficiency of gene delivery (Belting and Petersson, 1999).

3.2.3 Cellular uptake

After successful attachment to the cell membrane, the second challenge for a gene delivery system is being taken up by the cell. Due to size restrictions, passive diffusion through the cell membrane is not possible for these systems. In general, cationic carrier systems enter the cell via endocytosis with non-specific electrostatic interaction between positively-charged lipoplexes or polyplexes and negatively-charged cell membrane GAGs. As it is described in the section 2.3.1, endocytosis occurs mainly in 5 different pathways: phagocytosis, pinocytosis, clathrin-dependent, caveolae-mediated and clathrin- and caveolae independent endocytosis. Most of the lipid carrier systems are explained to be taken up via clathrin-dependent endocytosis (Pichon et al, 2010). The uptake mechanism of polyplexes is more diverse depending on the cell size and type, the charge and side group characteristics of the polymer (Midoux et al, 2008).

In addition to the non-specific endocytotic entry to the cell, targeting is a strategy to obtain cell specific gene delivery and increase the uptake specificity for the internalization of the carrier system. Targeting the gene delivery system to a specific cell can be employed by using target specific receptors or ligands. This strategy gives the chance to design the delivery system containing the target-ligand according to the aimed cell type. Mainly, electrostatic, conjugative or covalent coupling are being used for ligand binding purposes. The most favored and successful targeting molecules are transferring (Schatzlein, 2003), galactose (Zanta et al, 1997) and the RGD (arginine-glycine-aspartate) peptide (Kunath et al, 2003). Additionally, cell-penetrating peptides are being investigated as a strategy to enhance the cellular

uptake (Heitz et al, 2009). These are positively charged peptides which are derived from viral proteins and have a length of 5-40 amino acids. They can be conjugated to the cargo material either covalently or non-covalently and their uptake mechanism is clearly explained by El-Andaloussi et al. (2005).

Moreover, as cellular internalization and uptake of polyplexes are mediated by cell surface GAGs, it has been shown that the use of high concentrations of exogenous GAGs for targeting purposes increased the uptake and transgene expression efficiency of complexes (Mounkes et al, 1998). One example of the GAGs is hyaluronic acid (HA) which is used as a shielding and coating material to increase specific cellular uptake. The uptake mechanism of HA-coated particles has been explained to be receptor-mediated endocytosis that is facilitated by CD-44 receptors (Knudson et al, 2002). HA and CD44-mediated uptake and targeting is specifically used in tumor targeting (K. Y. Choi et al, 2010).

3.2.4 Endosomal escape

Once the complexes are internalized by endosomal vesicles, the endosomal compartment becomes acidified by proton pumps (H^+ -ATPase) and the luminal pH drops. The therapeutic polymer-gene complexes undergo a pH drop from 7.4 on the cellular surface to 5.5 inside the endosomal lumen. As the vesicle matures from endosome to lysosome the pH gets even more acidic around pH 4.5-5.0, and the therapeutic DNA is faced with different types of nucleases in the lysosome. Hence, to avoid degradation of the therapeutic nucleic acids in the lysosomes and ensure high transfection in the diseased cell, it is essential for any gene delivery vector to be able to escape from the endosomes in time (Wiethoff and Middaugh, 2003).

For cationic lipid based gene delivery systems, their escape from endosomes is thought to be mediated by lipid mixing (flip flop mechanism) between endosomal and cationic lipid membranes and subsequently destabilization of the membrane and release of DNA into cytoplasm (Xu and Szoka, 1996).

In case of the cationic polymer vectors, there are two possible hypotheses involved in their endosomal escape mechanism. One of them supports that the direct electrostatic interaction between negatively charged endosomal membrane and cationic polymer causes membrane disruption. Such a mechanism has been suggested for poly(amido amine) (PAMAM) dendrimers and poly(lysine) vectors (Zhang and Smith, 2000).

The second and most common explanation for the endosomal escape mechanism of cationic polymers with ionizable amine groups is the proton sponge hypothesis (Boussif et al, 1995), even if it is debatable (Funhoff et al, 2004). This hypothesis came up with the poly(ethyleneimine) (PEI) polyplexes, since PEI has a high cationic-charge-density potential, due to the presence of multiple protonable amino groups. Besides, PEI is only 20% protonated at physiological pH and can have a buffering effect nearly at any pH (Boussif et al, 1995). During the maturation of the endosomal vesicle, as it pumps protons and becomes more acidic, PEI-like polymers can act like a proton sponge, accept the protons and effectively buffer the decreasing pH. On the other hand, these accumulated protons disturb the endosomal pH and endosomal ATPases tend to keep the pH constant in the endosomes (See Figure 3.3). They balance the H^+ influx by the influx of counter Cl^- anions to maintain the electroneutrality. This huge increase of ionic concentration inside the endosomes causes osmotic swelling by the influx of water and results in the bursting of endosomal membrane, eventually releasing its content.

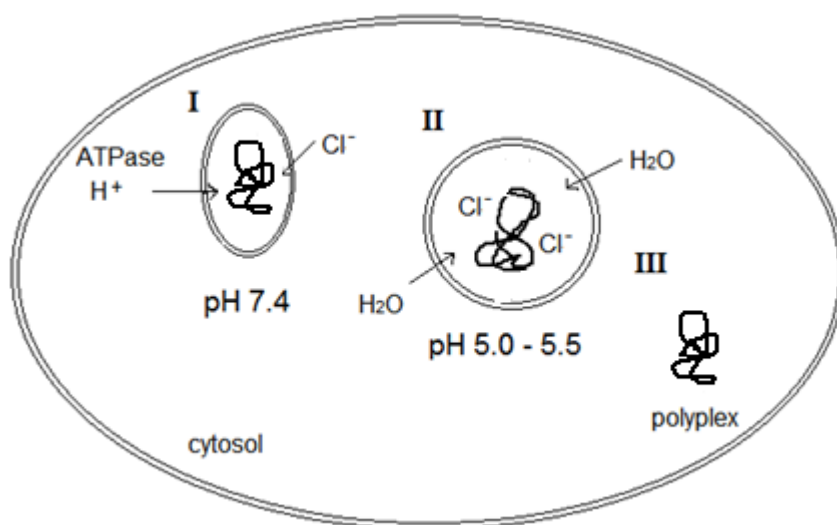


Figure 3.3 : Schematic illustration of proton sponge hypothesis.

3.2.5 Cellular translocation to the nucleus

Polyplexes that enter to cytosol following the endolysosomal release, are immediately faced with a contentious environment. The nucleolytic degradation enzymes are ready to degrade unprotected DNA, and the actin and tubulin filaments from the cytoskeleton form a dense network which can act as a diffusional barrier. The diffusion coefficient of the naked DNA in the cytoplasm is found to be highly

dependent on the plasmid size. However, the cytoskeleton does not allow the diffusion of naked DNA greater than 85 nm, thus polyplexes (150-200 nm) can reach to the nucleus only through active transport, provided by molecular motor proteins which are attached to the MTs or MFs (Luby-Phelps, 2000), (Dauty and Verkman, 2005).

3.2.6 Nuclear import

The translation of mRNA occurs in cytosol while pDNA transcription occurs in the nucleus. For this reason, pDNA therapy has to deal with one additional barrier during the entry to nucleus.

There are three possible routes for a molecule to overcome the nuclear envelope and enter the nucleus. One of them suggests that as the nuclear membrane breaks down during cell division, the DNA molecule can diffuse into the nuclear environment of the dividing cell (Gorlich and Mattaj, 1996). Most of the gene delivery systems are thought to transport their genetic material by this way. Second way is the passive diffusion of the molecules less than 5 nm through nuclear membrane (Wente and Rout, 2010). However, this way is not applicable due to size restrictions of the DNA molecule. The third route depends on the ability of a macromolecule to interact with the nuclear transport system. Highly selective membrane proteins -the nuclear pore complexes (NPCs) - present on this transport system, recognize a macromolecule by the guidance of nuclear localization signals (NLSs) (Pouton, 1998). Particles less than 26 nm in diameter can be actively transported through NPCs. DNA molecules can be condensed by NLSs via electrostatic interactions or NLSs can be bound to the polymer vector for nuclear targeting. Zanta et al. have shown that a 10- to 1000-fold enhanced transfection can be achieved with NLS conjugated DNA compared to DNA without NLS (1999).

Another important barrier to obtain an effective gene transfer for a non-viral vector system is the unpacking of the vector (Schaffer et al, 2000). A successful transcription and enhanced gene expression require safe and effective dissociation of the vector/DNA complex. As polymeric vectors are the subject of this thesis, gene unpacking strategies for polymers will be discussed in the next section.

Overall, the successful transfer of nucleic acids to the nucleus and dissociation of DNA is followed by the transcription of the genes to mRNA and subsequently translation to the therapeutic protein in the cytosol.

3.3 Methods for Gene Delivery

The previously mentioned challenges for gene delivery, make the delivery of naked DNA inefficient and enforces to use a physical method or combine it with a vector. Many types of physical methods and vector systems have been developed for this purpose.

3.3.1 Physical methods

3.3.1.1 Gene gun

This is a method based on applying physical force for the gene transfer. For the delivery process, DNA-coated gold nanoparticles are accelerated by a high-pressure helium steam (Mhashilkar et al, 2001). This method is also called “needle-free injection” because the method allows gene delivery injection without the use of needles (Mountain, 2000). The created force can deliver the DNA directly into the cytoplasm and can be used as a promising alternative to the intramuscular injection of naked DNA for genetic vaccination (Condon et al, 1996). Because of the easier physical accessibility the gene gun method has been widely applied for gene delivery to the skin and encouraging immune responses are reported in initial clinical studies (Tacket et al, 1999).

Large amounts of DNA can be delivered by this method, however, the introduction of foreign materials such as gold particles, the relatively low transfection efficiency and possible physical damage to the cells remain disadvantages of the gene gun (Bleiziffer et al, 2007).

3.3.1.2 Electroporation

Electroporation is a method based on the administration of short (nanosecond range) high-voltage pulses to temporarily disrupt the cell membrane barrier (Gehl, 2003). The effect of the electric field disrupts the lipid and lipid-protein interactions and the membrane becomes porous and permeable, allowing reversible transitions (Neumann

et al, 1999). In short, cells and DNA are put into a cuvette *in vitro* and then placed between electrodes. After the electrical field is applied for a short incubation time to allow the DNA pass the cell membrane, cells are restored to normal culture conditions (Makrides, 2003). Cell size, temperature, post-pulse manipulation and composition of electrodes and pulsing medium are important parameters to be considered while performing electroporation (Gehl, 2003). Improved transfections for *in vivo* electroporation applications have been reported as electrochemotherapy, for the delivery of drugs and genes to malignant tumors, in brain (Nishi et al, 1997), skin (Dujardin et al, 2001) and muscle (Mir et al, 1999) tissues.

Nevertheless, the need for a surgical procedure to place the electrodes into the organs (Gao et al, 2007) and the applied high voltage which results in inevitable tissue damage because of thermal heating (Durieux et al, 2004), limit the applicability of electroporation facilitated gene delivery methods

3.3.1.3 Gene transfer by ultrasound radiation

The first statement that ultrasound (US) may improve the transdermal penetration of drugs was established in 1954 (ter Haar, 2007). Following the developments in therapeutic applications of US, it was discovered that US waves can be used for gene transfer purposes both on the cellular (Kim et al, 1996) and tissue (Liang et al, 2004) levels. The term sonoporation is also used for this method, which is based on creating temporary plasma membrane defects by using US to generate acoustic cavitation (Mehier-Humbert and Guy, 2005). During each ultrasonic cycle, the tissue absorbs the energy of the propagating wave which results in thermal heating that affects the cell membrane structure (Al-Dosari and Gao, 2009). This way, the DNA can be transferred into the cytoplasm via passive diffusion through created membrane pores (Kim et al, 1996). The transfection efficiency of the system is controlled by the frequency, the output strength of the US wave, the duration of the treatment and the amount of the plasmid DNA used (Gao et al, 2007).

The major improvement was observed in US mediated gene transfer when the technique was combined with contrast agents or microbubbles (Endoh et al, 2002). Microbubbles are compressible gas-field vesicles which are stabilized by surface active molecules such as cholesterol (Al-Dosari and Gao, 2009). Their ability to expand and shrink immediately under US application enhances the transfection

efficiency (Bao et al, 1997). Furthermore, two successful *in vivo* examples can be stated for US-mediated gene delivery combined with a contrast agent: one of them with the aim of intravenous injection (Unger et al, 2001) and the second for disrupting the blood-brain barrier (BBB) (Sheikov et al, 2008).

3.3.2 Viral vectors

The use of viral vectors for gene delivery purposes has been the most efficient way (Loser et al, 2002). Viral particles contain a nucleic acid genome surrounded by a capsid of proteins. The introduction of a gene of interest into a host cell by a virus is defined viral transduction. They can easily gain entry to host cells where the genetic information is replicated by the host's machinery. In the ideal case, these viral vectors utilize the viral infection pathway but avoid the subsequent expression of viral genes as this may lead to self-replication and potential toxic effects. Thus, the gene must be combined into a virus that is replication-deficient (Jang et al, 2004). There are large number of viral vector systems (i.e. retrovirus, adenovirus and adeno-associated virus) used for gene therapy applications but the most frequently used adeno-associated virus will be explained in this section.

3.3.2.1 Adeno-associated virus

Adeno-associated virus (AAV) is frequently chosen because it is able to transduce a variety of cells, including non-dividing cells, provide long-term gene expression, and offer minimalised immune response (Jang et al, 2004). However, applications are limited with AAV vectors due to a small packaging capacity, inefficient transgene expression and the need for duplication of the single-stranded DNA genome (Thomas et al, 2003).

In addition to these issues, the reported failures of clinical trials with viral vectors accelerated the developments of safer, less pathogenic and immunogenic gene delivery alternatives such as non-viral vectors including lipid and polymer based delivery systems.

3.3.3 Non-viral vectors

Non-viral vectors have been developed as alternative gene delivery systems to viral vectors because they offer a number of potential advantages. These advantages can be listed as non-immunogenicity, ability for repeated administration, ease of

production and lower costs (Brown et al, 2001). The introduction of DNA by means of non-viral delivery system is defined as transfection process. This process includes a successful gene transfer and expression (Mountain, 2000). Most commonly used synthetic non-viral delivery systems will be described in the following.

3.3.3.1 Lipid-based gene delivery systems

Lipid-based systems have a variety of applications for drug and gene delivery in pharmaceutical industry. Liposomes are spherical bilayered phospholipid structures which are formed by the self assembly of a hydrophilic polar head group and hydrophobic hydrocarbon tail. In an aqueous media, this bilayered structure consists an internal aqueous phase and a water phase between the alternating bilayers (Remaut et al, 2007). Due to the earlier mentioned physicochemical characteristics of DNA molecule, cationic liposomes are the most frequently investigated carriers to encapsulate the anionic surface charge of DNA by electrostatic interactions. The cationic liposome and nucleic acid complexes are called as lipoplexes.

Commonly used cationic lipids include *N*-(1-(2,3-dioleoyloxy)propyl)-*N,N,N*-trimethyl-ammoniumchloride (DOTMA) and 1,2-dioleoyl-3-trimethylammoniumpropane (DOTAP) as illustrated in Figure 3.4.

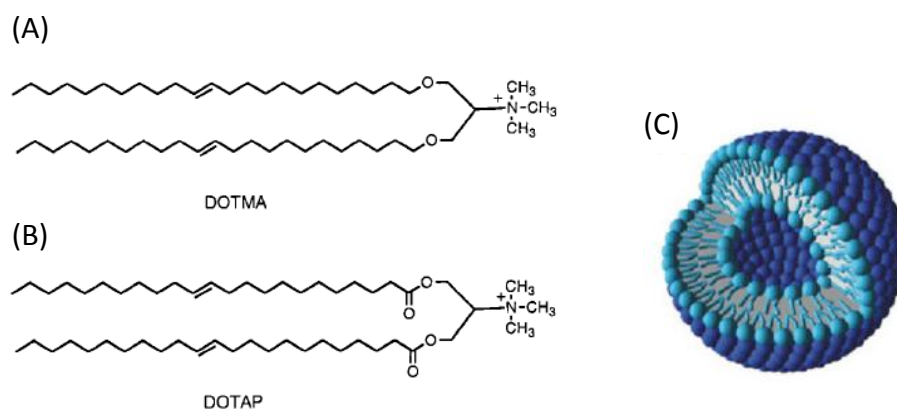


Figure 3.4 : Chemical structure of cationic lipid (A) DOTMA, (B) DOTAP and (C) an illustration of liposome, adapted from (Remaut et al, 2007).

The use of lipids as gene delivery systems offers some advantages, such as their lack of immunogenicity which makes repeated delivery *in vivo* possible. Another advantage is the potential to deliver large amounts of DNA and the protection of DNA against physical forces and enzymatic degradation. However, there are some

major limitations of these liposomes such as the duration and level of transgene expression (Brown et al, 2001).

3.3.3.2 Polymer-based gene delivery systems

As it was explained in the previous section that the understanding of the barriers that a vector system should overcome provides the development of safe and efficient vectors for the delivery of the plasmids. With this in mind, an ideal polymeric vector should meet the requirements of being able to neutralize the negative charge of the DNA to avoid charge repulsion against the anionic cell surface, to condense the DNA molecule to an appropriate length scale, and to protect the DNA from degradation by extracellular nucleases. Since cationic polymers are capable of condensing the negative charge of DNA, tremendous research has been done to improve their potential as non-viral gene carriers. They offer enhanced bio-safety and biocompatibility, a high flexibility regarding the size of the delivered nucleic acid, repeated administration and can be synthesized at low cost in large quantities (Wagner and Kloeckner, 2005).

The nano-sized self assemblies of positively charged polymers and negatively charged DNA are defined as polyplexes (pplexes). The packaging of therapeutic genetic material by a cationic polymer can be based on three different ways including electrostatic interactions, encapsulation within the spherical polymer structure and adsorption onto biodegradable nanosphere (Wong et al, 2007).

There have been many novel polymer structures developed for gene therapy applications but the most frequently investigated polymer systems include poly(L-lysine) (PLL) (Pack et al, 2005), poly(ethyleneimine) (PEI) (Akinc et al, 2005), methacrylate polymers (Dubruel et al, 2003) and poly(amidoamine) (PAA) (Liu et al, 2010), (See Figure 3.5).

The ratio of amine groups present in the cationic polymer to phosphates on the plasmid affects the effective diameter and determines the surface charge of the polyplex.

Poly(L-lysine) (PLL) was one of the first polycations used for polyplex formation. At physiological pH the amino groups of PLL are positively charged and interact ionically with the negatively charged phosphate groups of the DNA.

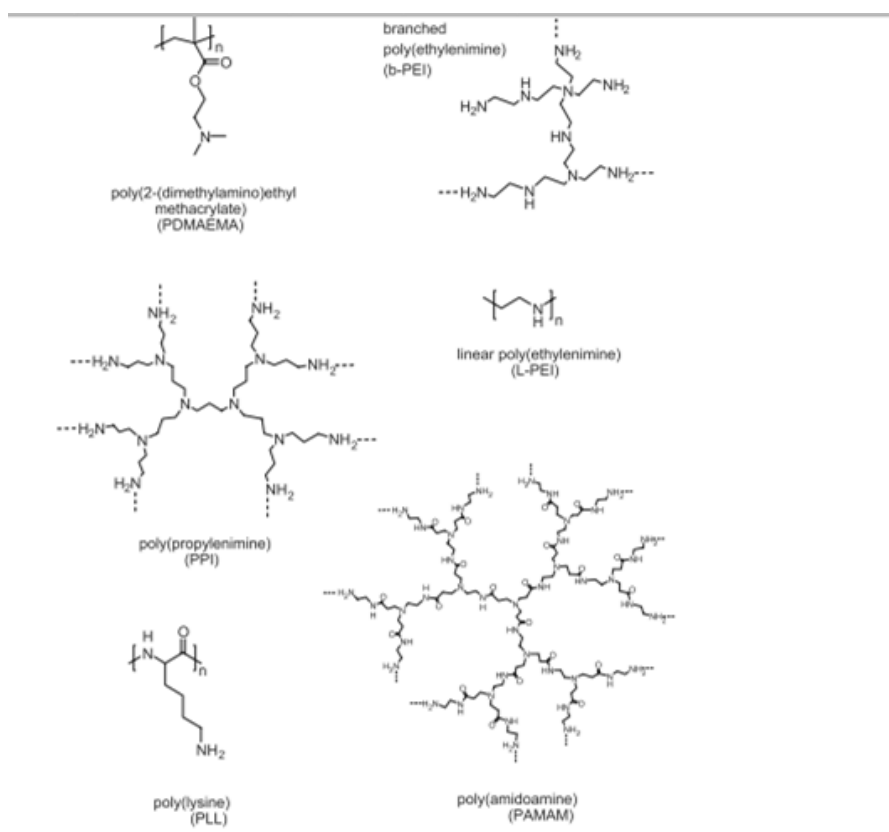


Figure 3.5 : Chemical structures of selected polymers, adapted from (Wong et al, 2007).

PLL/DNA polyplexes have a highly positive zeta potential, interact electrostatically with a negatively charged cell surface, and are taken up by absorptive endocytosis (Wagner and Kloeckner, 2005). The efficiency of uptake can be enhanced by covalently coupling PLL with ligands that can specifically target cells and promote receptor-mediated uptake (Zauner et al, 1998).

Poly(ethylenimine) (PEI) is an organic macromolecule with the highest cationic charge-density potential, allowing for a tight compaction of nucleic acids (Boussif et al, 1995). Linear PEI is solid at room temperature and contains only secondary amines, while branched PEI (bPEI) is liquid at all molecular weights and contains primary, secondary and tertiary amine groups (Ogris, 2004). Usually the branched form of PEI is used for gene delivery purposes. Because every third amino nitrogen atom is protonated, PEI has a buffer capacity at virtually any pH value (Boussif et al, 1995).

Methacrylate based polymers including poly(2-(dimethylamino)ethyl methacrylate)) (pDMAEMA) can be easily synthesized by radicalic polymerization. pDMAEMA apparently has advantageous properties to escape the endosome due to its average

pKa value of 7.5. This polymer is partially protonated at physiological pH and might behave as a proton sponge that can cause a disruption of the endosome, which results in the release of both the polyplexes and cytotoxic endolysosomal enzymes into the cytosol (van de Wetering et al, 1998). Moreover, pDMAEMA was shown to be an efficient vector for gene delivery to OVCAR-3 cells (van de Wetering et al, 1999).

Poly(amidoamine)s (PAAs) are synthetic tert-amino polymers obtained by stepwise polyaddition of primary or secondary aliphatic amines to bisacrylamides. Linear polymers are produced during the polymerization of both primary and secondary amines (Ferruti, et al, 2002). A novel bio-reducible, disulfide containing family of PAAs were introduced by Lin et. al. (2007a). These polymers showed relative stability in physiological conditions but were rapidly degraded in reductive environment. SS-PAAs possessed higher buffer capacities than PEI in endosomal pH range, which may contribute to the endosomal escape of the polyplexes. Some members of SS-PAA family also showed higher transfection efficiency in COS-7 cells than PEI with low cytotoxicity (Lin et. al, 2007a). Dendrimer form of polyamidoamines (PAMAM) also shows high transfection potential in the absence of any additional membrane-active agent. Due to the low pKa of its terminal and internal amines this polymer can act as an endosomal buffering agent by this way preventing DNA degradation within the endolysosomes (Wagner and Kloeckner, 2005).

A variety of polymer systems have been developed to maintain an efficient DNA/vector dissociation. These strategies include thermoresponsive polymers, bio-reducible disulfide bonds and ester bonds (Wong et al, 2007).

The polymeric gene delivery vectors have relatively low transfection efficiency when it is compared with viral and lipid based systems. Mainly, this delivery inefficiency of the polymeric vectors relies on their inability to overcome numerous barriers encountered between the site of administration and the localization of nucleus (Wiethoff and Middaugh, 2003). Thus, numerous strategies were applied to improve the efficiency of polymer vector systems.

4. MATERIALS AND METHODS

The aim of the research described in this work is to evaluate cationic polymers in terms of their physicochemical and biological suitability for gene therapy applications. For this purpose, non-biodegradable poly((2-dimethylamino)ethyl methacrylate) (pDMAEMA) polymer and bio-reducible disulfide containing poly(amidoamine)s (SS-PAA)s were synthesized and evaluated.

4.1 Polymer Synthesis

4.1.1 Synthesis of pDMAEMA by radical polymerization

As a leading compound, poly((2-dimethylamino)ethyl methacrylate) (pDMAEMA), is chosen as a candidate for gene delivery studies since it is relatively easy to obtain by radical polymerization from dimethylaminoethyl methacrylate (DMAEMA) and its molecular weight (M_w) can be controlled by controlling the amount of initiator and monomer.

$$DP = \frac{[M]}{[I]} \quad (4.1)$$

DP = Degree of Polymerization (units of monomers in a polymer chain).

[M] = concentration of monomer.

[I] = concentration of initiator.

Moreover, DMAEMA has amine groups which are protonated at physiological pH. Due to a neighboring effect present in the polymer, some groups remain unprotonated and therefore enable the polymer to express buffering capacities. In gene therapy, the buffering capacity of a polymer is extremely important as it enables the polymer to escape from endosomes.

The low M_w pDMAEMA (50 kDa) and high M_w pDMAEMA (600 kDa) which are evaluated in this thesis were obtained from Ghent University Polymeric Biomaterials Group (Ghent, Belgium).

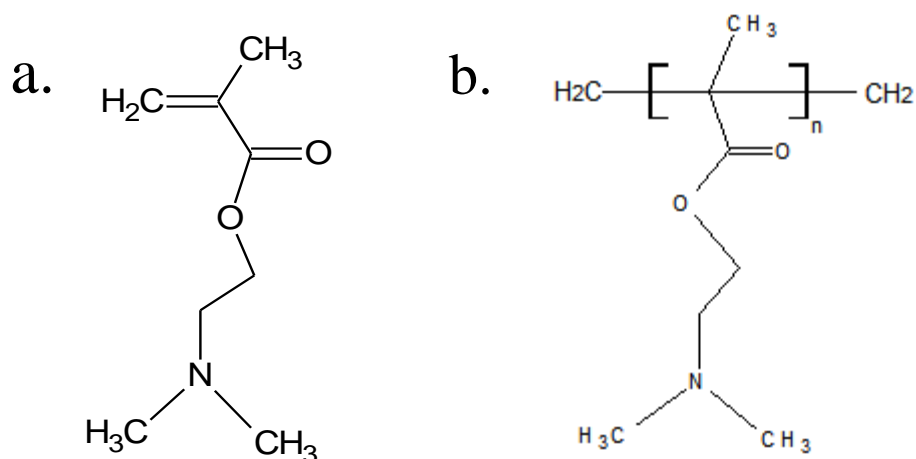


Figure 4.1 : Chemical structures of a. DMAEMA monomer, b. pDMAEMA polymer.

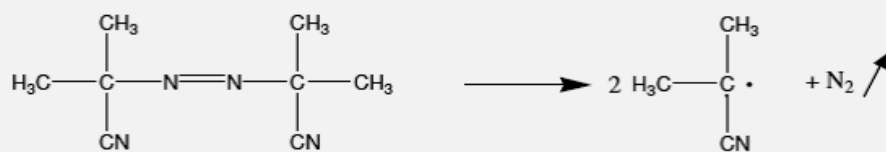
The synthesis of pDMAEMA (250 kDa) was performed by thermally initiated radicalic polymerization reaction, as a model reaction for this study.

It should be noted that even though the general set up and mechanisms are the same for low and high Mw pDMAEMA synthesis, it is not possible to synthesize high Mw pDMAEMA with the same initiator. As it was previously stated by van de Wetering et. al., high Mw (>300 kDa) pDMAEMA polymers were obtained when ammonium persulfate (APS) radicalic initiator was used in aqueous solution conditions (1998).

As it is illustrated in Figure 4.2, the AIBN initiator splits into two radical molecules in the initiation step. Afterwards, the propagation occurs while the radical attacks to the DMAEMA monomer. Then the monomer radical attacks to the other DMAEMA monomer and the polymerization continues by the formation of polymer radicals. The termination of the polymerization can be either via combination of two radicalic polymers with each other or disproportionation.

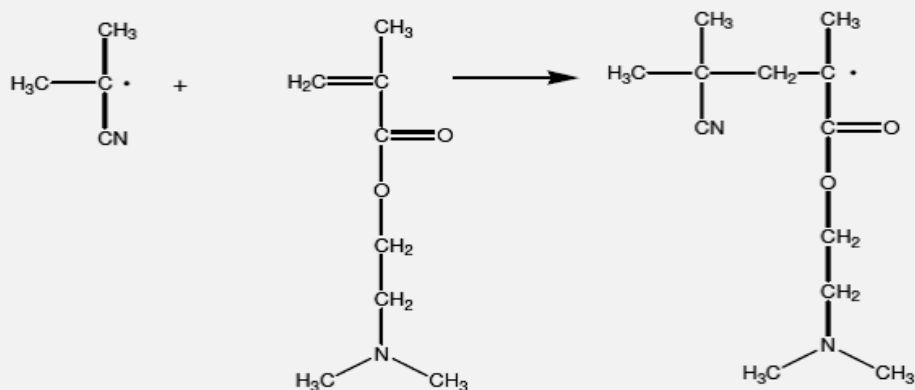
The DMAEMA monomer is commercially available from Fluka Analytical (Belgium). The pDMAEMA polymer was synthesized according to a previously published protocol (Dubruel et al, 2000). In short, first the monomer is stabilized with inhibitors and it is necessary to carry out a vacuum distillation prior to polymerization. Therefore, the monomer was vacuum distilled for 2 hours. Although it contained polymerization inhibitor, 10% of the monomer was polymerized and stucked to the flask. At the end of the distillation, the distilled monomer liquid was decanted gently from the flask.

I. Initiation

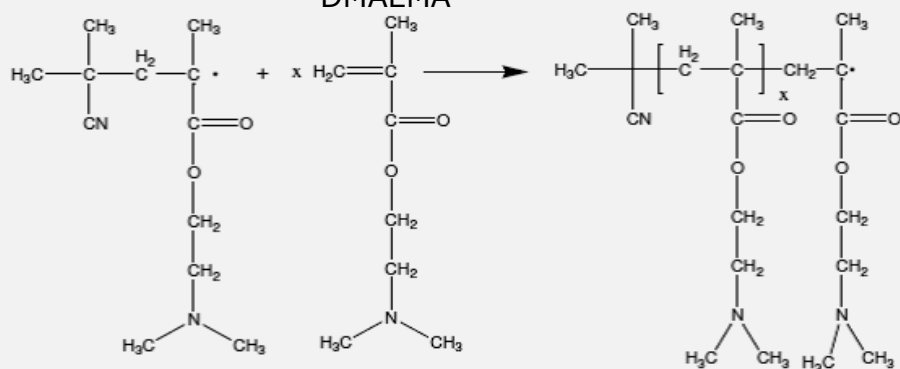


II. Propagation

AIBN



DMAEMA



III. Termination by combination

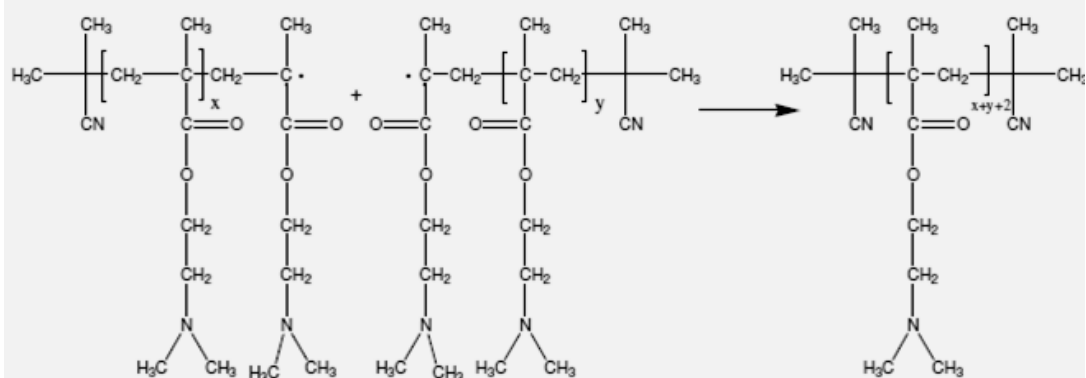


Figure 4.2 : Illustration of radicalic polymerization reaction mechanism.

IV. Termination by disproportionation

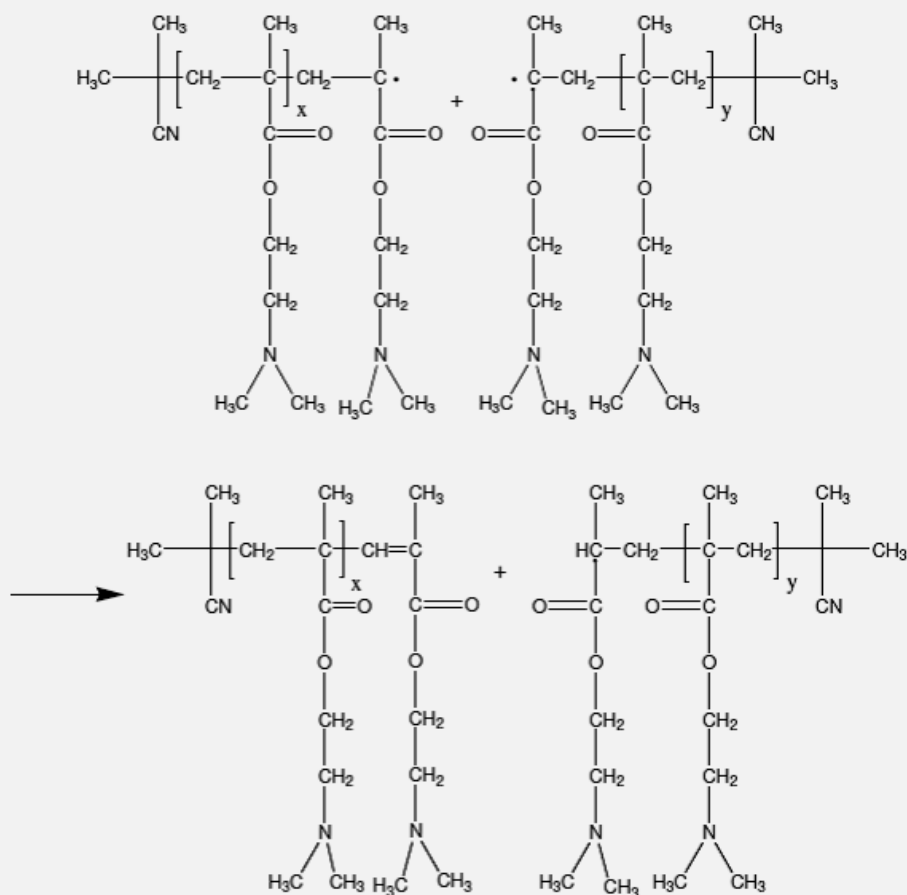


Figure 4.2 (continued) : Illustration of radicalic polymerization reaction mechanism.

Meanwhile, the solvent of the reaction was distilled nearly for 3 hours in order to get rid of any possible impurities. The solvent purification was performed in the presence of $\text{Ca}(\text{OH})_2$ to dry out existing water or moisture in the solvent. The choice of the solvent and initiator depends on the solubility of the monomer as well as the polymer which will be synthesized inside and the desired Mw of the polymer. As an appropriate solvent, both for monomer and polymer, toluene was used and azo-bis-isobutyronitrile (AIBN) was chosen as an initiator for the polymerization reaction.

Prior to polymerization, a cooler, a valve and a two neck, round-bottomed flask were put in the drying oven, to remove any possible moisture. Firstly, the flask was placed in an oil bath which was placed on a magnetic stirrer, to allow monitoring of both the temperature and the stirring speed. Secondly, the reflux cooler was fixed to the flask and above this cooler the valve was placed with a connection to a balloon filled with

N₂. The other neck of the flask was covered with a septum to avoid air-contact. Finally, after addition of monomer and solvent, all contacts and seals were checked.

Before and after the addition of the appropriate amount of initiator, the reaction mixture is degassed and purged with N₂, by means of a vacuum pump and a balloon filled with N₂. This procedure was performed in order to remove the O₂ present in the set up as it may disturb the polymerization due to trapping of initiator radicals (O_{singlet} – O_{triplet} transition) which may lead to the absence of the initiator-propagation transition (Cherng et al, 1996).

When all of the reagents were purified and ready for the synthesis, the reaction was started by adding the calculated amounts of reagents according to the desired Mw of polymer. . A Mw of 250 kDa (250000 g/mol) was desired, 7.74 mg of AIBN was added to 10 % DMAEMA (25.3 mL) in toluene as shown by the following calculation. The density and Mw of DMAEMA are 0.93 g/ml and 157.21 g/mol respectively. The Mw of AIBN is 164.21 g/mol. Based on these values, the following calculations were made :

$$\begin{aligned}\text{Aimed DP} &= \text{Mw}_{\text{polymer}} / \text{Mw}_{\text{monomer}} \\ &= (250000\text{g/mol}) / (157.21\text{g/mol}) = 1590.23 \text{ units}\end{aligned}$$

Amount of monomer : If we start with 0.15 moles of monomer [M],

$$n = m / Mw ;$$

$$0.15 \text{ mol} = m_{\text{monomer}} / 157.21\text{g/mol}$$

$$m_{\text{monomer}} = 23.58 \text{ g}$$

$$d = m / V ;$$

$$0.93 \text{ g/ml} = 23.58 \text{ g} / V_{\text{monomer}}$$

$$V_{\text{monomer}} = 25.3 \text{ mL}$$

Amount of initiator : [I] = [M]/ DP

$$[I] = 0.15 \text{ mol} / 1590.23 = 9,43 \times 10^{-5} \text{ mol}$$

$$m_{\text{initiator}} = [I] \times \text{Mw}$$

$$m_{\text{initiator}} = 9,43 \times 10^{-5} \text{ mol} \times 164,21 \text{ g/mol} = 0,01548 \text{ g}$$

At the initiation step of the reaction, as every 1 mole of initiator gives rise to 2 moles of radicals as illustrated in figure 4.2, the calculated amount of the initiator should be divided by 2. This results in, $0.01548 \text{ g} / 2 = 0.00774 \text{ g} = 7.74 \text{ mg}$ of AIBN.

After the addition of AIBN the polymerization reaction is started by heating the oil bath to approximately 75°C, in order to obtain a temperature of 65 - 70°C in the flask, for 24 hours. 24 hours later, the polymerization reaction was stopped and the obtained reaction mixture is brought to room temperature. The mixture in toluene was precipitated drop wise in ice-cooled distilled pentane (5x volume of the reaction mixture). As a non-polar solvent pentane can remove the solvent of the reaction (toluene), the residue of the monomer (DMAEMA) and the initiator (AIBN). The synthesized polymer was separated from the pentane by decantation. After the precipitation procedure, a sticky and gummy polymer was obtained. Then the polymer was left to be dried and re-precipitated in ice-cooled ultra pure acetone (5x volume of the reaction mixture) and again it was left to be dried. Finally, the polymer was dissolved in ultrapure water. To ensure a good dissolution of the polymer in water, a few drops of 0,5 M HCl are added. This solution was purified by dialysis through a membrane with a Mw cut-off of approximately 1/5th of the Mw of the polymer. The dialysis procedure was carried out for 48 hours against ultrapure water, 0,1 M NaCl solution and 0,1 M HCl solution respectively. Subsequently, the dialyzed polymer solution was freeze-dried, then the final product was characterized by NMR (300 MHz, CDCl₃, relative to TMS) and stored at -20°C for further experiments.

p(DMAEMA): ¹H-NMR (CDCl₃) δ (ppm) = 1.83 (CH₃C(CH₂)CH₂); 1.92 ((CH₃)CCH₂C(CH₃)); 2.29 (CH₂N(CH₃)CH₃); 2.57 (CH₂N(CH₃)CH₃); 4.06 (O=COCH₂CH₂).

4.1.2 Synthesis of SS-PAA by Michael-type polyaddition

Poly(amidoamine)s (PAAs) have attracted significant interest due to their biocompatibility and biodegradability as potential gene delivery systems. A new series of PAAs containing repetitive disulfide linkages (SS-PAA) in the polymer backbone was previously introduced by Lin et. al. (2007a). Moreover, Zintchenko et.al. have reported an improved synthesis strategy for SS-PAA by means of Ca²⁺ catalysis in order to increase polymerization times of conventional synthesis (2011).

In this study, three types of SS-PAA were synthesized by Ca²⁺ catalyzed Michael type polyaddition of a primary amine to N,N'-cycloaminebisacrylamide (CBA)

monomer according to published protocol (Zintchenko et al, 2011). The polymerization reactions are illustrated in following figures (Figure 4.3, 4.4, 4.5) :

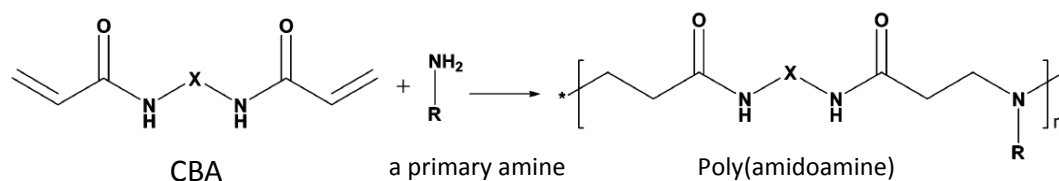


Figure 4.3 : Illustration of Michael type polyaddition of a primary amine to bisacryl amide monomer, adapted from (Lin et al, 2007a).

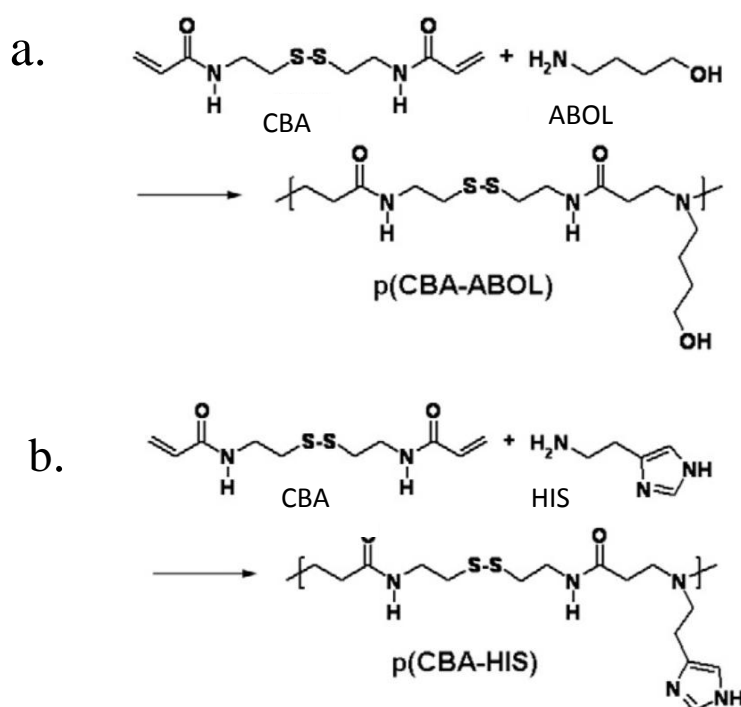


Figure 4.4 : Illustration of Michael type addition polymerization of a. p(CBA-ABOL), b. p(CBA-HIS), adapted from (Coue and Engbersen, 2011).

All monomers, 4-amino-1-butanol (ABOL, Aldrich), histamine (Fluka), *N,N'*-cystaminebisacrylamide (CBA, polysciences, USA), were purchased in the highest purity and no further purification was used. All reagents and solvents were of reagent grade and were used without further purification.

Solutions of CaCl_2 in methanol and in water (0.4 M) were prepared separately and mixed together at the ratio of 3/1 (v/v) just before the synthesis. The polymerizations were carried out with 1:1 molar ratio between the reactants.

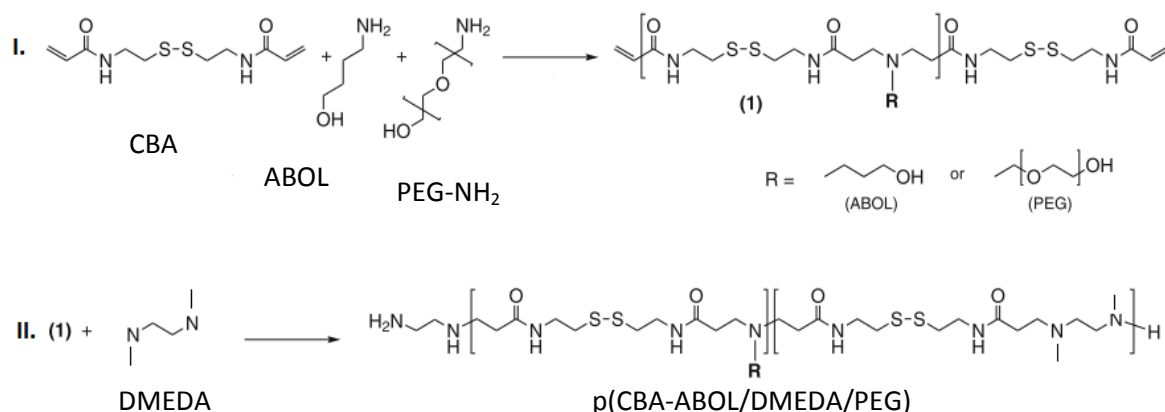


Figure 4.5 : Illustration of Michael type addition polymerization of a p(CBA-ABOL/DMEDA/PEG) copolymer, adapted from (Vader et al, 2012).

Solutions of CaCl_2 in methanol and in water (0.4 M) were prepared separately and mixed together at the ratio of 3/1 (v/v) just before the synthesis. The polymerizations were carried out with 1:1 molar ratio between the reactants. As a typical reaction ABOL (0.34 g, 3.85 mmol) was added to CBA (1.0 g, 3.85 mmol), 2 ml of solvent was added, and the reaction flask was sealed. The polymerization was performed at 50°C and the reaction was allowed to proceed for 30 h, yielding a viscous solution. Subsequently, the polymerization was quenched with 10 mol% excess of ABOL (0.034g, 0.385 mmol) in order to consume any unreacted acrylamide groups and stirring was continued for 1 h at 50°C . The resulting solution was diluted with water to about 20 ml, acidified with 6 M HCl to pH ~ 4 , and then purified using an ultrafiltration membrane (MWCO 1000 g/mol). After freeze-drying, the p(CBA-ABOL) polymer was collected as its HCl-salt form. The same procedures were applied for the synthesis of p(CBA-HIS) polymer. The p(CBA-ABOL/DMEDA/PEG) polymer was obtained from Engbersen Lab. (University of Twente, The Netherlands). The polymerization of PEGylated p(CBA-ABOL) was also performed with the same procedure. The Michael type addition of ABOL and PEG-NH₂ to CBA was followed by a second addition of DMEDA monomer as illustrated in figure 4.5.

NMR spectra of final products were recorded on Varian Unity 300 (^1H NMR 300 MHz) using tetramethylsilane (TMS) as the internal standard.

p(CBA-ABOL) : ^1H NMR (D_2O) δ (ppm) = 1.73 ($\text{CH}_2\text{CH}_2\text{OH}$, 2H); 1.94 ($\text{CH}_2\text{CH}_2\text{CH}_2\text{OH}$, 2H); 2.91($2 \times \text{NHCOCH}_2$, 4H); 3.00 ($2 \times \text{SSCH}_2\text{CH}_2$, 4H); 3.36 ($\text{NCH}_2\text{CH}_2\text{CH}_2\text{CH}_2\text{OH}$, 2H); 3.59 ($\text{CH}_2\text{CH}_2\text{NCH}_2\text{CH}_2$, 4H); 3.66 ($2 \times \text{SSCH}_2\text{CH}_2$, 4H); 3.75 (CH_2OH , 2H), 4.90 ($2 \times \text{NH}$, 2H) .

p(CBA-HIS) : ^1H NMR (D_2O) δ (ppm) = 2.77 ($2 \times \text{NHCOCH}_2$, 4H); 2.95 ($2 \times \text{SSCH}_2\text{CH}_2$, 4H); 3.17 (NCH_2CH_2 , 2H); 3.38 ($\text{CH}_2\text{N}(\text{CH}_2)\text{CH}_2$, 6H); 3.61 ($2 \times \text{SSCH}_2\text{CH}_2$, 4H); 7.26 ($\text{C}=\text{CH}-\text{N}$, 1H); 8.38 ($\text{C}-\text{N}=\text{CH}-\text{N}$, 1H).

The molecular weight and polydispersity (M_w/M_n) of the synthesized SS-PAA s were determined by gel permeation chromatography (GPC) relative to PEO standards (Polymer Labs) as suggested by Jiang et.al. (2006). A Viscotek GPCMax pump, autoinjector and two thermostated (30°C) PL aquagel-OH 30 columns ($8\ \mu\text{m}$, $300 \times 7.5\ \text{mm}$, Polymer Labs, with a low-molar-mass separation range 200 – 40,000) were used during the analysis. Data were collected using a TDA302 Triple detector with RI, Visc and LS (7 and 90°). 0.3 M NaAc aqueous solution, pH 4.4, with 30% methanol was used as eluent at a flow rate of 0.7 ml/min).

4.2 Cell Culture

In this project, *in vitro* studies were done with ARPE-19 cells (retinal pigment epithelial cell line; ATCC number CRL-2302), which are described by Dunn et al. as an adherent, human retinal pigment epithelium (RPE) cell line (1996).

4.2.1 Materials

Dulbecco's modified Eagle's medium (DMEM), serum-free transfection medium OptiMEMTM, L-glutamine, fetal bovine serum (FBS), penicillin-streptomycin solution (5000 IU/mL penicillin and 5000 $\mu\text{g/mL}$ streptomycin) (P/S), and phosphate-buffered saline (PBS) were provided from GibcoBRL (Merelbeke, Belgium). Trypsin was purchased from Sigma Aldrich (Bornem, Belgium) and used as 0.05% trypsin/ 0.02% ethylenediaminetetraacetate (EDTA) solution.

4.2.2 Methods used in cell culture

The cells are grown in polystyrene (PS) culture bottles in RPE cell culture medium (CCM), (DMEM:F12 supplemented with 10% fetal bovine serum (FBS), 2 mM

l-glutamine, and 1% penicillin/streptomycin (P/S)), and incubated at 37°C and in the presence of 5% CO₂ (Nu-5510 NuAire incubator).

All cell work is done under sterile laminar airflow conditions. When the monolayer of ARPE-19 cells has become 70-80 % confluent in culture bottle, the cell line is spliced to a new cell culture bottle. Prior to cell splicing procedure, the cells are always checked under the microscope for possible contamination. First of all, the old CCM is removed to waste. Then the cells are washed once with PBS solution without Ca²⁺ and Mg²⁺, to get rid of the dead cells floating inside the bottle and any remaining serum, which might inhibit trypsin activity. Afterwards, the flask is shaken gently and the PBS is aspirated from the bottle. Secondly, the cells are trypsinized with pre-warmed trypsin/EDTA solution and incubated at 37°C for 5 minutes. Trypsin provides the cell detachment from the bottle surface and EDTA chelates the remaining divalent cations, necessary for Ca²⁺-dependent cellular adhesion molecules. When cell detachment is verified by light microscopy, trypsin is neutralized and inhibited by means of pre-warmed fresh CCM since the serum in the CCM contains trypsin inhibitors. Fourthly, a certain amount of cell suspension is transferred to a new culture bottle. Then the cells are re-incubated at 37°C and in the presence of 5% CO₂ until the next passage. If the cells are needed the next day for a transfection experiment, then the cells are counted, seeded and plated following the trypsinization step.

4.3 Nucleic Acids Used in This Study

4.3.1 pGL4.13 plasmid

Bacterial plasmids are described as closed circular molecules of double-stranded DNA. Their size can range between 1-200 kb. There are genes which code for enzymes in plasmids. pGL4.13 is a plasmid of the series of pGL4-luciferase reporter vectors of Promega (Leiden, The Netherlands). It encodes for luciferase reporter gene (luc2) and is designed for high expression and reduced anomalous transcription. Besides, the genes of pGL4.13 plasmid encodes for ampicilline (Amp^r) resistance (See Figure 4.6).

During this thesis study, pGL4.13 plasmid is isolated from *Escherichia Coli* bacteria by using Qiafilter Plasmid Purification Kit (Qiagen, Venlo, The Netherlands) according to the instructions manual.

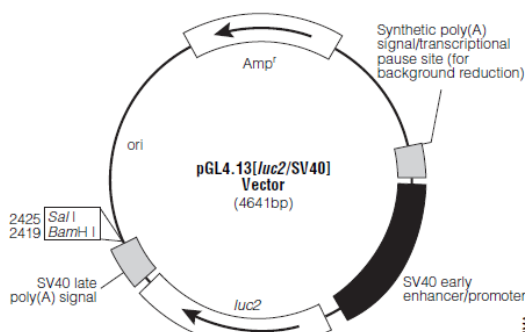


Figure 4.6 : Schematic representation of pGL4.13 plasmid. The plasmid encodes for luc2 gene under the control of SV40 promoter. Amp^r: ampicilline resistance marker [Url-4].

This assay is based on growing the bacteria containing the plasmid in appropriate medium and then isolation of the plasmid from the grown bacteria culture. The isolation includes filtration of alkaline lysate of the bacteria, centrifugation of lysate, anion-exchange chromatography for selective isolation of pDNA from lysate and finally purification of plasmid by alcohol precipitation (QIAGEN, 2005). The concentration and purity of isolated pDNA were determined by measuring the UV absorption at 260 and 280 nm with Nano Drop 2000c UV-Vis Spectrophotometer (Thermo Scientific, USA). Subsequently, pDNA solution was diluted to 1 mg/ mL and stored at -20°C.

4.3.2 gWizTM-GFP plasmid

The gWizTM-GFP plasmid which encodes for green fluorescent protein is an expression vector from the gWizTM series of Aldevron (Freiburg, Germany). As a bacterial selection marker, kanamycin (kan^r) resistance was used in this plasmid. The gWizTM-GFP plasmid is designed for the highest level of gene expression in various types of mammalian cells and tissues (See Figure 4.7). In this study, transfection efficiency studies were analyzed in terms of GFP expression by the use of gWizTM-GFP plasmid.

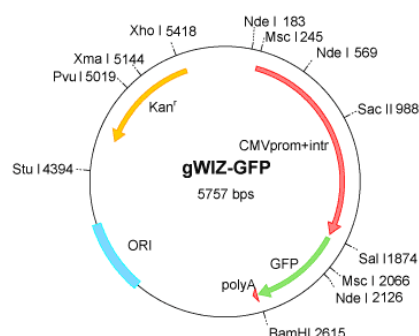


Figure 4.7 : Schematic representation of gWiz™-GFP plasmid. kan^r: kanamycin resistance [Url-5].

4.3.3 YOYO®-1 iodide labeled pGL4.13 plasmid

For uptake efficiency purposes, pGL4.13 plasmid was fluorescently labeled with YOYO®-1 iodide dye ($\lambda_{\text{ex}} = 491 \text{ nm}$, $\lambda_{\text{em}} = 509 \text{ nm}$). This is a green fluorescent dye from a series of dimeric cyanines obtained from Molecular Probes (Merelbeke, Belgium). The plasmid and YOYO-1 (1 mM in DMSO) iodide was mixed at a ratio of 0.15/1 (v/w), to provide a theoretical labeling density of 1 YOYO-dye molecule per 10 bp. Then the mixture was incubated at room temperature for 4 h in the dark. Free YOYO-1 dye and DMSO were removed by precipitating the labeled plasmid. For this purpose 2.5 volumes of ice-cold ethanol and 0.1 volume of 5 M NaCl were added to the plasmid/YOYO-1 solution. After incubation for 30 min at -80°C , the centrifugation (17000 g, 30 min) and washing with clean 70 % ethanol, fluorescently labelled plasmid was finally resuspended in 25 mM HEPES, pH 7.2. The concentration of the plasmid was again determined by UV absorption at 260 and 280 nm with Nano Drop 2000c UV-Vis Spectrophotometer (Vercauteren et al, 2011).

4.4 Preparation and Physicochemical Characterization of Polyplexes

4.4.1 Dynamic light scattering

4.4.1.1 Theory and working principle

Dynamic Light Scattering (DLS) is a technique which is used to measure the size-related Brownian motion of particles. Particles suspended within a liquid will move randomly under influence of the surrounding solvent molecules. The larger the particle, the slower the movement will be. The translational diffusion coefficient D is

a measure for the diffusional motion, from which the hydrodynamic diameter is calculated by using the Stokes-Einstein equation (4.2) :

$$d(H) = \frac{kT}{3\pi\eta D} \quad (4.2)$$

where:

$d(H)$ = hydrodynamic diameter (m)

D = translational diffusion coefficient ($\text{m}^2.\text{s}^{-1}$)

K = Boltzmann's constant ($1.38 \times 10^{-23} \text{ m}^2.\text{kg}.\text{s}^{-2}.\text{K}^{-1}$)

T = absolute temperature (K)

η = viscosity ($\text{kg}.\text{m}^{-1}.\text{s}^{-1}$)

The diameter that is obtained by DLS is the diameter of a sphere that has the same diffusion coefficient as the measured particle. This coefficient will depend not only on the size of the particle core, but also on any surface structure, as well as the concentration and type of ions in the medium.

The Brownian motion of particles is measured by determining the rate at which the intensity of light, scattered from the particles, fluctuates when detected with a suitable optical arrangement. The signal intensities at different time points are compared and a correlogram is constructed by a digital auto correlator in the DLS machine. This device will also determine the correlation function of the scattered intensity, from which the size of the particles can be calculated by using a suitable algorithm. The size distribution obtained from the DLS measurements is a plot of the relative intensity of light scattered by particles of various sizes and is therefore an intensity-dependent size distribution.

The other important parameter that determines the stability of nanoparticles is zeta potential which is defined as the measure of the magnitude of the electrostatic or charge repulsion or attraction between particles. Its measurement gives detailed information about the causes of dispersion, aggregation or flocculation, and can be used to improve the formulation of dispersions, emulsions and suspensions. When charged surfaces are put in aqueous solution an electric double layer forms at the particle-liquid interface. The electric double layer consists of two parts: an immobile layer of adversely charged ions where in this Stern layer the ions are bound tightly to the surface. Secondly, there is an outer layer, which is a diffuse layer where a

balance of electrostatic forces and random thermal motion determines the ion distribution. The potential in this region, therefore, decays with increasing distance from the surface until, at sufficient distance, it reaches the bulk solution value, conventionally agreed to be zero as illustrated in figure 4.6. The magnitude of the zeta potential gives an idea about colloidal stability of the suspension. If all the particles have a large value of positive or negative surface charge, then they will tend to repel each other and there will be no tendency for the particles to come together and form aggregates. In reverse case, if they have a low zeta potential then there will be no force to prevent the particles flocculating. The main factors that affect the zeta potential of a particle can be stated as pH of the solution, conductivity and concentration of a formulation component (See Figure 4.8).

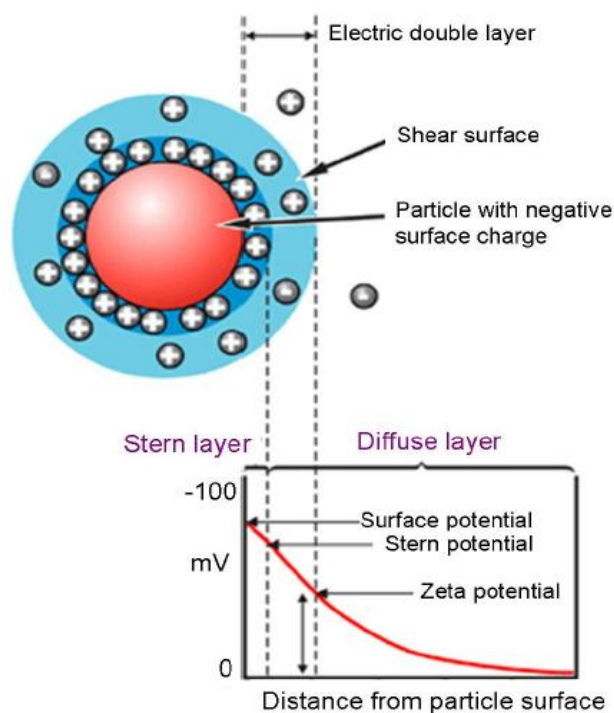


Figure 4.8 : Schematic illustration of zeta potential [Url-6].

The measurement of the zeta potential was performed on a Zetasizer. This apparatus calculates the zeta potential by determining the electrophoretic mobility (μ) of the polyplex. The latter is obtained by measuring the velocity of particles using Laser Doppler Velocimetry (LDV). The velocity and electrophoretic mobility are related by the following equation (4.3) :

$$\mu = \frac{v}{E} \cdot \frac{m \cdot sec^{-1}}{V \cdot m^{-1}} \quad (4.3)$$

By applying the Henry equation the zeta potential can be calculated from the following formula (4.4) :

$$\mu = \frac{\varepsilon \cdot \zeta \cdot f(ka)}{6 \cdot \eta} \quad (4.4)$$

where;

μ = the electrophoretic mobility in m²/Vs

ζ = the zeta potential in V

ε = the dielectric constant in F/m

η = the viscosity of the medium in cP

$f(ka)$ = Henry's function

In this project, a Nano-ZS (Malvern Instruments, Hoeilaart, Belgium) is used for DLS measurements. This instrument consists of the following main components (See Figure 4.9) : a laser beam (1) illuminates the sample contained in a cell (2). To prevent that the detector becomes saturated or that an insufficient amount of light reaches the detector, a variable attenuator (4) is placed between the laser and the sample, allowing to reduce or increase the intensity of the laser source and hence the intensity of scattering. The laser beam is scattered by the particle within the sample at all angles and a detector (3) measures the scattered light. In the Nano-ZS model, the detector is positioned at 173°. The signal from the detector is then passed to a correlator (5) that compares the scattering intensity at successive time intervals to derive the rate at which the intensity is varying. The information obtained by this digital processing board is then passed to a computer, equipped with Nano software to analyze the data and derive size information.

4.4.1.2 Particle size and surface charge measurements

All DLS measurements were performed in triplicate on a Nano-ZS (Malvern Instruments, Hoeilaart, Belgium), equipped with an Argon laser beam (488 nm) at a scattering angle of 173° and a temperature of 25°C. The preparation of polyplexes occurs as described in the following section.

4.4.2 Preparation of polyplexes

Polymer/DNA complexes were obtained by mixing the cationic polymer solution and anionic pDNA as illustrated in Figure 4.10.

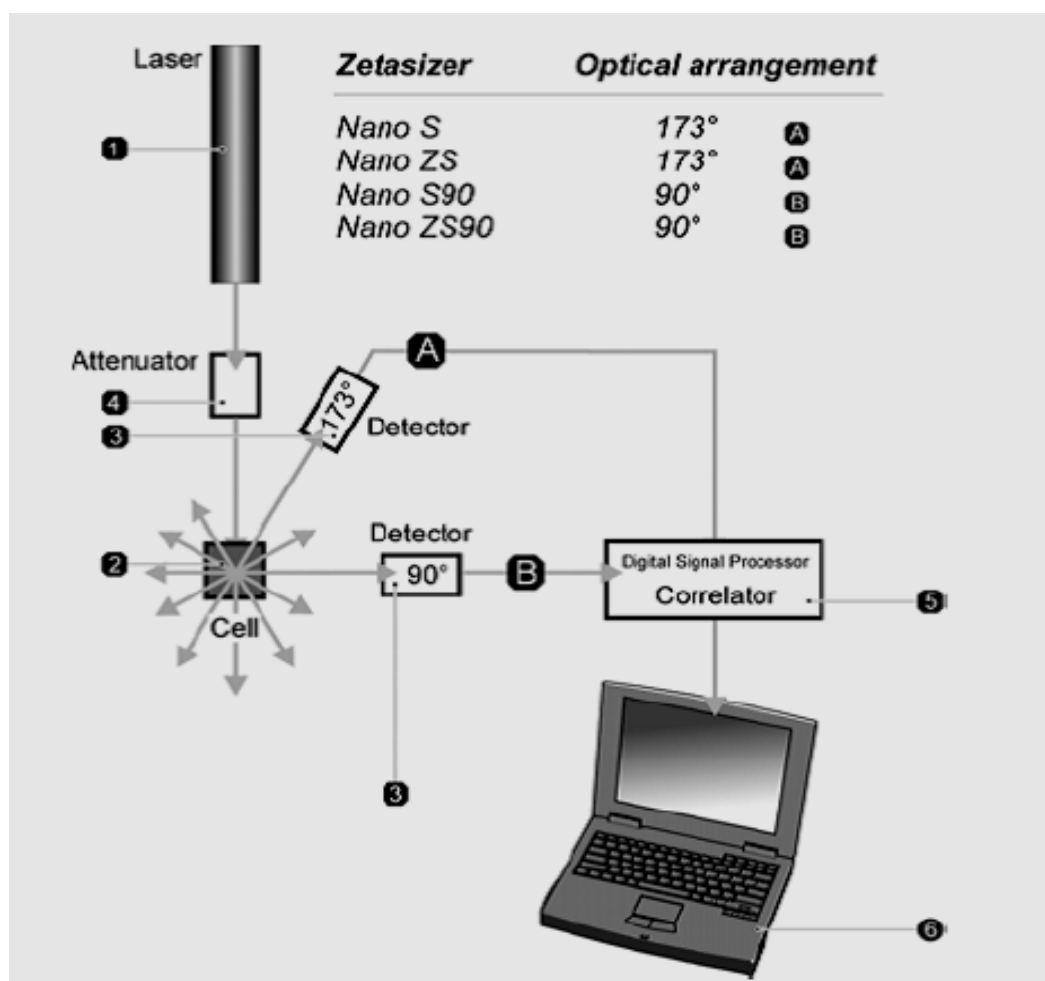


Figure 4.9 : Main components and optical configurations of a Nano Zeta-sizer instrument for DLS measurements [Url-7].

The formation of polyplexes are spontaneous and depends on electrostatic interaction between polymer and pDNA. All the polyplexes in this study were prepared in a filtered (0.2 μm mesh size), 25 mM, pH 7.2 HEPES buffer solution under dust-free laminar air flow conditions.

4.4.2.1 pDMAEMA polyplexes

pDMAEMA polyplexes were prepared with two different polymer Mw 50 kDa and 600 kDa, and in two different polymer/pDNA mass ratios of 1.5/1 and 12/1. As plasmid DNA, pGL4.13 plasmid is used for all DLS measurements in this thesis. The DLS samples with different polymer/pDNA mass ratios were prepared with changing amounts of polymer but the same amount of plasmid (10 μL). The polymer stock solution (5 mg/mL) was diluted in HEPES buffer solution to have a concentration of 0.6 mg/mL. The pDNA stock solution (1mg/mL) was also diluted until a concentration of 0.05 mg/mL. Then the formation of polyplexes were achieved

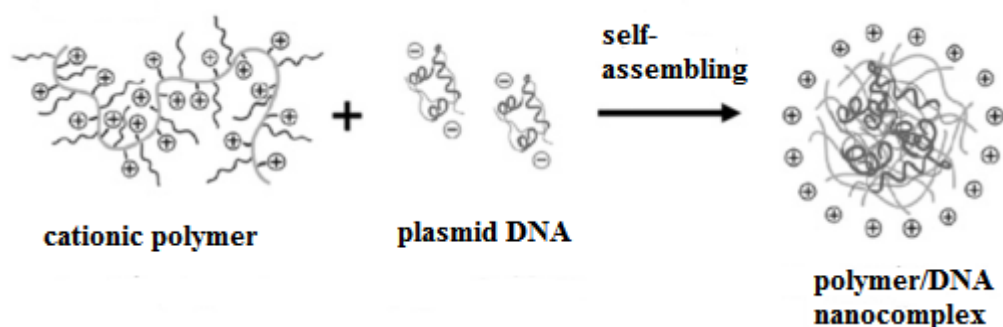


Figure 4.10 : Formation of polymer/DNA nanocomplex (polyplex) by self-assembly, adapted from (Coue and Engbersen, 2011).

by mixing the appropriate amount of polymer with pDNA solution which corresponds to 10 μg of plasmid. The amount of polymer for each ratio was calculated as follows :

(1.5/1) Polyplex preparation :

$$M1.V1 = M2.V2$$

8.33x dilution of polymer stock (100 μL polymer + 733 μL HEPES)

$$\rightarrow 5 \text{ mg/mL} \times 100 \mu\text{L} = M2 \times 833 \mu\text{L}$$

$$M2 = 0,6 \text{ mg/mL}$$

20x dilution of pDNA stock (10 μL pDNA + 190 μL HEPES)

$$\rightarrow 1 \text{ mg/mL} \times 10 \mu\text{L} = M3 \times 200 \mu\text{L}$$

$$M3 = 0,05 \text{ mg/mL}$$

Add 25 μL of 0,6 mg/mL polymer to 200 μL of 0,05 mg/mL pDNA then dilute to 1ml with 775 μL HEPES.

1.5/1 polyplex contains:

$$[(5\mu\text{g}/\mu\text{L} \times 100 \mu\text{L}) \times 25/833] = 15 \mu\text{g} \text{ of polymer}$$

$$(1\mu\text{g}/\mu\text{L} \times 10 \mu\text{L}) = 10 \mu\text{g} \text{ of pDNA}$$

$$(w/w) \text{ ratio} \rightarrow 15 \mu\text{g} / 10 \mu\text{g} = 1.5/1$$

When the polyplexes were formed after 20 minutes, first of all the particle size and polydispersity index (pDI) of the samples were measured in low volume polystyrene (PS) cuvettes to avoid any electrical effect that may disturb the polyplex formation. Subsequently, ζ -potential measurements were performed in clear disposable zeta cells.

Additionally, prior to the *in vitro* evaluation studies which are performed in OptiMEM™ GibcoBRL (Merelbeke, Belgium) serum free transfection medium, the

particle size and pDI measurements were also applied for the polyplexes in OptiMEM, representative for the stability in physiological media. For this purpose, polyplexes were prepared in the previous way but after the polyplex formation in HEPES, polyplexes were diluted 2 times in OptiMEM. Since OptiMEM media is rich in different types of proteins and dissolved ions, charge measurements were not carried out in OptiMEM media.

4.4.2.2 SS-PAA polyplexes

The polyplexes with p(CBA-ABOL), p(CBA-ABOL/DMEDA/PEG) and p(CBA-HIS) polymers were prepared in the same way as the pDMAEMA polyplexes were done. The amounts of polymers and pDNA that are calculated for polyplex formation are shown as a model for 48/1 ratio below :

48/1 (polymer/pDNA) polyplex preparation :

$$M1.V1 = M2.V2$$

8.33x dilution of 5 mg/mL polymer stock (100 μ L polymer + 733 μ L HEPES)

$$\rightarrow 5 \text{ mg/mL} \times 100 \text{ } \mu\text{L} = M2 \times 833 \text{ } \mu\text{L}$$

$$M2 = 0.6 \text{ mg/mL}$$

20x dilution of 1 mg/mL pDNA stock (10 μ L pDNA + 190 μ L HEPES)

$$\rightarrow 1 \text{ mg/mL} \times 10 \text{ } \mu\text{L} = M3 \times 200 \text{ } \mu\text{L}$$

$$M3 = 0.05 \text{ mg/mL}$$

Add 800 μ L of 0,6 mg/mL polymer to 200 μ L of 0,05 mg/mL pDNA.

48/1 polyplex contains:

$$[(5 \mu\text{g}/\mu\text{L} \times 100 \text{ } \mu\text{L}) \times 800/833] = 480 \text{ } \mu\text{g of polymer}$$

$$(1 \mu\text{g}/\mu\text{L} \times 10 \text{ } \mu\text{L}) = 10 \text{ } \mu\text{g of pDNA}$$

(w/w) ratio $\rightarrow 480 \text{ } \mu\text{g} / 10 \text{ } \mu\text{g} = 48/1$

For HA-coated p(CBA-ABOL) polyplexes, research grade HA with a known Mw range of 20-40 kDa was purchased from Lifecore Biomedical (MN, U.S.A). The chosen optimum polymer/pDNA ratio 48/1 was applied for the preparation of polyplexes. Polyplexes with 48/1 ratio were prepared as previously explained. When the polyplexes were formed, HA-coating was performed on 200 μ L pplx (corresponding to 2 μ g pDNA), with varying amounts of HA for the same amount of pDNA. Afterwards, the polyplex-HA mixture was vortexed for 10 seconds and allowed to stabilize for 15 minutes. Particle size and polydispersity of HA-coated

polyplexes were measured both in HEPES and OptiMEM™ media. As is mentioned before, the ζ - potential is only measured for the complexes in HEPES.

For 25.5/1 (HA/pDNA) ratio :

12,4 μ L of 5 mg/mL stock HA solution is diluted to 800 μ L with HEPES

$$5 \text{ mg/mL} \times 12.4 \text{ } \mu\text{L} = 62 \text{ } \mu\text{g HA}$$

Mw HA = 402 g/mol

Mw pDNA = 330 μ g/ μ mol

Molar ratio (HA/pDNA) $\rightarrow (62 \text{ } \mu\text{g} / 402 \text{ } \mu\text{g}/\mu\text{mol}) / (2 \text{ } \mu\text{g} / 330 \text{ } \mu\text{g}/\mu\text{mol}) = 25.5/1$

4.4.3 Agarose gel electrophoresis

4.4.3.1 Principles

Gel electrophoresis is a technique in which a gel matrix and an electric field are used to separate molecules based on their size and surface charge. DNA molecules will migrate to the positively charged electrode when forced over a gel by an electric current due to the negative charge on their phosphate backbone. Larger molecules will migrate more slowly because they move less easily through the gel network. After the separation is completed, the DNA fragments can be visualized with ethidium bromide, a fluorescent dye that intercalates between the heterocyclic bases in DNA helices. This intercalation strongly intensifies the signal obtained when the gel is exposed to UV light. Thus, different DNA fragments in the sample can be distinguished and their size can be determined by adding a DNA ladder (a sample containing different DNA molecules of known size) on the gel in parallel with the unknown sample.

In this study, agarose gel electrophoresis was used as a tool in determining the pDNA condensation ability of polymers and optimal polymer/pDNA ratio for polyplex formation. It allows to detect if there is still uncomplexed DNA present in the samples after complexation. If so, a migration band located toward the positive electrode will clearly be visible after electrophoresis. Usually, free pDNA is added to the gel to confirm the band in the polyplex well indeed corresponds to free pDNA. As this is unwanted, this indicates that a higher polymer ratio is needed to form stable polyplexes.

4.4.3.2 Experimental part

To visualize the pDNA complexation ability of polymer, polyplexes were applied on agarose gel electrophoresis.

For the preparation of TBE Electrophoresis buffer; 10.8 g/L Tris-base (Sigma, Bornem, Belgium), 2.5 g/L Boric acid (Merck, Brussels, Belgium) and 0.58 g/L EDTA (Titriplex®; Merck, Brussels, Belgium) were dissolved in double distilled water.

A 1% agarose gel was prepared using electrophoresis grade agarose powder (Invitrogen, Merelbeke, Belgium) and 10x TBE electrophoresis buffer (10 mL buffer in 100 mL water). The powder was dissolved by heating the suspension to 90°C in microwave. When the agarose was completely dissolved, the solution was cooled down till approximately 50°C, then solution was poured into a gel casting tray containing a sample comb and was allowed to solidify at room temperature. The solution is left to solidify gently at room temperature, to prevent clumping inside the agarose network.

In the meantime, the complexes were prepared with the appropriate ratios as explained in section 4.2.2. Then 20 µL samples (including 0.2 µg pDNA) were taken from each polyplex solution. The samples were mixed with 5µL loading buffer (50% sucrose solution in TBE) containing bromophenol blue as colorant. The loading buffer makes the samples more dense to remain at the bottom of the gel lane and bromophenol blue present in the loading buffer helps to visualize the migration of the complexes.

When the gel was formed, the polyplex samples were loaded into gel, and subjected to electric field at 100 V for 40 minutes in 1x TBE buffer. 1 kbp DNA ladder (BIORON) was added as a Mw marker and pure pGL4.13 plasmid as a reference were applied into gel. Heparin, as a molecule with the highest known anionic charge density was used as a control for DNA displacement. After that, the gel was stained by incubation on ethidium bromide (EtBr) bath for ±1 hour. Subsequently, the gel was observed by UV-illumination. At last, the photograph of the gel was recorded by a camera and processed by the software (Kodak Digital Sience).

4.5 *In vitro* Biological Evaluation of Polyplexes

The major goal of gene therapy is the introduction of a vector carrying the gene of interest into cells and to allow these cells to express that specific gene. Besides, during this transfer process, the carrier should not harm the exposed cells. In this study, after the polymer/pDNA complexes were investigated for their stability and DNA condensation ability, it is aimed to evaluate the synthesized polymers by means of their cellular uptake and gene expression efficiencies as well as the viability response of the ARPE-19 cells to the introduction of cationic vectors synthesized in this thesis.

4.5.1 Flow Cytometry

4.5.1.1 Principles

Flow cytometry is a technique that is capable of performing simultaneous measurements such as counting, examining and analyzing cells in a flowing suspension depending on the certain chemical and physical properties of cells. With a flow cytometer, a cell suspension is analyzed cell per cell using a capillary tube through which the cell suspension passes along a laser beam that is perpendicular to the capillary tube (See Figure 4.11). The instrument can measure up to 3000 cells passing in the capillary tube per second. The laser light is scattered in the forward (forward scatter, FS) and sideward scatter (SS) direction, and by using a combination of dichroic mirrors and filters, fluorescence emission light is sent to individual detectors and in different spectral channels. The detectors convert the optical signal to an electrical signal. The scatter signal is used to derive information on cell size and granularity, while fluorescence is used to obtain additional information, such as uptake and transfection efficiency of the non-viral particles which are being evaluated.

The equipment contains 3 subsystems: fluidics, optics and detectors. In the fluidics-subsystem, a stream of cells is introduced into the flow and prepared for single cell measurement. This is done by hydrodynamic focusing: pressure causes the sheath buffer to be driven through a flow cell. The sample stream, entering the system between two sheath buffer streams, is compressed by these surrounding streams,

which causes the arrangement of the cells in the sample like pearls on a string. This way, the cells are passed through the flow cell one at a time.

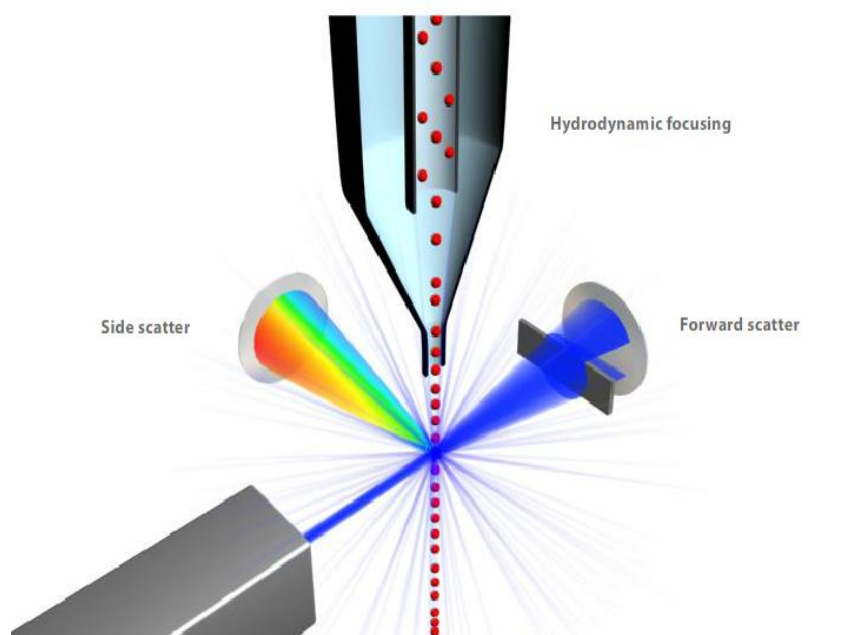


Figure 4.11 : The scattering of laser in flow cytometer [Url-8].

4.5.2 Uptake and transfection efficiency studies

For uptake and transfection efficiency studies cells were seeded as follows: after the trypsinization of the ARPE-19 cells, the cells were counted with Burker Counting Chamber and diluted to a concentration of 10×10^4 cells per mL. Then cells were seeded into 12-well plates with a confluence of 10×10^4 cells per well ($2,5 \times 10^4$ cells per cm^2 , 1 mL of diluted cell suspension). Next, they were allowed to attach on the plate overnight. The day after, CCM was removed from the wells and freshly prepared polymer/pDNA complexes in OptiMEM were added to the cells, with a pDNA concentration of 2 μg per well (for polyplex preparation see section 4.4). During the uptake experiments, YOYO-1 labelled pGL4.13 plasmids were used for the preparation of the polyplexes. One set of the cells with the same polyplexes were put at 4°C as it is known that 4°C almost completely inhibits cellular uptake. After 2 h incubation, the extracellular fluorescence of the cells, caused by the fluorescent polyplexes attached to the cell surface but not taken up, was quenched with trypan blue (0,20%) for 5 minutes at RT after which the cells were washed with PBS. Subsequently, they were detached by trypsinization. When they were loosened enough, cell pellets were collected by centrifugation for 7 min at 300g. Prior to the

measurements, the cells were resuspended in flow buffer (PBS with 0,1% azide, 1% BSA).

For transfection experiments, the gWizTM-GFP plasmid was used which expresses the green fluorescent protein (GFP) and enables the quantification of a green fluorescent signal in ARPE-19 cells. Non-treated cells and the cells which were transfected with non-fluorescent pGL4.13 plasmid were negative controls for transfection experiments. 2 hours after the addition of polyplexes, the complexes were removed and cells were incubated 22 h more in full CCM. After 22 h, the cells were washed, trypsinized and centrifuged. Appropriate gating was applied by means of the scatterplot of untreated cells to select for intact cells. Then the cells were resuspended in flow buffer and the average GFP expression of the total gated population of cells and the amount of GFP-positive cells in the same gate were subsequently measured by FACS Calibur flow cytometer (Beckton Dickinson, Erembodegem, Belgium). The analyses were done by using Cellquest software (Beckton Dickinson, Erembodegem, Belgium).

4.5.3 Cell viability

In order to analyze the cytotoxicity related to the application of different polymers with different Mw's and mass ratios, viability measurements were performed. Cell viability measurements determine healthy cells in a sample. This can be accomplished either by directly counting the number of living cells or by measuring an indicator related to the amount of living cells in cell populations. An increase in cell viability shows cell proliferation, while a decrease in viability may be the result of either toxic effects of the particular polymer or inappropriate culture conditions (Roche, 2003).take and transfection efficiency studies.

4.5.3.1 MTT assay

Most viability assays are based on one of two characteristic parameters, namely metabolic activity or cell membrane integrity of healthy cells. In this study, the metabolic activity was measured in cell populations by incubating the cells with a product, called MTT reagent. MTT (3-(4,5-dimethylthiazol-2-yl)-2,5-diphenyltetrazolium bromide) reagent is a yellow colored tetrazolium salt, that is reduced into a purple colored product, which is formazan, by metabolically active cells.

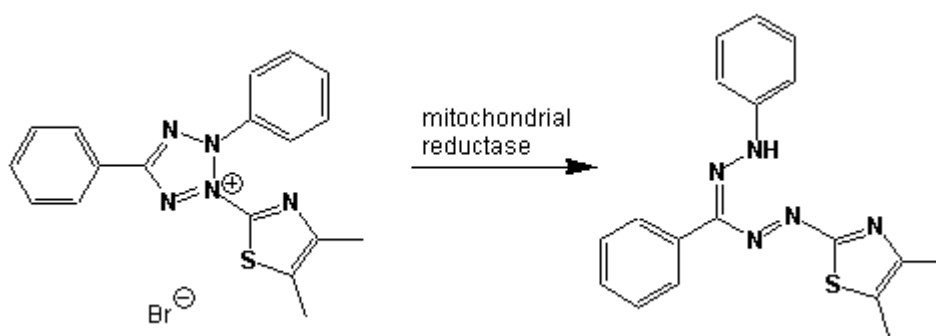


Figure 4.12 : Reduction of MTT reagent to formazan.

This colorimetric test also gives the possibility to see the color change and viability of cells visually. More dense purple color indicates more MTT reagents that is reduced to formazan which means more living cells. Finally, the analyses were quantified by measurement of the absorbance by Micro Plate Reader.

4.5.3.2 Experimental

The cells were seeded into 96-well plates with a confluence of $1,0 \times 10^4$ cells/well ($0,25 \times 10^4$ cells per cm^2) and allowed to adhere overnight. The next day, freshly prepared polyplexes, including 0,2 μg of plasmid/well, were added to the cells. The concentration of pDNA was proportional to the amount of cells, thus the same concentration was used as uptake and transfection experiments. Then, the same procedure as transfection studies was applied. 24 h after the addition of polyplexes, the old CCM was removed with fresh CCM and 10 μL MTT labeling reagent was added per well. After 4 h incubation, 100 μL ($\times 10$ of first reagent) of solubilizing reagent was added incubated overnight. As a negative control, some wells were only treated with MTT reagents. Next, the cell viability was analyzed by measuring the absorbance at 590 nm with a reference at 690 nm by a Micro Plate Reader.

5. RESULTS AND DISCUSSIONS

5.1 Polymer Synthesis

5.1.1 Characterization of polymers

5.1.1.1 pDMAEMA

Characterization of pDMAEMA polymer was performed at the end of purification and lyophilization steps. The ^1H -NMR (300 MHz) spectrum of pDMAEMA was recorded in CDCl_3 solvent after the radical polymerization with AIBN initiator. The measurement was applied relative to tetramethylsilane (TMS) at 25°C.

The absence of sharp monomer peaks at 5.5 ppm and 6 ppm (See Figure 5.1) which represent the double bonds verifies the purity of the polymer. As these peaks are not observed in the spectrum of synthesized pDMAEMA (See Figure 5.2), it can be concluded that complete conversion of DMAEMA monomer to pDMAEMA polymer took place or that unreacted monomers were removed during the purification process.

5.1.1.2 SS-PAAs

Three different types of linear, disulfide linkage containing PAA were synthesized via Michael type polyaddition of corresponding primary amine monomers to *N, N'*-cystaminebisacrylamide (CBA). The addition polymerization occurs in a stepwise process thus in order to obtain a polymer with highest theoretical Mw equal monomer ratios were used for the synthesis. Any possible toxic acrylamide end group residues that were not polymerized during the reaction were consumed by adding excess amine monomer to the reaction media in the final stage. The obtained polymers are easily soluble in water, alcohols and dimethyl sulfoxide, but not in chloroform or ether (Lin and Engbersen, 2009). The ^1H -NMR spectrum of the HCl salts of the synthesized SS-PAA in D_2O were recorded on Varian Inova spectrometer operating at 300 MHz.

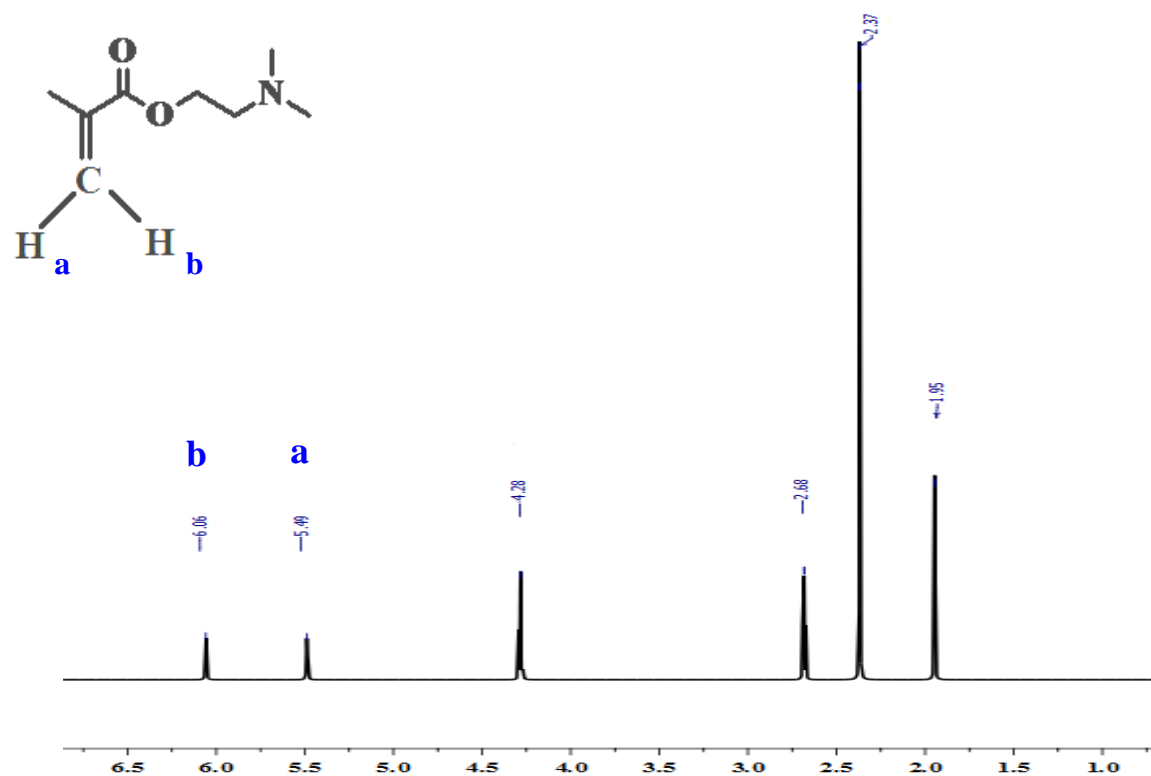


Figure 5.1 : Illustration of ^1H -NMR spectrum of DMAEMA monomer.

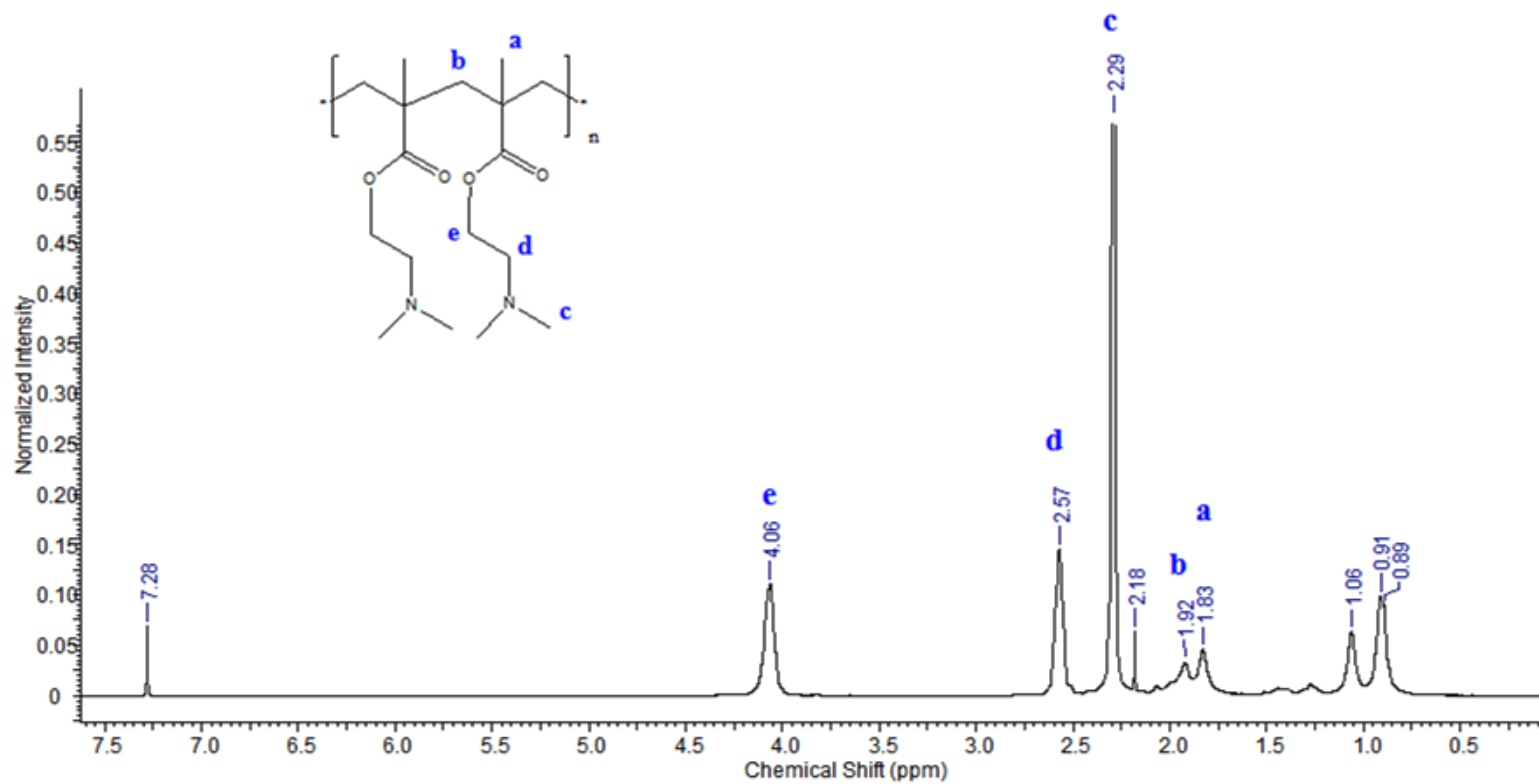


Figure 5.2 : The ^1H -NMR spectrum relative to TMS (CDCl_3 , 300 MHz and expressed in ppm) of pDMAEMA. The spectrum was recorded after radicalic polymerization of DMAEMA monomer with AIBN initiator. The corresponding H-atoms are shown on the polymer molecule structure.

As the double bond proton signals of acrylamide monomer at 5 and 7 ppm were not observed in ^1H -NMR spectra of final products, the purity of synthesized polymers was verified (See Figure 5.3 and 5.4).

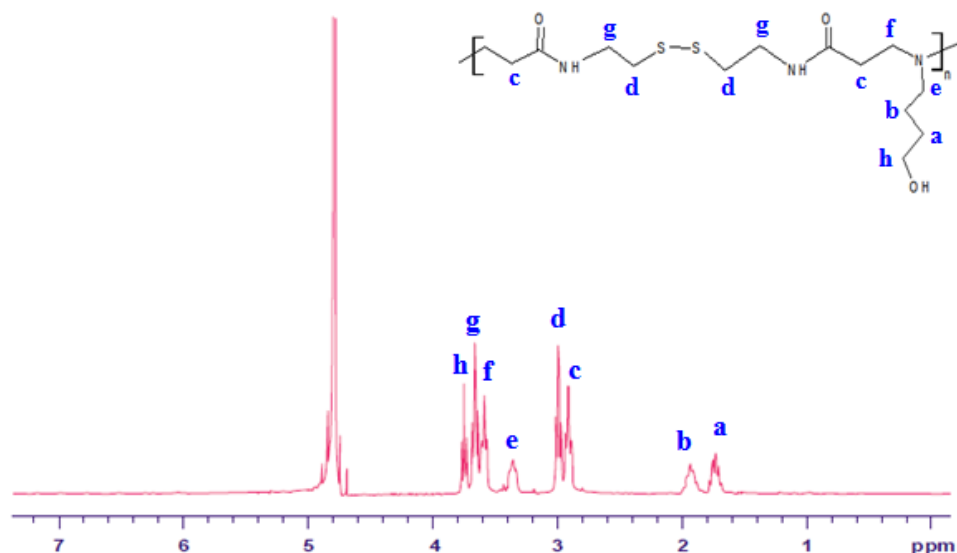


Figure 5.3 : The ^1H -NMR spectrum relative to D_2O (D_2O , 300 MHz and expressed in ppm) of p(CBA-ABOL).

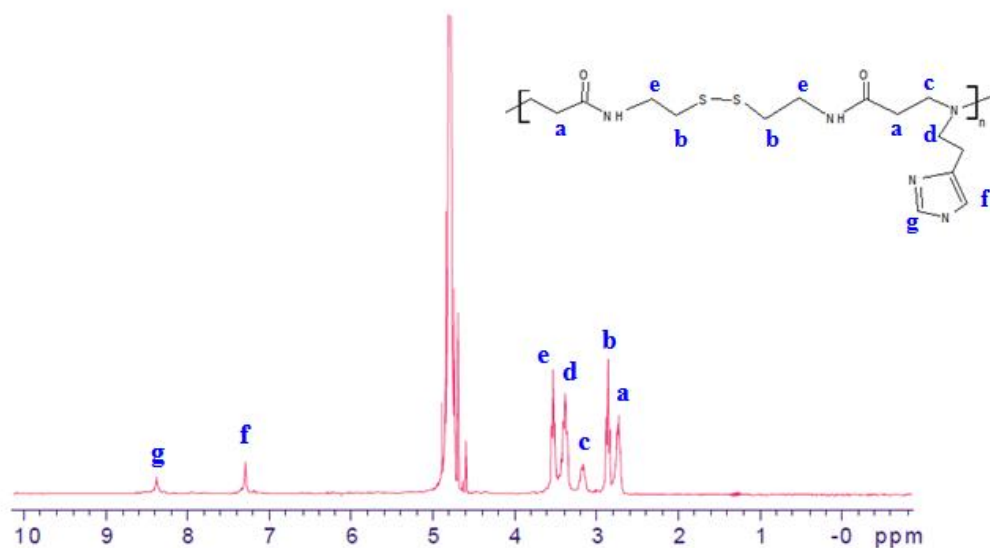


Figure 5.4: The ^1H -NMR spectrum relative to D_2O (D_2O , 300 MHz and expressed in ppm) of p(CBA-HIS).

Gel Permeation Chromatography (GPC) measurements were performed using a Waters 2695 LC system and two thermostated (30°C) PL aquagel-OH 30 columns (8

μm , $300 \times 7.5\text{mm}$, with a low-molar-mass separation range (200 ~ 40,000)) as previously described by Lin et. al. (2007a). Data were collected using a differential refractometer (Model 2414). 0.3 M NaAc aqueous solution (pH 4.4) plus methanol (70/30, v/v) was used as eluent at a flow rate of 0.5 mL/min. The GPC chromatograms (GPC) showed that the weight-average molecular weight (M_w) of p(CBA-ABOL) was 5.24 kDa and p(CBA-HIS) 7.48 kDa, with polydispersity indexes (pDI) 1.29 and 1.66, respectively (See Figure 5.5 and 5.6).

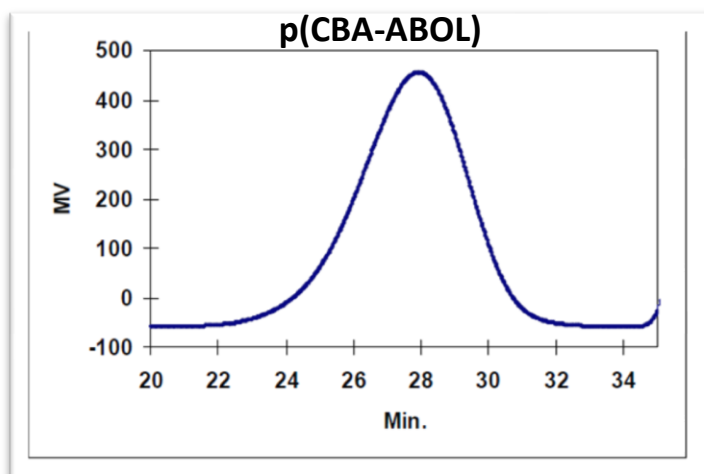


Figure 5.5: Illustration of the M_w distribution of p(CBA-ABOL) obtained by gel permeation chromatography.

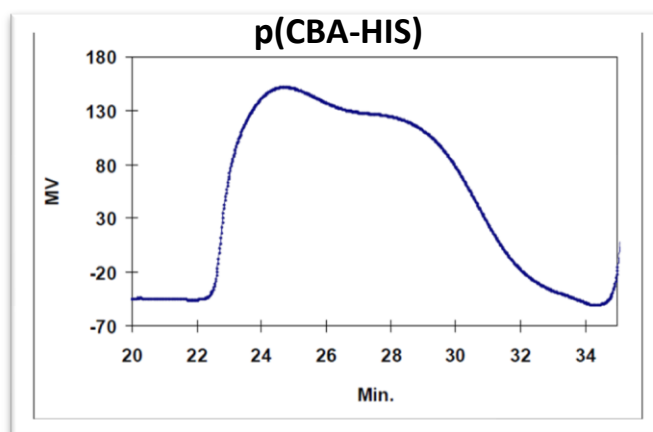


Figure 5.6: Illustration of the M_w distribution of p(CBA-HIS) obtained by gel permeation chromatography.

Additionally the buffering capacity and polymer degradation studies were previously performed by Lin et. al. (2007a). The buffer capacity of the SS-PAA polymers, defined as the percentage of amine groups that becomes protonated when pH decreases from 7.4 to 5.1 (i.e., the pH change from the extracellular environment to

the lower pH of the endosomes), was measured by acid-base titration. A known amount of polymer which was isolated as its HCl-salt form was dissolved and titrated by 0.1 M NaCl. p(CBA-ABOL) that is a polymer lacking a proton-acceptor side group shows good buffer capacity of 72% whereas, p(CBA-HIS) with imidazole side chain has a buffer capacity of 58%. These values are reported to be significantly higher than that of PEI (24%). The hydrolytic and reductive degradation profile of SS-PAAAs was analyzed by GPC in the absence and presence of reduction agent dithiothreitol (DTT, 2.5 mM), mimicking the physiological and intracellular environment, respectively. The analyses indicated that SS-PAAAs were reduced very slowly in the absence of DTT however, in the reductive environment with DTT a rapid degradation of polymers within 5 min. was reported.

5.2 pDMAEMA Polyplexes

Since naked DNA is not capable of passing the cellular membrane efficiently, a carrier system is needed for gene delivery purposes (Behr, 1993). Cationic polymers were widely investigated as safe carrier systems. As a promising candidate of cationic polymer vectors, pDMAEMA was evaluated in terms of its physicochemical characteristics and biological efficiency on ARPE-19 cells.

5.2.1 Physicochemical characterization

Stability in the extracellular environment is the first necessary condition for an efficient vector system. The size and surface charge of pDMAEMA/pDNA complexes were characterized by DLS. The influence of Mw and different polymer/pDNA (w/w) ratios on the polyplex stability was investigated this way. Moreover, agarose gel electrophoresis was applied to analyze the pDNA condensation ability of pDMAEMA.

5.2.1.1 Particle size and surface charge measurements

Prior to the *in vitro* evaluation of the pDMAEMA polymer, the complex stability characteristics such as particle size, pDI and surface charge of pDMAEMA/pDNA complexes were analyzed. The amounts of polymer and plasmid that are used to prepare the polyplexes are given in Table 5.1.

It can be seen from Table 5.2 that the average particle size of all polyplexes are in the range 100-150 nm. The increase in the Mw does not have an indicative effect on charge and pDI of the polyplexes (See Figure 5.7). However, as the polymer/pDNA ratio increases particles get smaller. It is observed that in OptiMEM, polyplexes with higher polymer/pDNA ratio are more densely condensed than the polyplexes with a lower amount of polymer.

Table 5.1 : The amounts of pDMAEMA polymer and pDNA which was used to obtained desired polymer/pDNA (w/w) ratios.

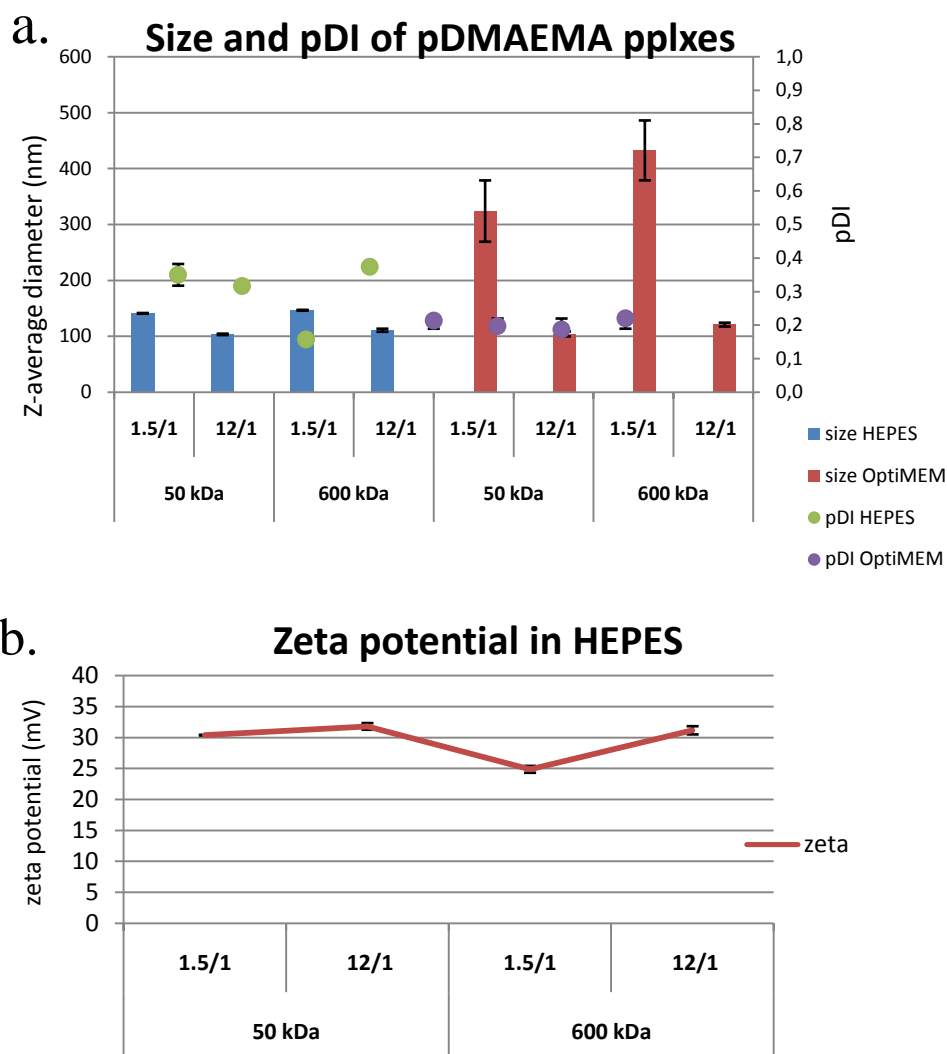
pDMAEMA	Polymer Mw	mass ratio	m _{polymer} (µg)	m _{pDNA} (µg)
	50 kDa	1.5/1	15	10
		12/1	120	10
	600 kDa	1.5/1	15	10
		12/1	120	10

Table 5.2 : Illustration of average size, pDI and charge values for pDMAEMA polyplexes.

pDMAEMA pplx		HEPES			OptiMEM	
Mw	mass ratio	size (nm)	pDI	Z-potential (mV)	size (nm)	pDI
50 kDa	1.5/1	140,9	0,35	30,4	323,9	0,21
	12/1	103,3	0,32	31,8	104,1	0,2
600 kDa	1.5/1	146,4	0,16	24,9	432,5	0,19
	12/1	110,8	0,37	31,2	120,8	0,22

5.2.1.2 pDNA complexation efficiency

The influence of both Mw and mass ratio of pDMAEMA on pDNA condensation and polyplex formation ability was analyzed by agarose gel electrophoresis, the results of which are presented in Figure 5.8. Lane number 3,4,5 and 6 indicate the different polyplexes prepared in HEPES buffer (25 mM, pH 7.2). The following four lanes, numbers 7,8,9 and 10, are loaded with the same polyplexes which are diluted in OptiMEM after polyplex formation. Finally, the last four lanes show the polyplexes prepared in HEPES buffer, to which 20 µL heparin solution (7 µg/µL) was added. The Et-Br signals are localized in the wells, indicating that all the complexes condense the pDNA efficiently. Surprisingly, pDNA displacement by heparin did not yield a similar signal as observed in lane 2, yet it was still different from the normal complexed pDNA in the former 8 lanes.



The charts give the output of DLS analyses. The results are average of 3 measurements and shown with standard deviations. For size and pDI measurements complexes were prepared both in HEPES buffer solution (25 mM, pH 7.2) and OptiMEM serum free transfection medium. Since OptiMEM media is rich in different types of proteins and dissolved ions, charge measurements were only carried out with the polyplexes that are prepared in HEPES. In Figure a., the primary y-axis shows the Z-averaged size in nm and secondary y-axis shows the corresponding pDI. The x-axis indicates the polymer type, the polymer/pDNA (w/w) ratio and Mw of the polymer used. It can be seen in figure a. only influence of polymer ratio is that a lower ratio gives rise to large particles in OptiMEM, possibly aggregates. Figure b. shows the zeta potential measurements in HEPES media, which appear more or less constant around +30 mV for all ratios and MW's.

Figure 5.7 : Illustration of a. particle size and polydispersity, b. ζ -potential of pDMAEMA polyplexes with different Mw and mass ratios.

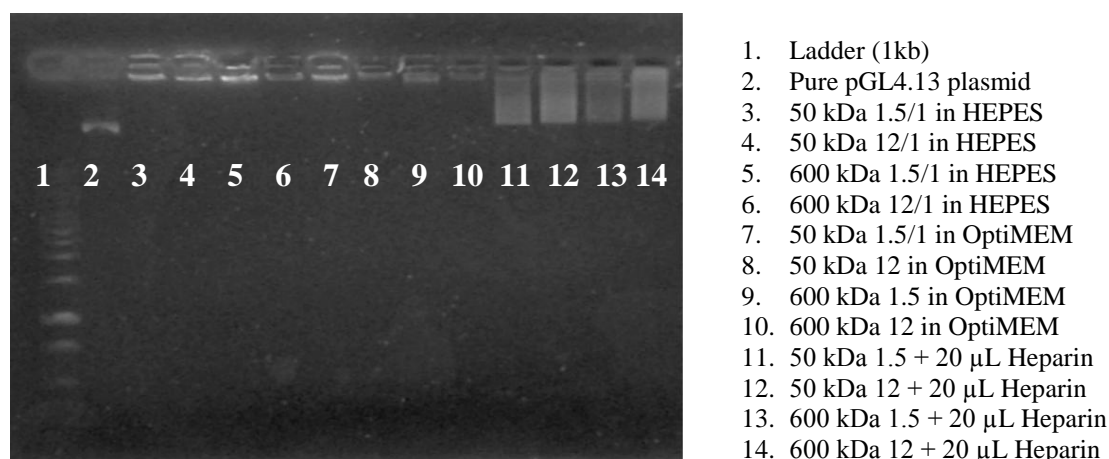


Figure 5.8 : Agarose gel electrophoresis of pDMAEMA polyplexes Mw 50 kDa and 600 kDa with different mass ratios. The lanes with the polyplexes contain 20 μ L of sample (corresponding to 200 ng of pDNA per well). As a negative control, 20 μ L of heparin (7 μ g/ μ L) was added to last 4 samples to simulate pDNA displacement.

5.2.2 *In vitro* biological evaluation

The ability of the polymer to form stable complexes and condense the pDNA efficiently is the first key for an efficient cellular uptake and transfection. Following the complex characterization measurements, *in vitro* biological evaluations of the polyplexes both with different Mw and polymer mass ratios, in terms of uptake and transfection efficiency and cell viability were investigated.

5.2.2.1 Uptake efficiency

The uptake efficiency of stable pDMAEMA/pDNA complexes was analyzed by flow cytometry. The negative control samples of both untreated cells and the cells at 4°C did not show any cellular uptake more than the autofluorescence of the cells, as expected. Because as it is known, at 4°C the metabolic activity of cells slows down as well as the uptake. Figure 5.9 shows the uptake efficiency results of pDMAEMA polyplexes based on two different Mw and mass ratios with their negative controls. It can be seen from figure that the percentage of positive cells is higher for the cells treated with 12/1 polyplexes, indicating a more efficient uptake. Moreover, the effect of Mw is clear for the complexes with 1.5/1 mass ratio. The increment in the Mw for the same polymer/pDNA ratio shows 3 times increase for the uptake efficiency.

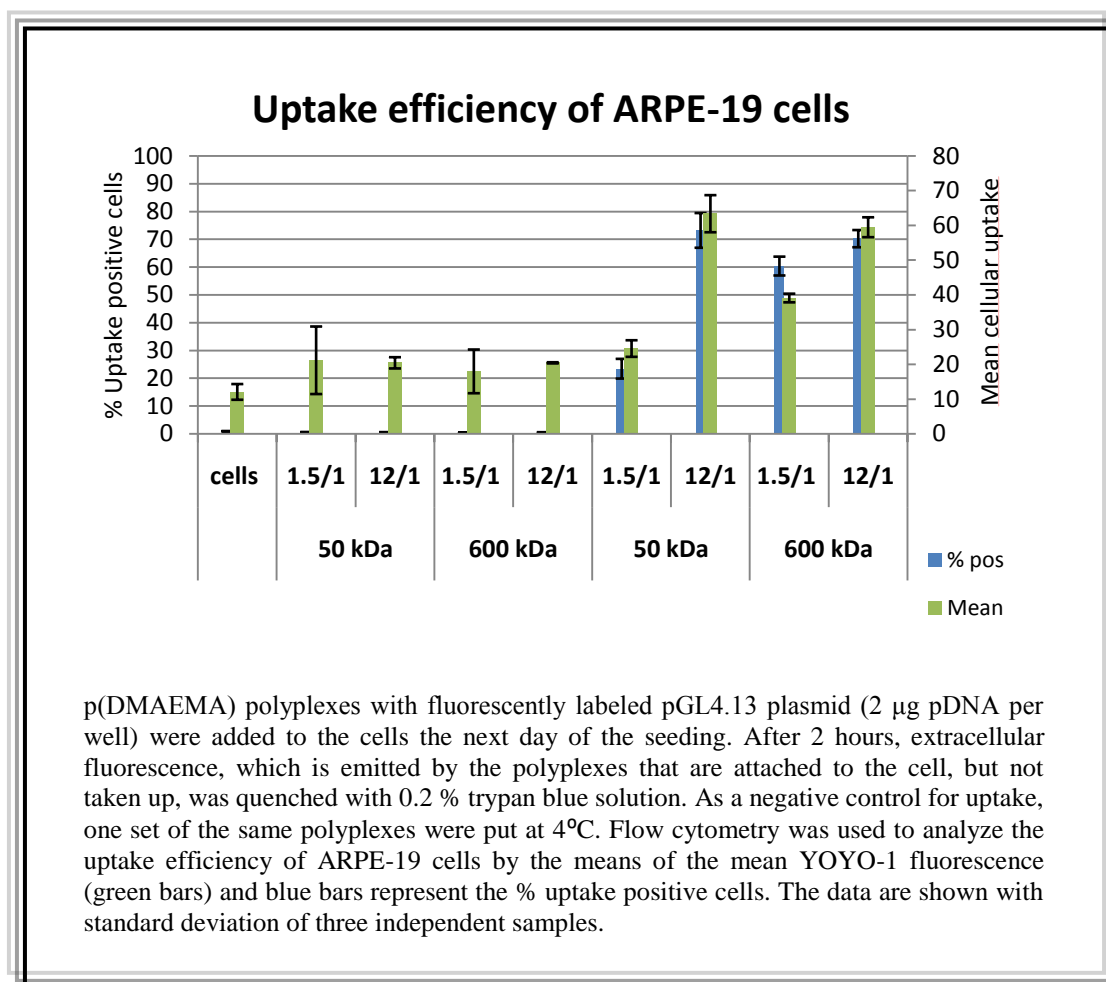


Figure 5.9 : Comparison of cellular internalization of p(DMAEMA) polyplexes with different Mw and mass ratios.

5.2.2.2 Transfection efficiency

The influence of pDMAEMA Mw and polymer mass ratio on transfection efficiency of ARPE-19 cells was determined by flow cytometry. The samples were analyzed 24 h after the addition of polyplexes. % positive GFP expression of polyplex samples and their controls is shown in Figure 5.10. Similar to uptake negative control, no transfection was observed for cells and the negative control for transfection. The positive control, LF transfected nearly 50% of the cells. The pDMAEMA complexes with lower polymer amount almost did not transfect the cells. On the other hand, the polyplexes with 12/1 ratio showed very low transfection efficiency.

5.2.2.3 Cell viability

The cytotoxic effect of pDMAEMA polyplexes on ARPE-19 cell viability was analyzed with MTT assay by means of absorbance measurement of formazan dye that comes from the reduced MTT by metabolically active cells.

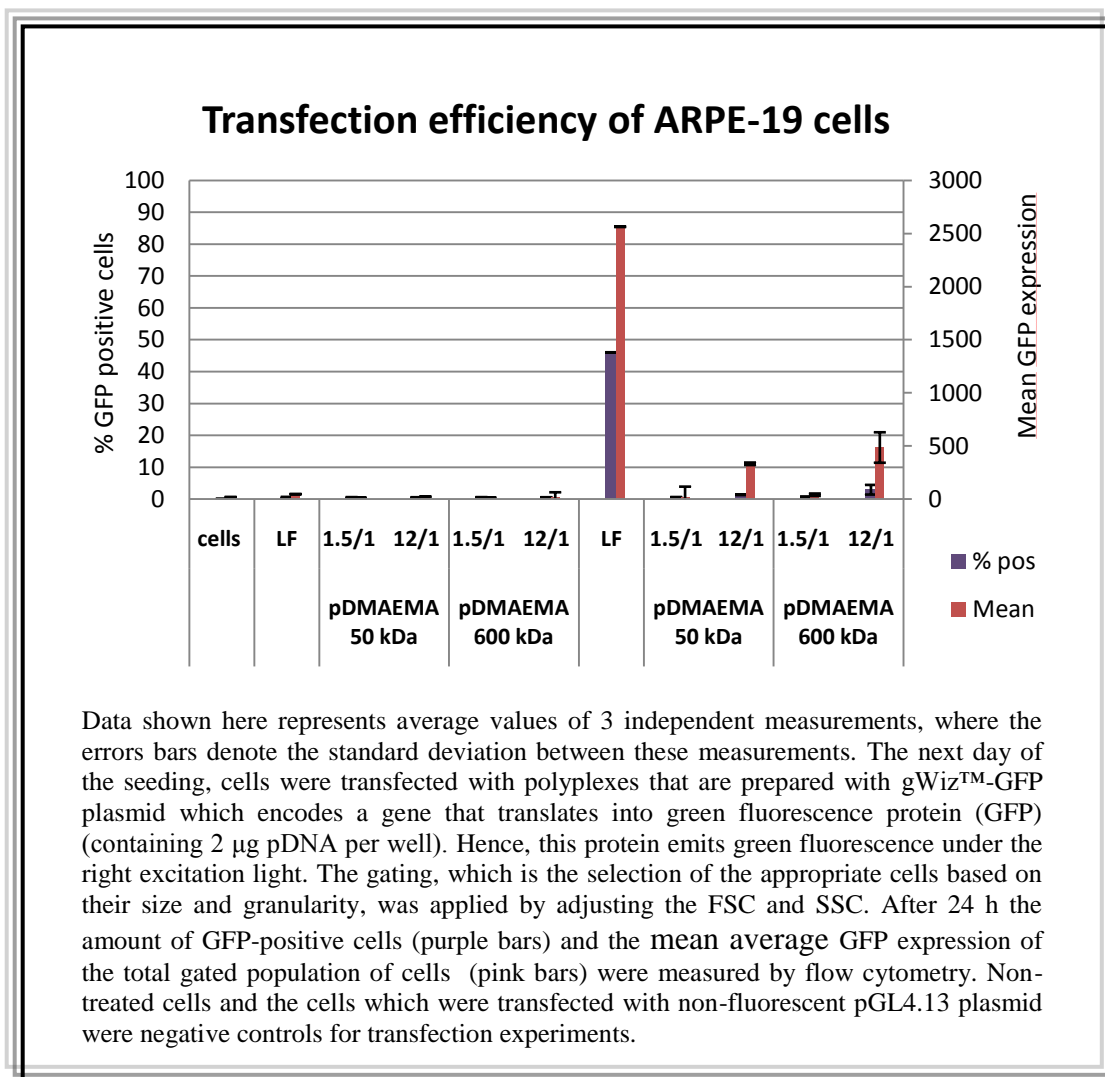


Figure 5.10 : Comparison of transfection efficiency of pDMAEMA polyplexes with different Mw and mass ratios and LF as a positive control.

In Figure 5.11, it can be seen that adding more polymer to the cells resulted in a significant decrease of metabolic cell activity, which can indicate higher cytotoxicity. The effect of polymer Mw on toxicity of polyplexes is less clear in case of 1.5/1 ratio as both Mws show relatively moderate viability of cells.

5.2.3 Discussion

In this part of the study, pDMAEMA homopolymers were synthesized and evaluated as a candidate to be a gene delivery vector. Since the stability in the extracellular environment is the primary condition for an efficient carrier, the size and surface charge of pDMAEMA/pDNA complexes were characterized by DLS in both HEPES buffer and OptiMEM, the latter being representative for physiological conditions.

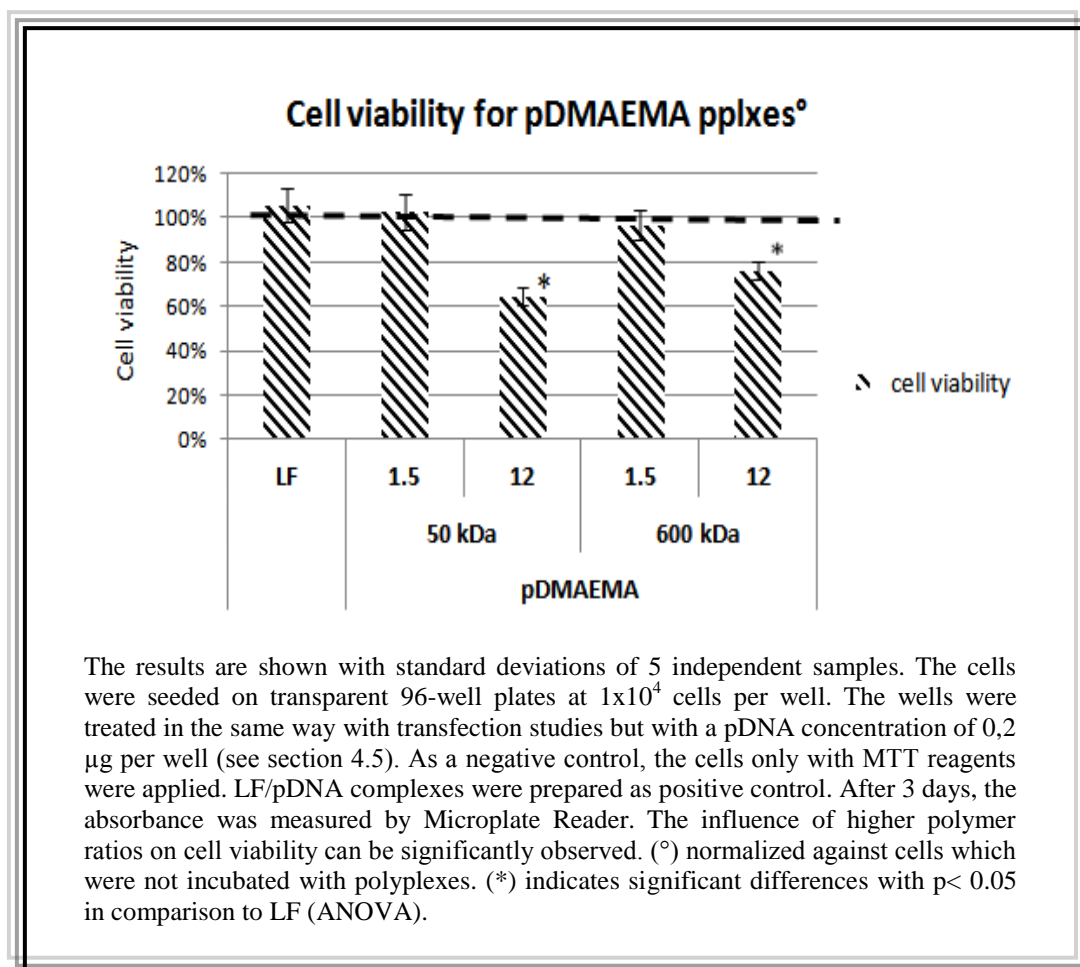


Figure 5.11 : Cell viability results of pDMAEMA polyplexes with different Mw and polymer ratios.

The difference in Mw for the same polymer/pDNA (w/w) ratios did not show a significant effect on the polyplex stability (See Figure 5.7). This was not surprising because the charge density per weight would be the same both for 50 kDa and 600 kDa polymer. Hence the amount of positive charges of polymer that will bind the negative charge of pDNA and form complexes does not change in both cases. However, the increase in polymer/pDNA ratio resulted in smaller particles that could be because more positive charges lead to stronger complexation. For the complexes with lower polymer mass ratio in OptiMEM, the interactions between proteins and polyplexes may cause an increase in particle size, resulting in more stable complexes than the ones in HEPES buffer. Secondly, agarose gel electrophoresis was applied to analyze the pDNA condensation ability of polyplexes as shown in Figure 5.8. It was reported by Arscott et al. that DNA condensation occurs when 90% of the anionic charges of pDNA is condensed by the positive charges of the polymer (1990). All the samples showed a great ability to form stable complexes and condense the pDNA

efficiently, even the 1.5/1 polyplexes with lowest polymer/pDNA mass ratio. Heparin was added to the complexes as a negative control to simulate the pDNA displacement. The effect of heparin did not displace the pDNA completely as expected, which could be due to the plasmid still being bound to smaller fractions of polymer. Nevertheless, even if the complete pDNA displacement effect of heparin cannot be observed, it should be emphasized that when it is compared with the polyplex samples that were not treated with heparin, no pDNA displacement was seen for them.

The physicochemical characteristics of pDMAEMA polyplexes were verified with the satisfying results of stable complexes and efficiency for pDNA complexation. Afterwards, the cellular processing of the pDMAEMA/pDNA complexes on ARPE-19 cells was performed. In terms of biological evaluation of pDMAEMA polymers the uptake and transfection efficiency of polyplexes were investigated by flow cytometry and then cell viability was analyzed by an MTT assay. The MTT assay measures metabolic activity by the increase of absorbance by formazan crystals that are reduced. pDMAEMA/pDNA complexes with higher Mw and higher polymer/pDNA ratio showed promising results for cellular uptake (See Figure 5.9). They were taken up by the cells with a maximum of 70%. The influence of polymer amount on pDMAEMA uptake efficiency was previously explained by van de Wetering et al. that the amount of free polymer would increase as the polymer ratio in the polyplex increases which results in higher membrane destabilization thereby facilitating the cellular uptake of polyplexes (1997). Moreover, the increment in the Mw for the same polymer/pDNA ratio showed 3 times increase for the uptake efficiency. It was also stated that higher Mw polymers form smaller particles because they can condense the pDNA more strongly. Thus polyplexes can permeate through the membrane easily and this results in relatively increased uptake and number of transfected cells (van de Wetering et al, 1997). However, the fact that this effect did not observed for cellular uptake of the polyplexes with 12/1 mass ratio with 600 kDa polymer could be explained by the maximization of uptake around 80% for pDMAEMA polyplexes.

Following the cellular entry by means of endosomal vesicles, another key is the escape from endosomes prior to the transport to the nucleus. The pDMAEMA homopolymer has tertiary amine groups which are partially protonated at

physiological pH and therefore can be further protonated at endosomal pH. As it was indicated by van de Wetering et.al, pDMAEMA shows an average pKa value of 7.5 where 50% of the amino groups in the polymer chain are protonated (1999). This answers the requirement for endosomal escape for methacrylate based polymers according to the proton sponge hypothesis (Dubruel et al, 2003). However, the transfection efficiency of pDMAEMA was very limited. The polyplexes both with the ratio of 1.5/1 and 12/1 showed almost no transfection for ARPE-19 cells. This fact was previously explained by Jones et. al. that although, pDMAEMA disrupts the endosomes when internalized by the endosomal vesicles, it does not induce the release of therapeutic material into the cytosol (2004). This could be because of the strong DNA binding ability of the polymer that does not allow the plasmid to be released once it reaches the cytosol or there may be another factor that limits the disassembly of the complexes to be released in the cytosol.

Subsequently, when the cell viability was evaluated by MTT assay, it was also observed that higher polymer ratio gave rise to higher cytotoxic effect on ARPE-19 cells *in vitro*. Since many cationic polymers, including pDMAEMA, were reported to have higher cytotoxicity (Layman et al, 2009), the investigation of an alternative delivery system with higher transfection efficiency and less cytotoxic effects was necessary.

5.3 SS-PAA Polyplexes

Cationic polymers have been attractive research materials as non-viral gene delivery vectors due to their lack of specific immune response, large scale DNA loading capacity and ease of production (Pack et al, 2005). Besides numerous types of cationic polymers which are investigated as gene carriers, poly(amidoamine)s (PAAs) are a unique family of cationic polymer therapeutics. They are reported to have a good solubility in water, be hydrolytically more stable and biodegradable (Ferruti et al, 2002). Recently, a new series of linear PAAs containing repetitive disulfide linkages in their main chain has been developed by the Engbersen Lab. (Lin et. al, 2007a). The disulfide linkage present in SS-PAAs, which are relatively stable in extracellular environment, provides bioreducibility in the intracellular media.

In this project, physicochemical and biological properties of SS-PAAAs with different polymer/pDNA (w/w) ratios, variable coating strategies and buffering capacity were evaluated.

5.3.1 p(CBA-ABOL) polyplexes

p(CBA-ABOL) is one of the examples of SS-PAAAs as a potential gene delivery vector. It was obtained by Michael type polyaddition of 4-amino-1-butanol (ABOL) to *N,N'*-cystaminebisacrylamide (CBA). The ABOL-side group provides the positive charge and buffering capacity, while the repetitive disulfide linkage present in its main chain makes the polymer bio-reducible and a good candidate for gene delivery applications.

5.3.1.1 Physicochemical characterization

Particle size and surface charge measurements

The particle size and surface charge measurements of p(CBA-ABOL) polyplexes with various polymer/pDNA mass ratios were determined by DLS, in order to have an idea about the stability range of the p(CBA-ABOL) polyplexes. The amount of polymer and pDNA which was used while preparing the complexes is illustrated on Table 5.3 and the measurement values can be found on Table 5.4. As it is shown in Figure 5.12 a, the complexes in HEPES indicates a narrow size range between 120-150 nm with a stable pDI value. Polyplexes with the ratio of 96/1 has the most positive surface charge with +45.53 mV. However, in OptiMEM media the increasing amount of polymer resulted in very large aggregates.

Table 5.3: The amounts of p(CBA-ABOL) polymer and pDNA which was used to obtain desired polymer/pDNA (w/w) ratios. The polyplexes were prepared with increasing amount of polymer while the amount of plasmid was the same for each.

mass ratio	m _{polymer} (μg)	m _{pDNA} (μg)
12/1	120	10
24/1	240	10
48/1	480	10
96/1	960	10

Table 5.4 : Illustration of size, pDI and charge values for p(CBA-ABOL) pplxes with different polymer/pDNA mass ratios.

p(CBA-ABOL)	mass ratio	HEPES			OptiMEM	
		size (nm)	pDI	Z-potential (mV)	size (nm)	pDI
	12/1	147,93	0,1	27,57	449,70	0,14
	24/1	134,27	0,11	29,83	511,00	0,20
	48/1	122,47	0,11	43,1	744,00	0,37
	96/1	132,17	0,07	45,53	1335,00	0,62

pDNA complexation efficiency

The relation between the amount polymer and DNA condensation ability while forming stable complexes were analyzed by agarose gel electrophoresis. Polyplexes which were prepared in HEPES buffer with increasing mass ratio of p(CBA-ABOL) were loaded into lanes number 3,4,5 and 6, respectively (See Figure 5.13). It can be seen from the figure that the free DNA bands become less clear above a polymer/pDNA mass ratio of 12/1. This indicates that increasing polymer ratios form complexes with increased pDNA complexation efficiency. The following four lanes, number 7,8,9 and 10, were loaded with the same polyplexes which were diluted in OptiMEM after polyplex formation in HEPES buffer. The bands of the pDNA that migrated from the polyplexes in OptiMEM become more visible which corresponds to more pDNA release.

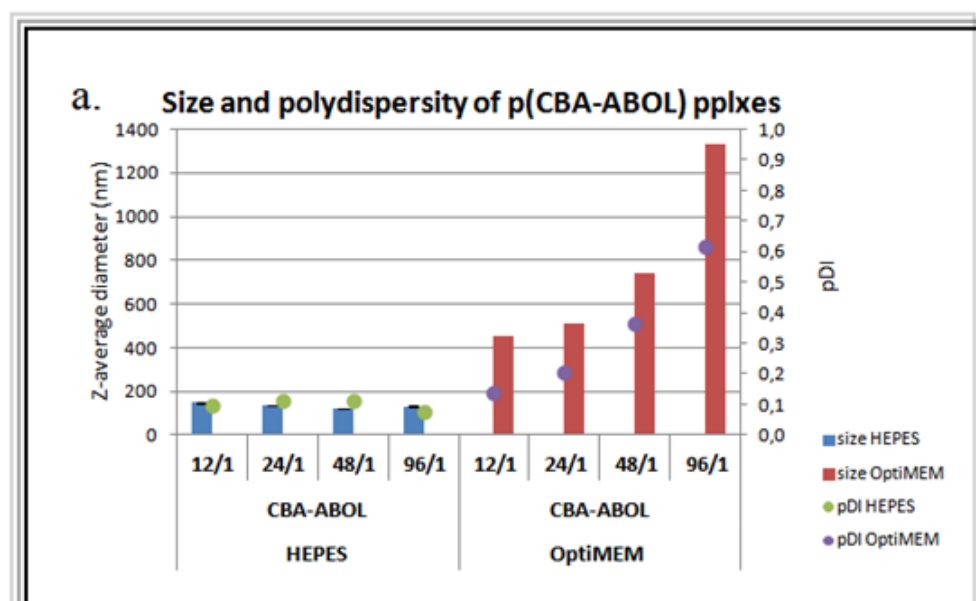


Figure 5.12 : Illustration of a. particle size and polydispersity, b. ζ -potential of p(CBA-ABOL) polyplexes with different mass ratios.

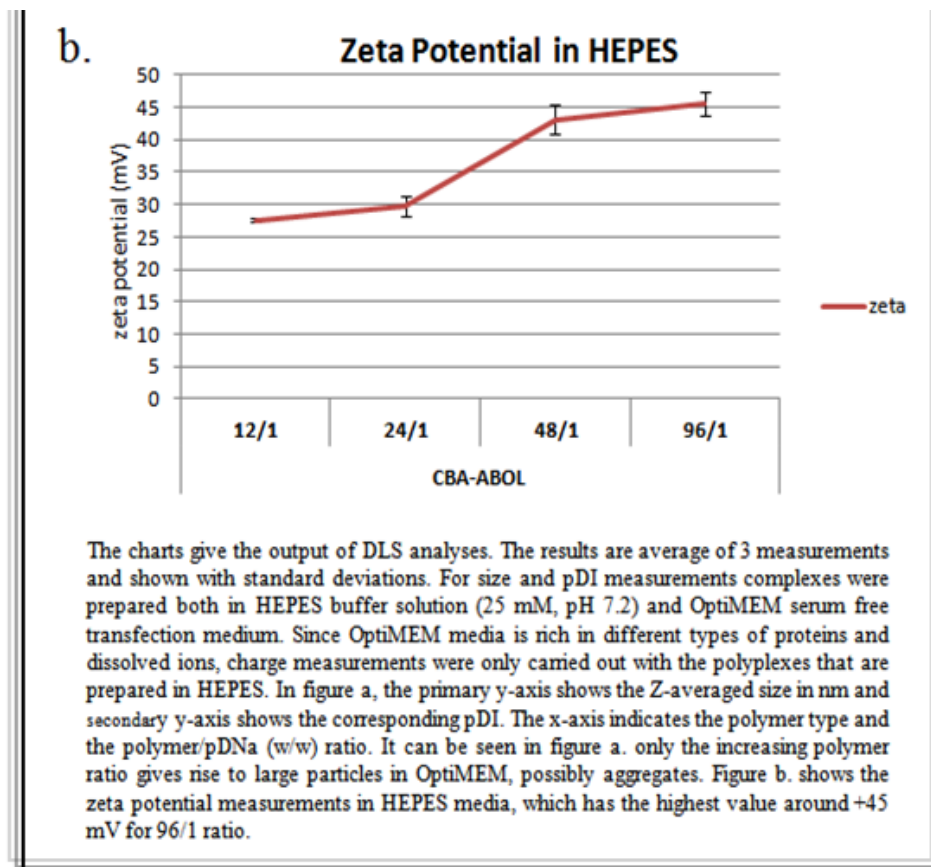


Figure 5.12 (continued) : Illustration of a. particle size and polydispersity, b. ζ -potential of p(CBA-ABOL) polyplexes with different mass ratios.

When it is compared with lane numbers 7,8,9 and 10, it can be concluded that the release in OptiMEM is not negligible but there is still some plasmid left in the wells. The pDNA binding ability of the polyplexes with 48/1 ratio supports the stable results which were obtained from DLS, as well.

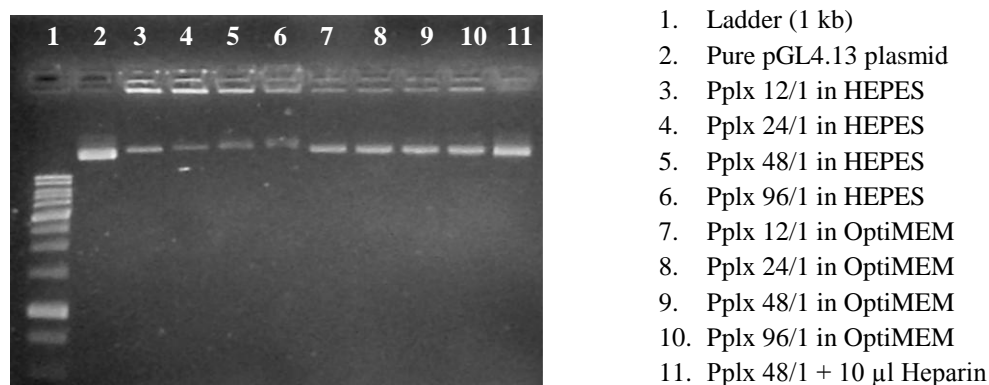


Figure 5.13 : Agarose gel electrophoresis of p(CBA-ABOL) pplxes with different mass ratios. Each sample was colored with 5 μ L loading buffer. The polyplex samples contain 0.2 μ g of pDNA. As a negative control, 10 μ L of Heparin (7 μ g/ μ L) was added to last sample.

5.3.1.2 *In vitro* biological evaluation

After the physicochemical characterization of p(CBA-ABOL) polyplexes, the effect of polymer/pDNA ratio on biological evaluation of the polyplexes in terms of uptake and transfection efficiency and cell viability was analyzed.

Uptake efficiency

In order to determine effect of mass ratio on the uptake efficiency of p(CBA-ABOL) polyplexes, ARPE-19 cells were incubated with polyplexes and analyzed by flow cytometry (Figure 5.14). It can be seen from the figure that for the samples at 37°C, an increasing amount of polymer results in a higher uptake efficiency. The uptake efficiency of 96/1 ratio reaches to 90% whereas it results in 10% for 12/1.

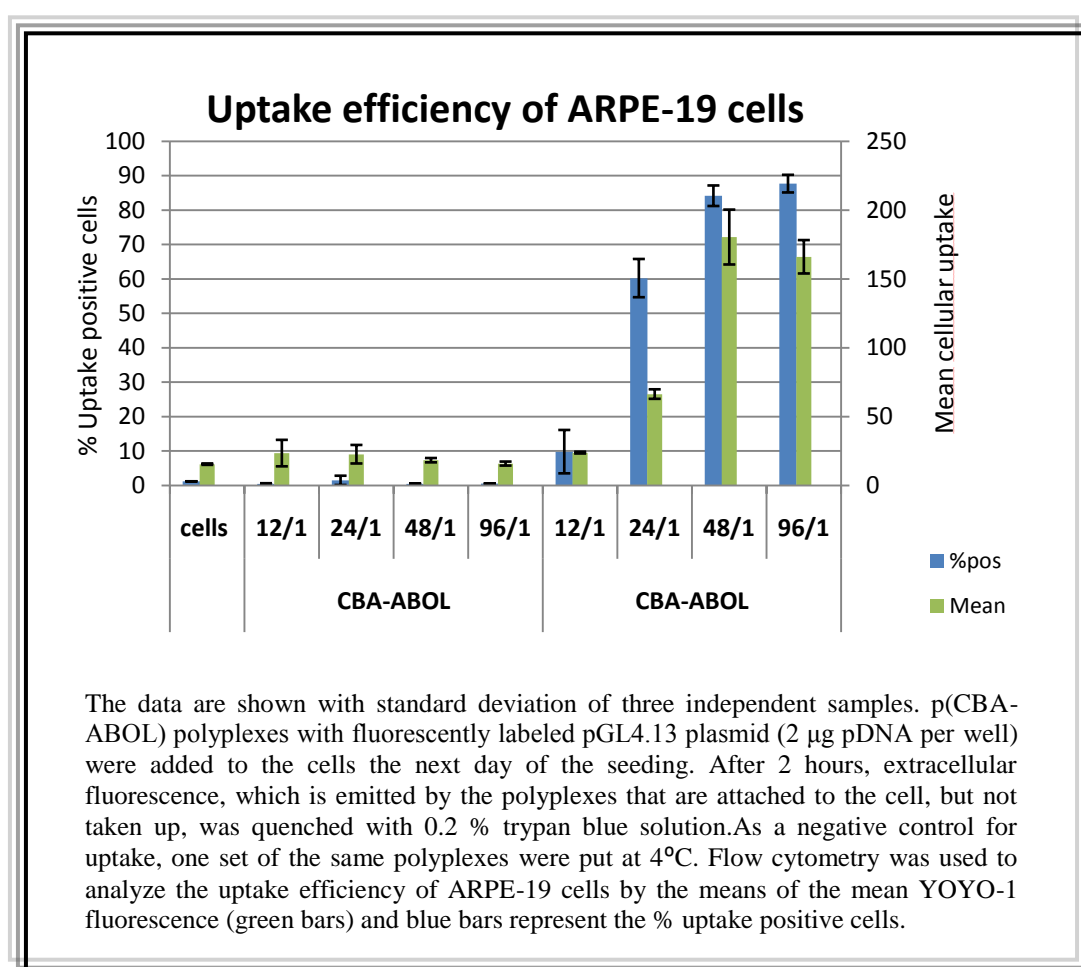


Figure 5.14 : Comparison of cellular internalization of p(CBA-ABOL) polyplexes with different mass ratios.

Transfection efficiency

p(CBA-ABOL) polyplexes with different polymer/pDNA (w/w) ratio were evaluated in terms of GFP expression on ARPE-19 cells. Figure 5.15 shows the transfection efficiencies of polyplex samples and their negative controls analyzed by flow cytometry. The negative control samples which were prepared with non-fluorescent pGL4.13 plasmid and cells showed no transfection, not more than auto-fluorescence. The polyplexes with 12/1 ratio indicate very low transfection efficiency while the complexes with higher polymer ratios show about 30% transfection efficiency. The GFP expression of 96/1 ratio reaches to 40%. Whereas, the transfection efficiency of positive control samples with LF that is commercially available and known to have good transfection, reaches to 30 %.

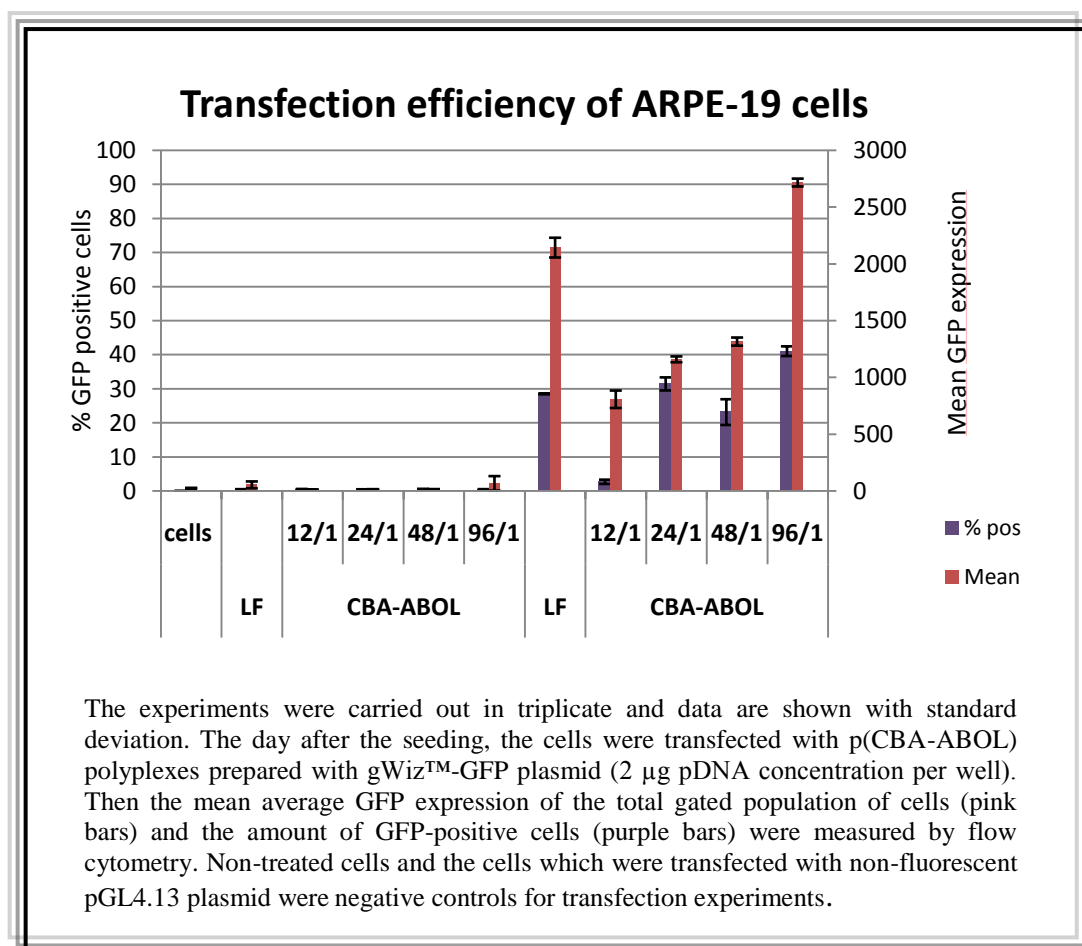


Figure 5.15 : Comparison of transfection efficiencies of p(CBA-ABOL) polyplexes with various mass ratios compared to LF.

Cell viability

The cytotoxic effects of p(CBA-ABOL) complexes with different polymer mass ratios (w/w) were analyzed by means of the MTT assay. The cells were incubated with the same polymer/pDNA ratios as was used for the transfection experiments. However, the amount of sample which was added to the cells was proportional to the cell confluence. The cell viability percentage of ARPE-19 cells which were treated with p(CBA-ABOL) complexes is shown in Figure 5.16. The 48/1 ratio was seen to have the lowest cytotoxic effect on the cells, equal to that of LF. The increase in the amount of polymer for 96/1 ratio resulted in more toxicity and less viability for ARPE-19 cells.

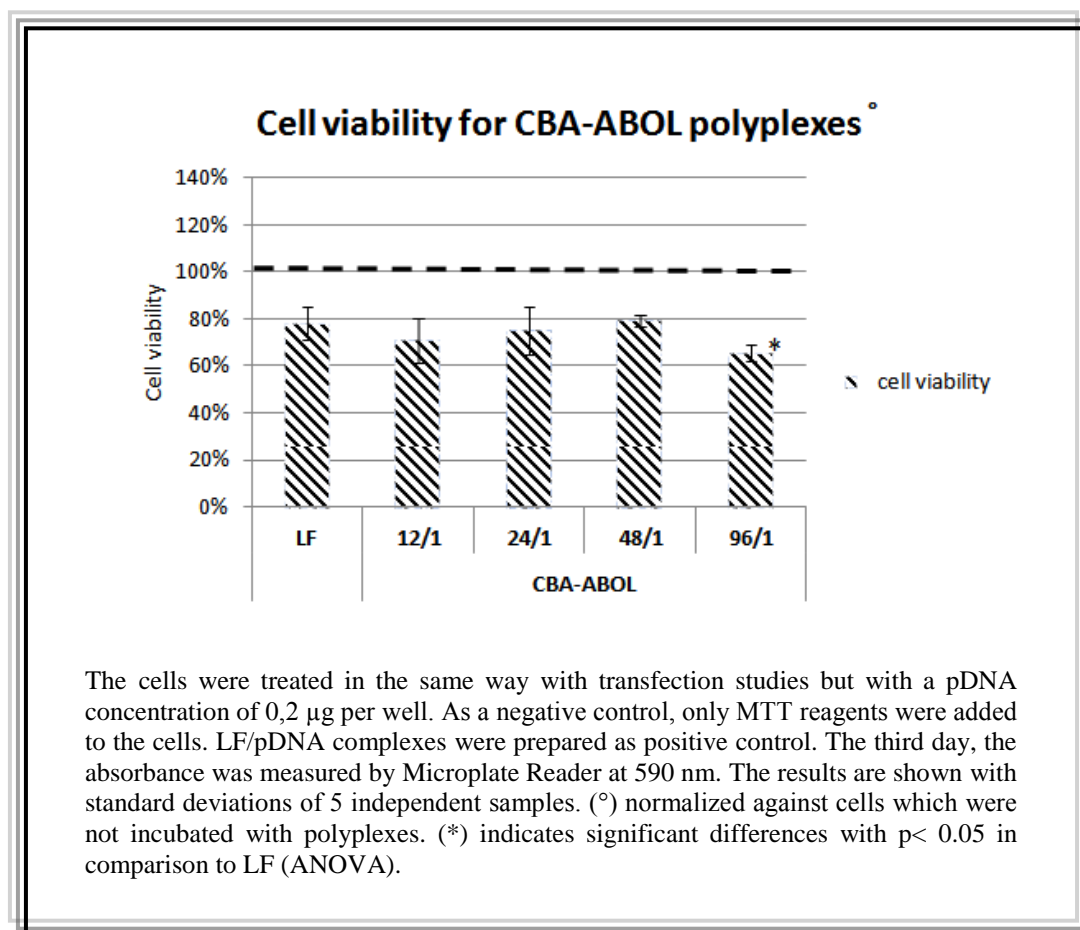


Figure 5.16 : Cell viability results of p(CBA-ABOL)/pDNA polyplexes with different mass ratios.

5.3.1.3 Discussion

In the first part of this study pDMAEMA polyplexes were evaluated as potential gene delivery vectors. Even though pDMAEMA formed stable complexes with

pDNA, it could only transfect the cells somewhat at polymer/pDNA ratios which were toxic to the cells. As SS-PAAAs were reported to be efficient p(CBA-ABOL) was chosen to be evaluated as a promising member of this family. The repetitive disulfide linkages present in the CBA monomer chain makes the polymer bio-reducible, whereas hydroxybutyl groups in the side chain originating from the ABOL unit enrich the efficiency in DNA transfection by increasing the endosomolytic properties of polyplexes (Lin et. al, 2007a).

In this section, prior to biological evaluation of p(CBA-ABOL), the polymer/pDNA complexes were physicochemically characterized. The ability of the polymer to form stable complexes with DNA and the influence of polymer/pDNA (w/w) ratios on colloidal stability of complexes were analyzed by DLS. The size, polydispersity and surface charge measurements of p(CBA-ABOL) polyplexes showed that the increase in the amount of polymer resulted in more stable and more positive complexes in HEPES buffer.. Hence, all polyplexes with 4 different mass ratios (12/1, 24/1, 48/1 and 96/1) were capable to form nanosized polyelectrolyte complexes by the means of self assembly in HEPES buffer. The same measurements were also performed in OptiMEM to simulate physiological conditions. However, due to the the interactions of proteins and various ions that are present in OptiMEM, polyplex particles caused very large aggregates as the polymer amount increases. According to agarose gel electrophoresis results, all p(CBA-ABOL) polyplexes were able to condense the pDNA but the ones with 48/1 and 96/1 polymer/pDNA ratio were more efficient in terms of DNA binding (See Figure 5.13). As the amount of polymer increases corresponding to the same amount of pDNA, when the pDNA is condensed with the cationic polymer at some point, this could be that free polymer causes the increment in surface charge and pDNA binding ability.

To further evaluate the effect of polymer/pDNA (w/w) ratio on biological efficiency of p(CBA-ABOL) polyplexes the same 4 ratios were used for uptake and transfection efficiency experiments as well as for MTT assay. The uptake efficiency results, which were determined by flow cytometry, clearly indicated that increasing amount of polymer resulted in higher percentages of cellular uptake (See Figure 5.14). When it is compared with pDMAEMA, p(CBA-ABOL) polyplexes have higher uptake that is probably due to more positive charges present in the polyplexes with higher amount of polymer. This effect could be facilitated the interactions between anionic

cell membrane HSPGs. Especially the ratios 48/1 and 96/1 were observed to be more efficient in terms of uptake. After the cellular entry via endocytosis, the escape from endosomes and the release of the pDNA from polymer are the requirements for gene expression. The p(CBA-ABOL) polyplexes showed highly efficient transfection relative to LF, which was used as a positive control, by increasing amount of polymer. If it is compared with previous carrier system pDMAEMA, we assume the effect of hydrophobic side chain such as ABOL and rapid release of pDNA following the endosomal escape by the means of disulfide cleavage in the intracellular reductive environment give rise to higher pDNA transfection and increased level of gene expression (Lin and Engbersen, 2009). Cell viability of p(CBA-ABOL) polyplexes with different mass ratios which was analyzed by MTT assay showed that p(CBA-ABOL)/pDNA complexes possess very low cytotoxicity on ARPE-19 cells relative to LF especially compared to pDMAEMA. Nevertheless, 96/1 ratio with the maximum transfection efficiency showed significantly lower viability on ARPE-19 cells.

In conclusion, p(CBA-ABOL) was determined as a good non-viral carrier. As the pDMAEMA polymer, it was able to form stable polyplexes, yet it also showed high cellular uptake and transfection efficiency results with very low cytotoxicity. As 96/1 ratio was stated to be relatively cytotoxic, 48/1 ratio polyplexes with similar physicochemical properties and biological efficiency but higher cell viability were chosen as a comparative reference for further experiments. Nevertheless, the tendency of the polyplexes to form large aggregates in physiological conditions dictate further optimizations for p(CBA-ABOL) to be a better vector.

5.3.2 p(CBA-ABOL/DMEDA/PEG) polyplexes

In order to increase the stability of gene delivery vectors in the extracellular environment, PEGylation is a universal strategy that is widely applied. This method is performed by grafting the non-ionic and hydrophilic polyethylene glycol (PEG) to the gene delivery vector. Since p(CBA-ABOL) polyplexes was promising non-viral carriers with good uptake and transfection efficiency and favorable cell viability, PEGylation was applied to increase their colloidal stability. In the following section, PEGylated particles were physicochemically and biologically evaluated.

5.3.2.1 Physicochemical characterization

Particle size and surface charge measurements

p(CBA-ABOL/DMEDA/PEG) complexes were characterized in terms of their particle size, surface charge and polydispersity by DLS. Complexes were prepared with the same amounts of polymer and pDNA of p(CBA-ABOL) polyplexes for the corresponding polymer/pDNA (w/w) ratio. It can be seen from Table 5.5 that polyplex particles in HEPES get smaller as the amount of polymer increases. On the other hand, complexes have very slight positive charge even with the highest amount of polymer for 96/1 ratio. For the measurements in OptiMEM, it is clearly observed from Figure 5.17 that polyplexes show a great stability with a size range between 120-160 nm.

Table 5.5 : Illustration of average size, pDI and charge values for PEGylated p(CBA-ABOL) polyplexes with different polymer/pDNA mass ratios.

p(CBA-ABOL/DMEDA/PEG)	mass ratio	HEPES			OptiMEM	
		size (nm)	pDI	Z-potential (mV)	size (nm)	pDI
	12/1	134,63	0,41	5,29	160,87	0,52
	48/1	114,6	0,34	8,35	121,33	0,40
	96/1	108,9	0,32	9,40	152,70	0,49

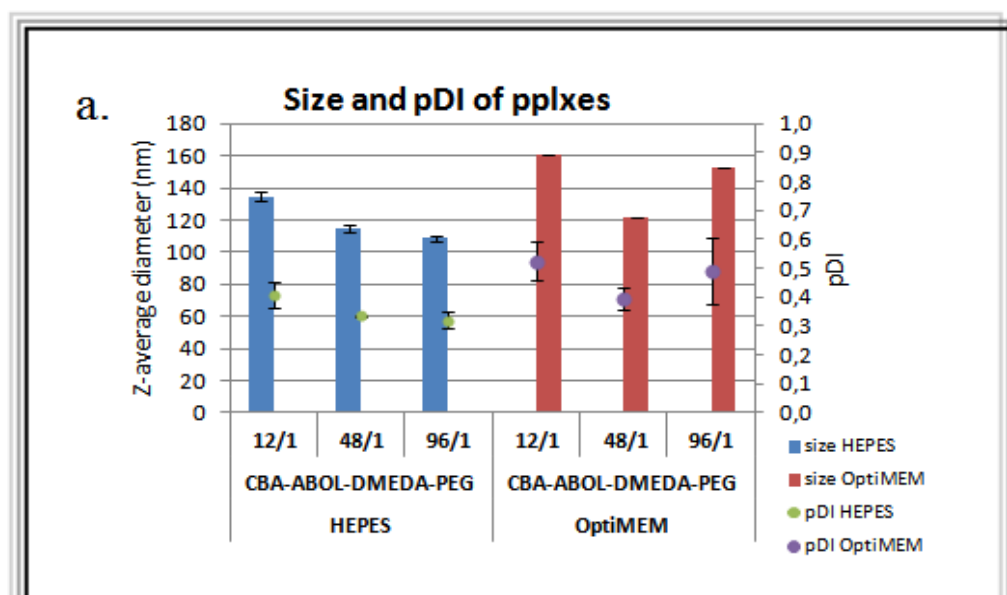


Figure 5.17 : Illustration of the effect of PEGylation on a. particle size and polydispersity, b. ζ -potential.

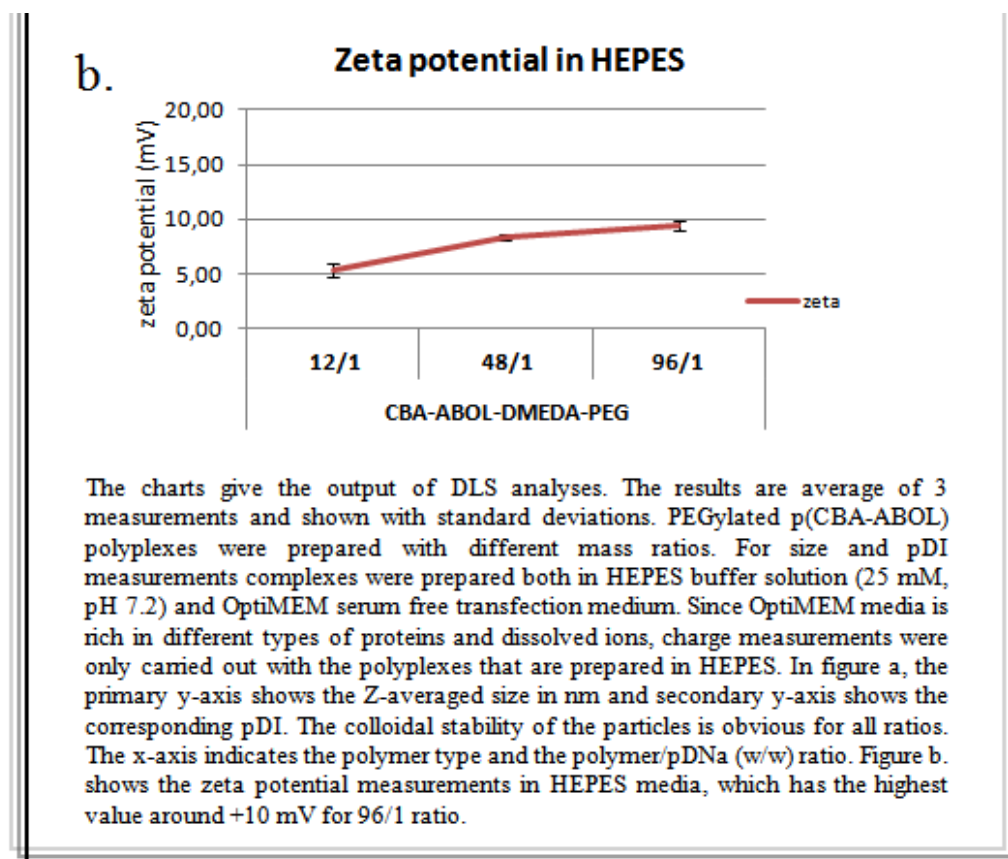


Figure 5.17 (continued) : Illustration of the effect of PEGylation on a. particle size and polydispersity, b. ζ -potential.

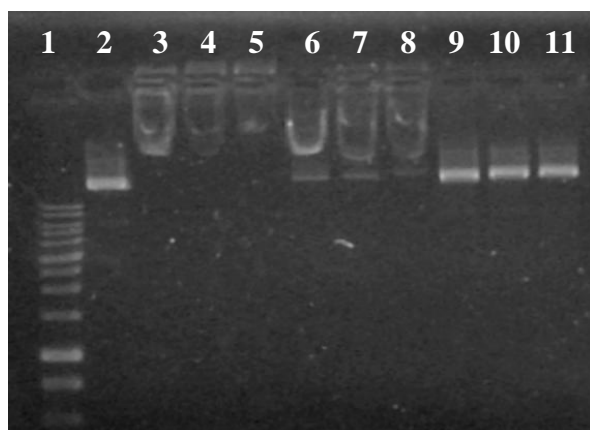
pDNA complexation efficiency

Agarose gel electrophoresis was applied to investigate the DNA binding capability of PEGylated polymers. Lane numbers 3,4 and 5 indicate the polyplexes prepared in HEPES and number 6,7 and 8 show the complexes diluted in OptiMEM (See Figure 5.18). It can be observed from the band intensities that PEGylated polymers have a more strong DNA binding ability both in HEPES and OptiMEM. Moreover, the polymer mass ratio above 48/1 show more stable complexes for PEGylated polymers.

5.3.2.2 *In vitro* biological evaluation

Uptake efficiency

The uptake efficiency of PEGylated p(CBA-ABOL) polymer complexes with different polymer/pDNA (w/w) ratios on ARPE-19 cells was evaluated by flow cytometry. According to the results of the stability and DNA condensation ability of



1. Ladder (1kb)
2. Pure pGL4.13 plasmid
3. PEG-pplx 48/1 in HEPES
4. PEG-pplx 72/1 in HEPES
5. PEG-pplx 96/1 in HEPES
6. PEG-pplx 48/1 in OptiMEM
7. PEG-pplx 72/1 in OptiMEM
8. PEG-pplx 96/1 in OptiMEM
9. PEG-pplx 48/1+ 5 µl Heparin
10. PEG-pplx 72/1+ 5 µl Heparin
11. PEG-pplx 96/1+ 5 µl Heparin

Figure 5.18 : Agarose gel electrophoresis for p(CBA-ABOL/DMEDA/PEG) complexes. The lanes with the polyplexes contain 20 µL of sample (corresponding to 200 ng of pDNA per well). As a negative control, 5 µL of Heparin (7 µg/µL) was added to last 3 samples to simulate pDNA displacement.

the polymer, the most capable two ratios, 48/1 and 96/1, were chosen and applied for the uptake experiment. The non-PEGylated 48/1 p(CBA-ABOL) polyplexes were also applied as a comparison. Figure 5.19 shows the efficiencies of polyplex samples and their negative controls. The negative control samples which were put at 4°C, showed no uptake, as expected. As expected, the cells showed positive uptake for p(CBA-ABOL)/pDNA complexes with 80%. However, it can be seen from Figure 5.19 that PEGylated p(CBA-ABOL) polyplexes were almost not taken up by ARPE-19 cells.

Transfection efficiency

In order to determine transfection efficiency of PEGylated p(CBA-ABOL) complexes ARPE-19 cells were treated with polyplexes having different mass ratios and the transfection efficiency was analyzed by flow cytometry. LF/pDNA complexes and non-PEGylated p(CBA-ABOL) polyplexes were applied as positive controls. As it is illustrated in Figure 5.20 that the positive control samples showed a GFP expression around 25% on the other hand, PEGylated p(CBA-ABOL) complexes did not transfect.

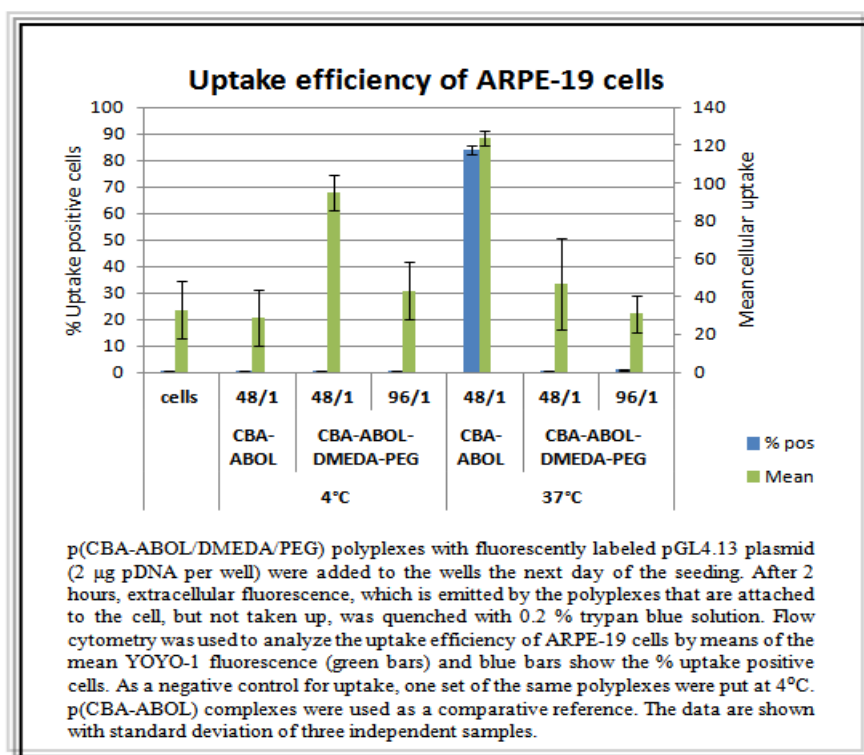


Figure 5.19 : The effect of PEGylation on cellular internalization of p(CBA-ABOL) polyplexes with different mass ratios in ARPE-19 cells.

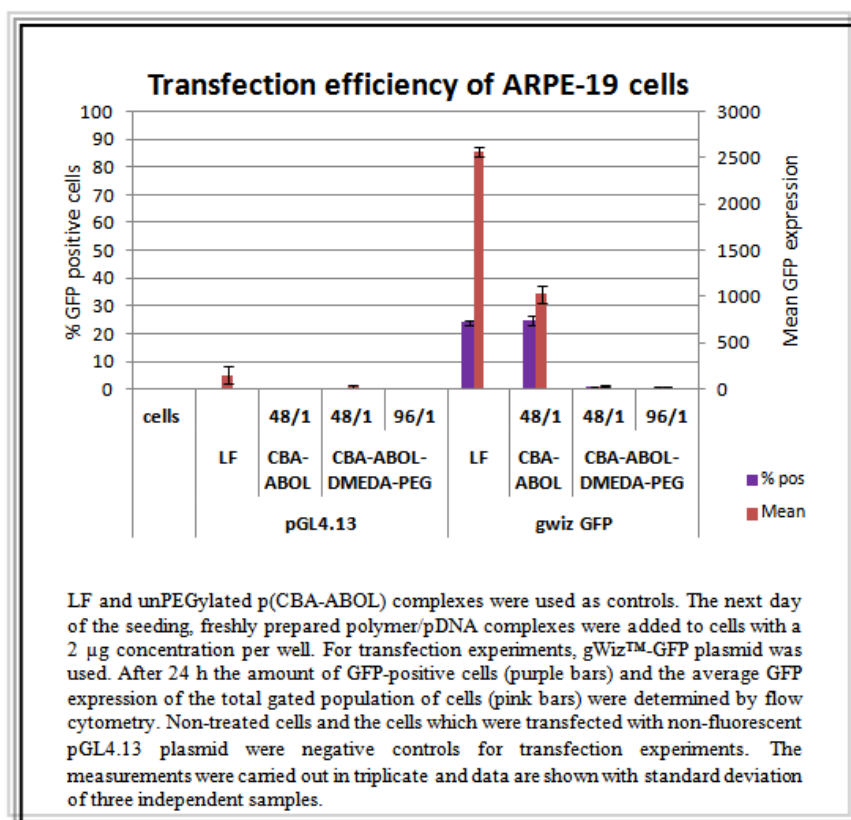


Figure 5.20 : Comparison of the effect of PEGylation on transfection efficiency of p(CBA-ABOL) polyplexes with various mass ratios in ARPE-19 cells.

5.3.2.3 Discussion

p(CBA-ABOL) polyplexes were evaluated as the first member of SS-PAA family in the previous section. p(CBA-ABOL) polymer was able to efficiently transfect the ARPE-19 cells, however, the complexes formed large aggregates in the extracellular environment. PEGylation was applied as a strategy to increase the colloidal stability of p(CBA-ABOL)/pDNA complexes in the extracellular environment. Synthesis of p(CBA-ABOL/DMEDA/PEG) was performed by Michael addition polymerization. p(CBA-ABOL/DMEDA) was first synthesized by the same reaction and then PEGylation was performed by PEG-NH₂ quenching. In addition to the bioreducibility and DNA transfection ability of p(CBA-ABOL), *N,N'*-dimethylethane-1,2-diamine (DMEDA) group increases the positive charges present in the polymer chain which improves complexation and electrostatic interactions between polymer and pDNA (Vader et al, 2011). The effect of PEGylation on polyplex particle size and surface charge was characterized by DLS. It was clearly seen that PEGylated polyplexes form more stable complexes than unPEGylated p(CBA-ABOL) polyplexes in OptiMEM with a hydrodynamic diameter of 152 nm in 96/1 ratio. The surface charge measurements indicated less positive complexes with p(CBA-ABOL/DMEDA/PEG) even with the highest polymer ratio of 96/1 which is because of PEG molecule that has a neutral surface charge in buffer conditions (Brumbach et al, 2010). To determine the ability of PEGylated polymer to condense the pDNA, agarose gel electrophoresis was applied. As it was shown in Figure 5.18, p(CBA-ABOL/DMEDA/PEG) polyplexes were able to condense DNA in HEPES for all applied ratios. Additionally, the samples in OptiMEM showed less clear bands that represent the pDNA than p(CBA-ABOL) polyplexes which means PEGylated polymers can condense the pDNA more densely with the facilitating effect of increased polymer/pDNA mass ratio.

In vitro biological evaluation of p(CBA-ABOL/DMEDA/PEG) polyplexes was analyzed by flow cytometry by the means of uptake and transfection efficiency which showed that these complexes showed almost no cellular uptake (See Figure 5.19). This fact was explained by Coi (1998) and Oupicky et al. (2002) that PEGylation reduces the cellular association and uptake of polyplexes due to the steric shielding of polyplex particles. When the PEGylated particles were investigated for transfection efficiency on ARPE-19 cells, they did not show any

GFP expression where the unPEGylated p(CBA-ABOL) has transfected similar to positive control lipoplexes. As Lin and Engbersen stated that PEGylated polyplexes indicated very low transfection efficiency because their neutral surface appears efficient cellular association and internalization (2009). Furthermore, the endosomal escape of polyplexes from acidic endosomes is also diminished by PEGylation (Knorr et al, 2007). Since the results of biological evaluation of PEGylated particles address the “PEG dilemma”, PEGylated polyplexes was not investigated in terms of cellular viability, because particles which are not taken up by the cell will have minimal influence on cell viability.

To conclude, PEGylation of polyplexes results in reduced interaction with OptiMEM components giving rise to more stable particles. Nevertheless, this extracellular stability comes at the cost of an inefficiency for uptake and transfection observations, possibly due to the shielding of the surface charge, which emphasizes the need for alternative strategies to increase colloidal stability of p(CBA-ABOL) particles.

5.3.3 HA-coated p(CBA-ABOL) polyplexes

Hyaluronic acid (HA) is a cell surface GAG which is highly abundant in extracellular matrix (ECM). It is popularly investigated for drug delivery purposes because of having good biocompatibility and biodegradability (Han et al, 2009). Moreover, it has been reported to be responsible of cellular internalization and uptake of gene therapy vectors. In this section, HA-coated p(CBA-ABOL) polyplexes were investigated in terms of increase in the stability of complexes and in the uptake efficiency.

5.3.3.1 Physicochemical characterization

Particle size and surface charge measurements

Particle size and surface charge measurements were carried out for a series of HA-coated p(CBA-ABOL)/pDNA complexes with different HA/pDNA molar ratios. The characterization was performed by DLS. The coating was applied on p(CBA-ABOL) polyplex with 48/1 ratio with different amount of research grade HA that is purchased from Life Core Scientific. As it is shown in Figure 5.21, increasing amount of HA results in smaller, more negative and stable complexes in HEPES

buffer. The effect of increasing amount of HA is less clear for size measurements in OptiMEM because all the complexes have an average size of 500 nm.

Table 5.6 : Illustration of the amount of HA and pDNA used to apply the coating in appropriate HA/pDNA molar ratio.

HA-coated p(CBA-ABOL)	molar ratio (HA/pDNA)	V _{HA} (μ L)	m _{HA} (μ g)	m _{pDNA} (μ g)
	25.5 /1	12.4	62	2
	63/1	30.6	153	2
	125/1	61.1	305.5	2
	190/1	92	460	2
	250/1	122.2	611	2
	313/1	153	765	2
	377/1	184	920	2
	505.5/1	244.4	1222	2

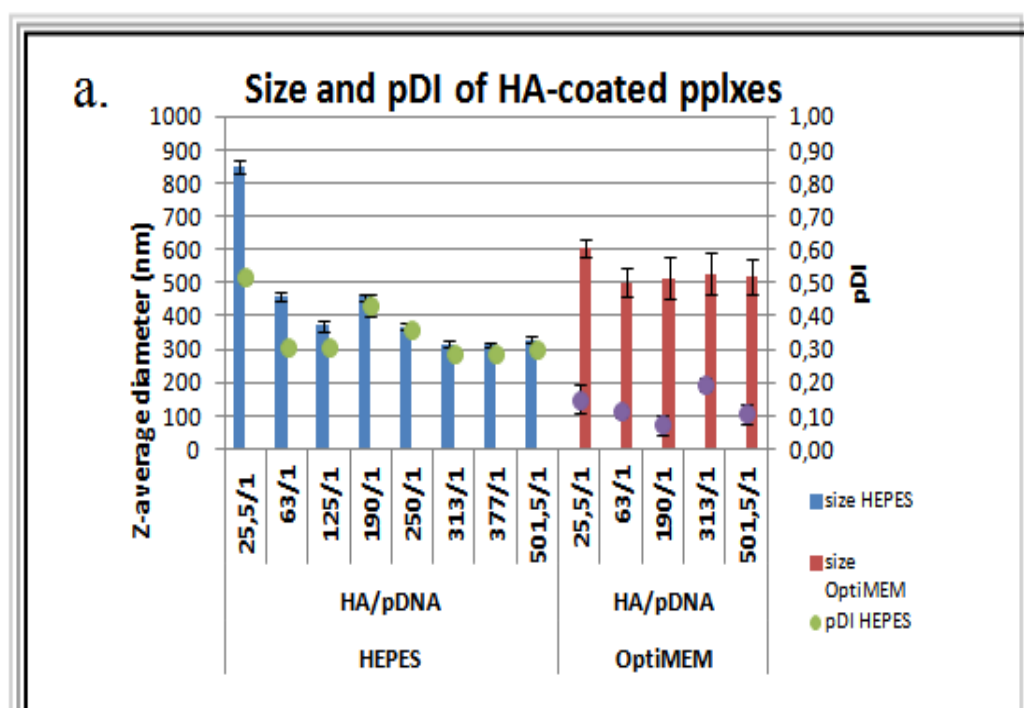


Figure 5.21 : Illustration of the effect of HA-coating on a. particle size and polydispersity, b. ζ -potential of p(CBA-ABOL) polyplexes with different HA/pDNA molar ratios.

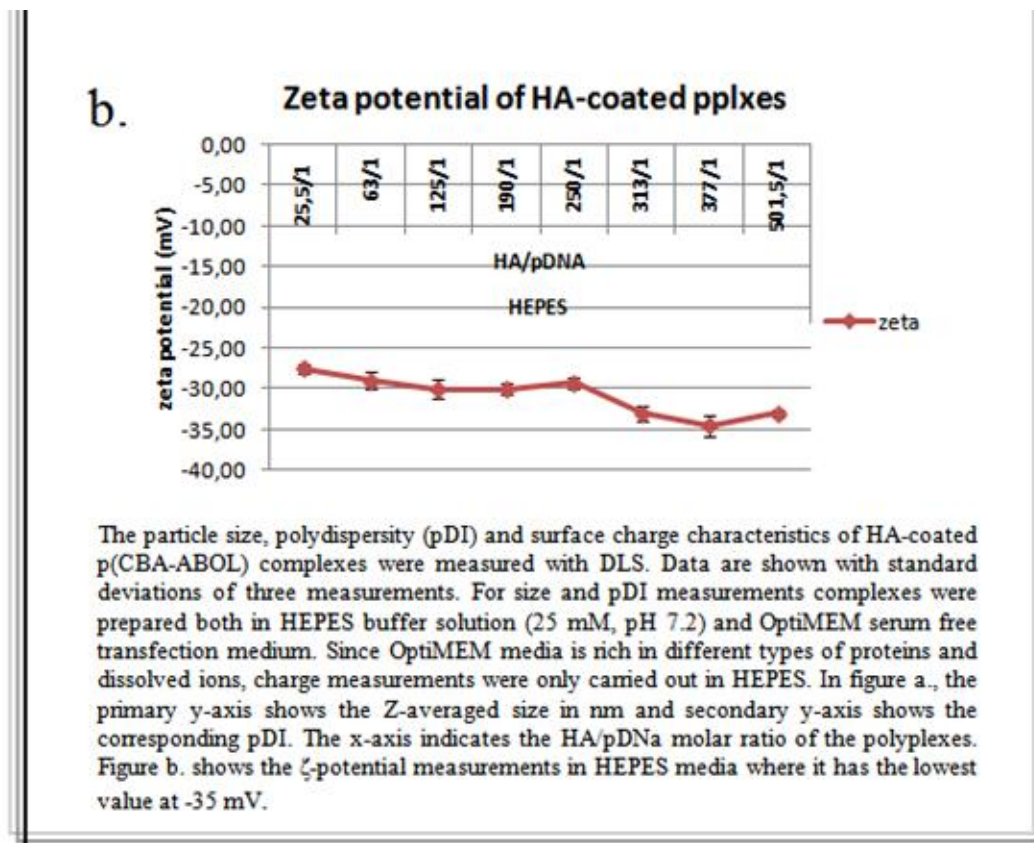


Figure 5.21 (continued) : Illustration of the effect of HA-coating on a. particle size and polydispersity, b. ζ -potential of p(CBA-ABOL) polyplexes with different HA/pDNA molar ratios.

pDNA complexation efficiency

The influence of HA-coating on the DNA condensation behavior of p(CBA-ABOL) complexes was observed by agarose gel electrophoresis. Based on DLS results, the most stable complexes were chosen and applied into gel. As a reference, non-coated p(CBA-ABOL) complexes with 48/1 ratio was also loaded in gel. Polyplexes which were prepared in HEPES buffer with increasing HA/pDNA ratio were loaded into lanes numbers 4,5 and 6 (See Figure 5.22). In terms of pDNA band intensity the complexes in HEPES, looks more or less have the same stability with non-coated polyplexes. Nevertheless, the slight bands of the lane numbers 8,9 and 10 that are loaded with HA-coated complexes in OptiMEM, clarify the effect of HA-coating on the stability of complexes.

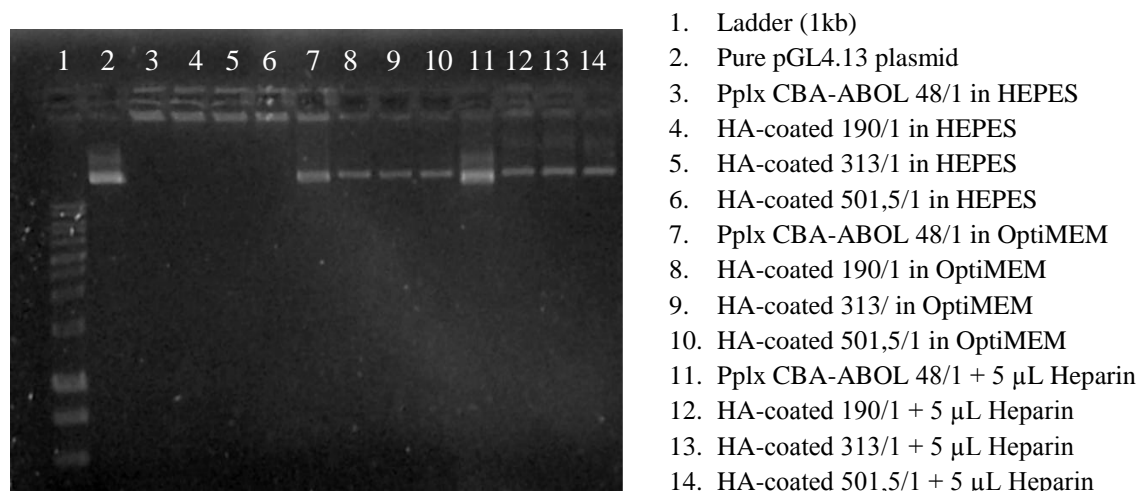


Figure 5.22 : Agarose gel electrophoresis of HA-coated p(CBA-ABOL) polyplexes with different HA/pDNA mass ratios. The lanes with the polyplexes contain 20 µL of sample (corresponding to 200 ng of pDNA per well). As a negative control, 5 µL of Heparin (7 µg/µL) was added to last 4 samples to simulate pDNA displacement.

5.3.3.2 *In vitro* biological evaluation

Uptake efficiency

The influence of HA-coating on the uptake efficiency of stable p(CBA-ABOL) complexes was analyzed by flow cytometry. A series of HA/pDNA ratios were applied for physicochemical characterization of HA-coated p(CBA-ABOL) polyplexes but only the more stable ones were chosen for the uptake experiment. Non-coated p(CBA-ABOL) complexes were also applied in order to compare the effect of HA-coating. Figure 5.23 shows the uptake efficiency results of HA-coated p(CBA-ABOL) polyplexes based on three different HA/pDNA molar ratios with their controls. The positive control samples with non-coated p(CBA-ABOL) polyplexes show 80% cellular uptake. The desired effect of HA-coating and increasing HA/pDNA ratio was not observed in terms of uptake efficiency because all the ratios show similar efficiency around 10% of uptake positive cells.

Transfection efficiency

The transfection efficiency of HA-coated p(CBA-ABOL) polyplexes with different HA/pDNA molar ratios was determined by flow cytometry. Polyplexes with non-coated p(CBA-ABOL) and LF/pDNA complexes were prepared as positive controls. The samples were analyzed 24h after the addition of the complexes. % positive GFP expression of HA-coated p(CBA-ABOL) polyplex samples and their controls is

shown in Figure 5.24. The positive control LF transfected nearly 30% of the plasmid while p(CBA-ABOL) had 15% GFP expression. The HA-coated polyplexes showed very low transfection, even with the highest HA/pDNA ratio for 400/1.

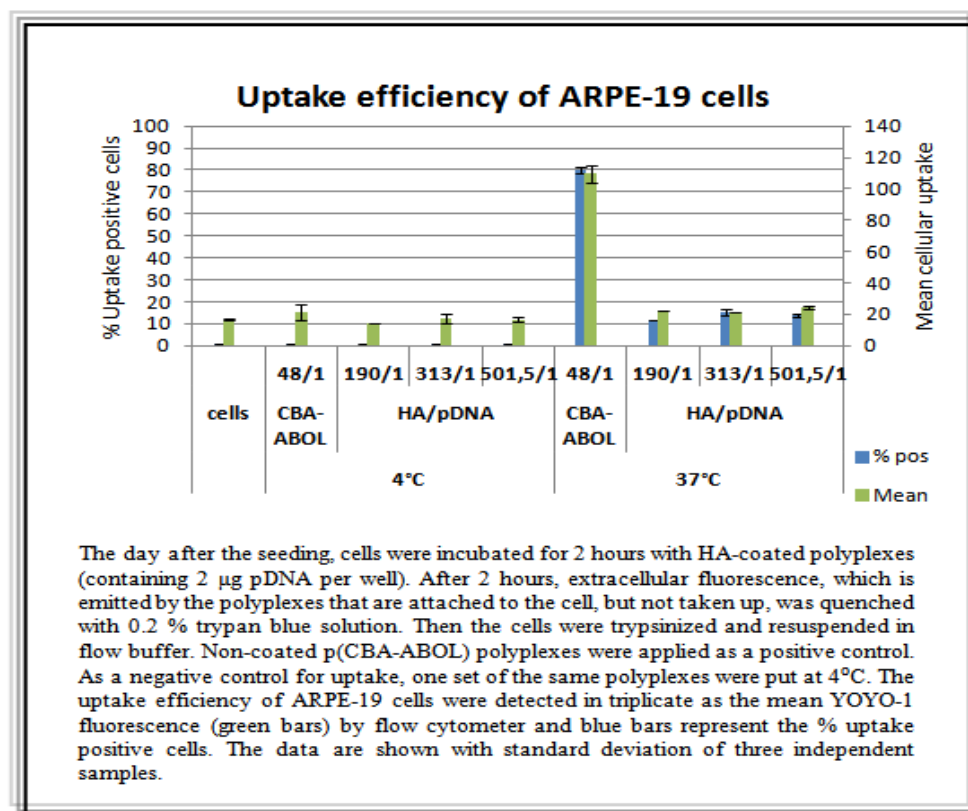


Figure 5.23 : The effect of HA-coating on cellular internalization of p(CBA-ABOL) polyplexes with different HA/pDNA molar ratios in ARPE-19 cells.

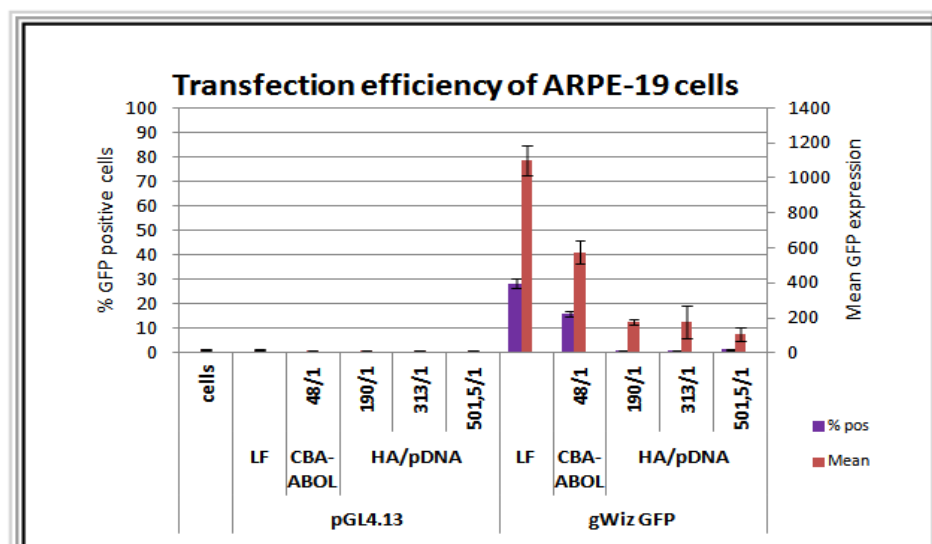


Figure 5.24 : Comparison of transfection efficiencies of different gene carriers HA-coated p(CBA-ABOL) with different HA/pDNA molar ratios, non-coated p(CBA-ABOL) and LF complexes.

To measure transfection efficiency, the cells were transfected with complexes, containing 2 μ g of a GFP reporter plasmid and GFP levels were determined by flow cytometry 24 h after transfection showing the percentage of fluorescent cells (purple bars) and the average transgene GFP expression (pink bars). The gating, which is the selection of the appropriate cells based on their size and granularity, was applied by adjusting the FSC and SSC. Non-treated cells and the cells which were transfected with non-fluorescent pGL4.13 plasmid were negative controls for transfection experiments. Data shown here represents average values of 3 independent measurements, where the errors bars denote the standard deviation between these measurements.

Figure 5.24 (continued) : Comparison of transfection efficiencies of different gene carriers HA-coated p(CBA-ABOL) with different HA/pDNA molar ratios, non-coated p(CBA-ABOL) and LF complexes.

Cell viability

The effect of HA-coating for p(CBA-ABOL) polyplexes on ARPE-19 cell viability was analyzed with MTT Assay and the absorbance was measured by Microplate Reader. LF/pDNA and non-coated p(CBA-ABOL)/pDNA complexes were applied as positive controls. It is clearly seen on Figure 5.25 that HA-coated complexes indicate higher cell viability when than the positive controls. This may because of they are taken up with a lower efficiency with comparison to the control samples.

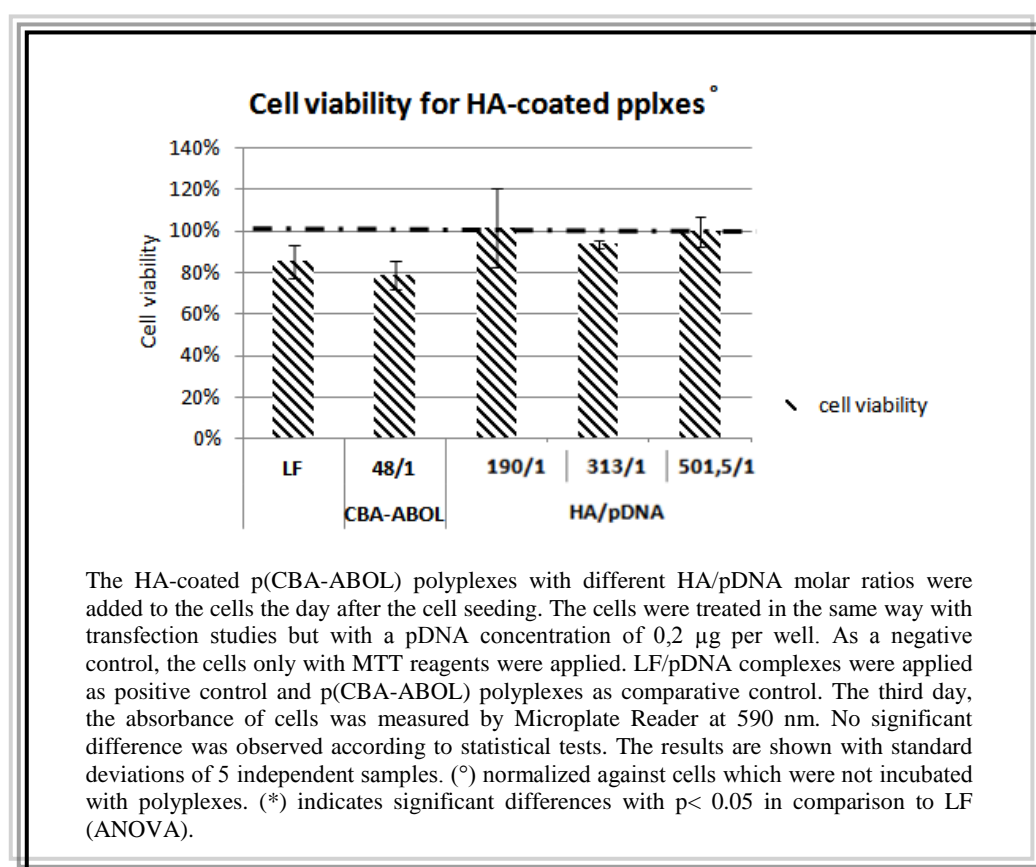


Figure 5.25 : Effect of HA-coating on the viability of ARPE-19 cells.

5.3.3.3 Discussion

In the previous sections, pDMAEMA polyplexes were reported to be stable but had a very low transfection efficiency. Then as an alternative vector system p(CBA-ABOL) polymer was chosen to be evaluated for its potential to be a gene delivery vector. p(CBA-ABOL) complexes were stable in HEPES and had promising results for transfection. However, they were not stable in the extracellular environment. Thus PEGylation was applied to increase the stability of p(CBA-ABOL) polyplexes in the extracellular environment. PEGylated particles formed stable complexes in the extracellular media, but were not taken up and did not transfect efficiently. p(CBA-ABOL) polyplexes should be improved in terms of stability in the extracellular environment and transfection efficiency. HA-coating was applied by means of electrostatic binding of negatively charged low molecular weight HA polymer to positively cored polyplexes. The choice of hyaluronan Mw was determined by the previous study of Hornof et. al. (2008) and the ratio of complexes based on the molar ratio between HA and pDNA. By adding the HA to the polyplexes as the outer core of the polyplexes was coated with anionic HA, the ζ -potential of complexes turned negative from positive (See Figure 5.21) and resulting in a lowest value of -35 mV. According to the Z-average diameter measurements in OptiMEM, particles with all ratios show a clear stability around 500 nm in average. When it is compared to uncoated polyplexes this drastic change in the size of particles could be because the polyplexes are completely restructured, perhaps with more plasmids per polyplex, and more polymer as well. The pDNA condensation efficiency of the polyplexes in OptiMEM can be seen from agarose gel electrophoresis (See Figure 5.22). The HA-coated particles with the lowest ratio showed a slight pDNA release and the other two ratios were able to completely condense the pDNA which means HA-shielding has a positive effect on pDNA binding ability of polymer.

For biological evaluation of HA-coated particles, uptake and transfection efficiency analyses were performed. In contrast to generally obtained results, the desired increasing effect of HA-coating could not be observed for p(CBA-ABOL) uptake efficiency studies. Previously, Wang et al. have reported a facilitating effect for cellular uptake of HA-shielded PEI/pDNA complexes (2011).

In a preliminary study, we obtained low Mw HA with enzymatic digestion of hyaluronan (See App. A). The transfection efficiency results showed higher gene

expression than the results obtained with research grade purity HA. This could be due to the purity and decreased effect of HA Mw. Although we aimed low Mw by the enzymatic digestion, there is a possibility that the high Mw HA particles could not be eliminated completely by ultrafiltration. Then the mixture of low and high Mw HA may have resulted in increased transfection efficiency in the preliminary study. Moreover, the MTT assay results indicated that the cell viability is higher for the cells treated with HA-coated particles than uncoated particles. This could be because they are less toxic for the cells, but it could also be because they are not taken up as much as uncoated particles. Hence, the application of HA-coating should be further investigated.

5.3.4 p(CBA-HIS) polyplexes

p(CBA-HIS) was chosen to be used as a gene delivery vector due to the imidazole groups present in the side chain. These groups have a good buffering capacity in physiological conditions that is expected to be more efficient in terms of delivery of the plasmid to the cell nucleus.

5.3.4.1 Physicochemical characterization

Particle size and surface charge measurements

The particle size and surface charge measurements of p(CBA-HIS) polyplexes with various polymer/pDNA mass ratio were determined by DLS. The p(CBA-HIS)/pDNA complexes were prepared with 4 different mass ratios which were the same ratios that applied for p(CBA-ABOL) polyplexes. By this way, it was possible to compare the polyplex formation characteristics of two types of polymers. The amount of polymer and pDNA which was used while preparing the complexes is illustrated on Table 5.7 and the measurement values are given on Table 5.8. As it is shown in Figure 5.26, increasing amount of polymer results in smaller, more positive and stable complexes in HEPES buffer. However, measurements in OptiMEM media indicates that the increase in the polymer/pDNA ratio causes very large particles, even $>1\ \mu\text{m}$ for 96/1 ratio.

Table 5.7: The amounts of p(CBA-HIS) polymer and pDNA which was used to obtain desired polymer/pDNA (w/w) ratios. The polyplexes were prepared with increasing amount of polymer while the amount of plasmid was constant.

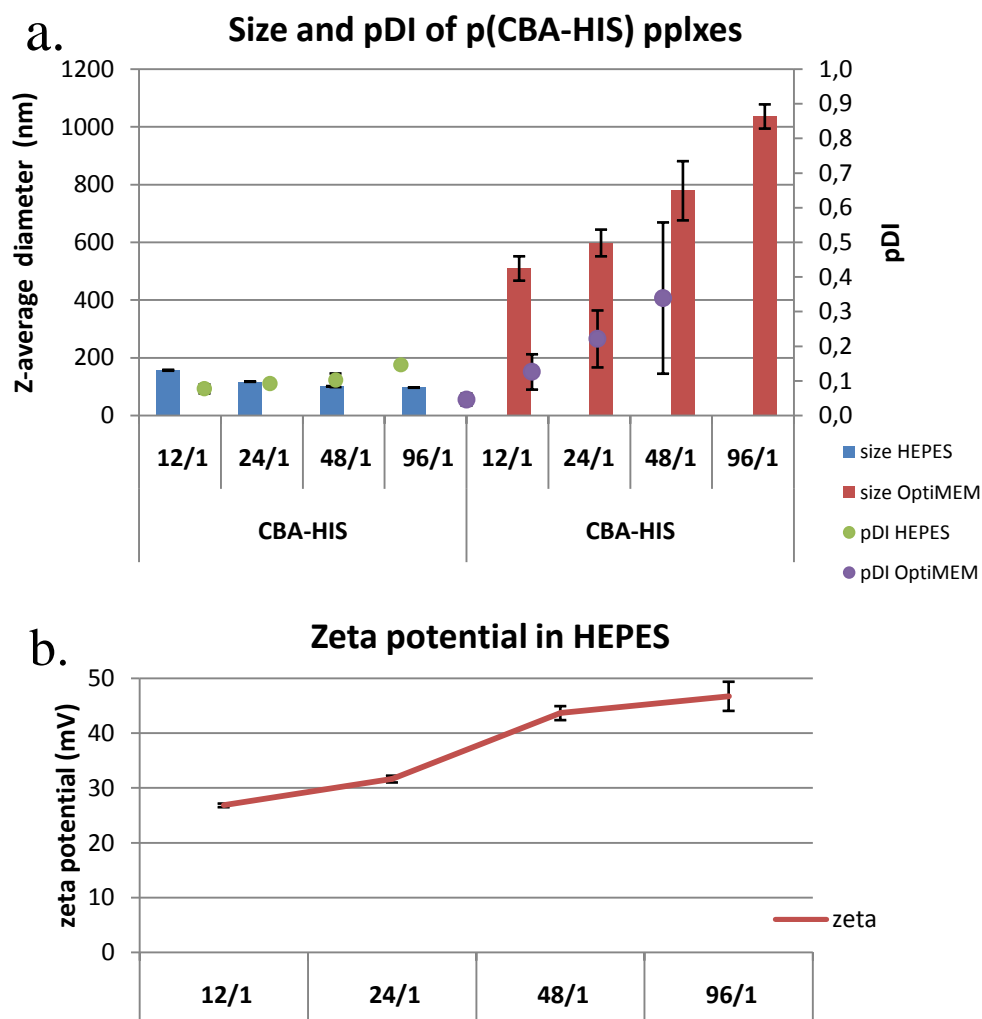
mass ratio	m _{polymer} (μg)	m _{pDNA} (μg)
12/1	120	10
24/1	240	10
48/1	480	10
96/1	960	10

Table 5.8 : Illustration of average size, pDI and charge values for p(CBA-HIS) polyplexes with different polymer/pDNA mass ratios.

p(CBA-HIS)	mass ratio	HEPES			OptiMEM	
		size (nm)	pDI	Z-potential (mV)	size (nm)	pDI
	12/1	157,07	0,08	26,87	509,70	0,05
	24/1	117,70	0,09	31,67	598,10	0,13
	48/1	101,80	0,10	43,70	778,97	0,22
	96/1	96,78	0,15	46,77	1036,33	0,34

pDNA complexation efficiency

Agarose gel electrophoresis was performed to analyze the pDNA condensation ability of homopolymer p(CBA-HIS)/pDNA complexes. As it is shown in the Figure 5.27, the polyplexes were loaded into gel starting from lane number 3 and polymer/pDNA ratio of 12/1. 48/1 p(CBA-ABOL)/pDNA complex was also applied as a reference. It can be seen from the figure that above the ratio of 24/1, the bands become almost invisible and polymer strongly binds the pDNA. If the polyplexes with the same amount but different type of polymer are compared (lane number 5 and 7), it can be concluded that p(CBA-HIS) has strong ability to condense the pDNA molecule. For the samples in OptiMEM, the release of pDNA is observed however, the bands are less bright than the ones with heparin where the pDNA was almost totally displaced.



The charts give the output of DLS analyses. The results are average of 3 measurements and shown with standard deviations. For size and pDI measurements complexes were prepared both in HEPES buffer solution (25 mM, pH 7.2) and OptiMEM serum free transfection medium. Since OptiMEM media is rich in different types of proteins and dissolved ions, charge measurements were only carried out with the polyplexes that are prepared in HEPES. In Figure a., the primary y-axis shows the Z-averaged size in nm and secondary y-axis shows the corresponding pDI. The x-axis indicates the polymer type and the polymer/pDNA (w/w) ratio. It can be seen in figure a. that the influence of increasing polymer ratio gives rise to large particles in OptiMEM, possibly aggregates. Figure b. shows the zeta potential measurements in HEPES media, which appear to be maximum around +50 mV for 96/1 ratio.

Figure 5.26 : Illustration of a. particle size and polydispersity, b. ζ -potential of pDMAEMA polyplexes with different Mw and mass ratios.

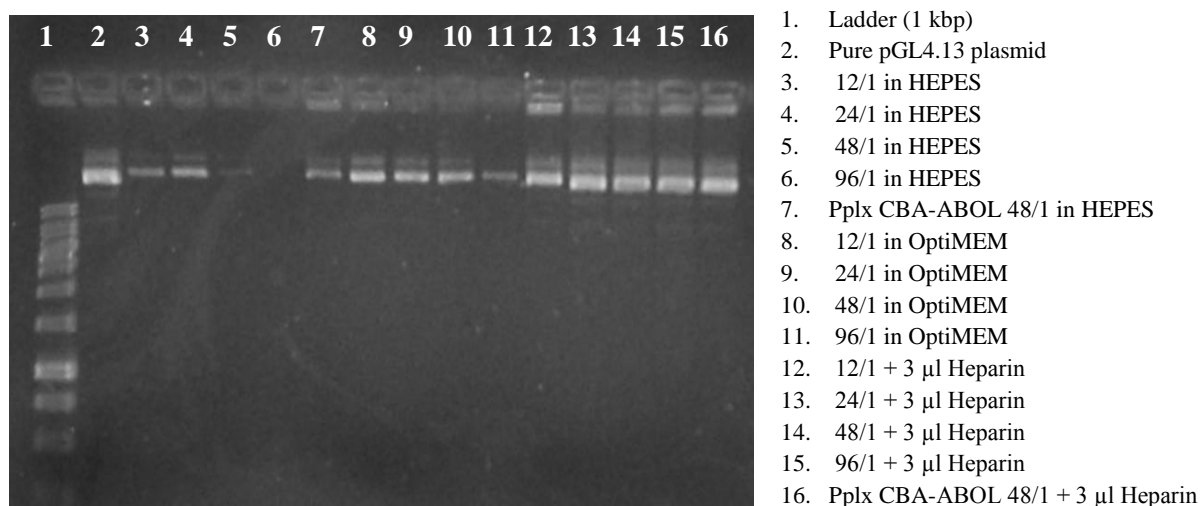


Figure 5.27: Agarose gel electrophoresis of p(CBA-HIS) polyplexes with different mass ratios. The lanes with polyplexes contain 20 µL of sample (corresponding to 200 ng of pDNA per well). As a negative control, 3 µL of Heparin (7 µg/µL) was added to last 5 samples to simulate pDNA displacement. 48/1 p(CBA-ABOL) polyplexes were applied as a comparative reference.

5.3.4.2 *In vitro* biological evaluation

Uptake efficiency

The influence of increased buffering capacity on the uptake efficiency of ARPE-19 cells was determined by flow cytometry (See Figure 5.28). Two mass ratios of p(CBA-HIS), 24/1 and 48/1, with the best physicochemical characteristics were chosen and applied for uptake experiment. p(CBA-ABOL) 48/1 ratio was used to prepare the positive control samples. Untreated cells and one set of the polyplexes were put at 4°C as negative controls. p(CBA-HIS) with 48/1 mass ratio polyplexes showed nearly 95% uptake which is higher than the p(CBA-ABOL) polyplexes with the same polymer/pDNA (w/w) ratio.

Transfection efficiency

Following the uptake efficiency experiment, the p(CBA-HIS) polyplexes were evaluated in terms of their transfection efficiency. ARPE-19 cells were treated with polyplexes having different mass ratios and the transfection efficiency was analyzed by flow cytometry. LF/pDNA complexes and p(CBA-ABOL) polyplexes were applied as positive controls. For positive control samples, nearly 30% GFP expression was observed while p(CBA-ABOL) showed a transfection efficiency

around 10% (See Figure 5.29). On the other hand, p(CBA-HIS) complexes showed very low transfection for both selected polymer/pDNA ratios.

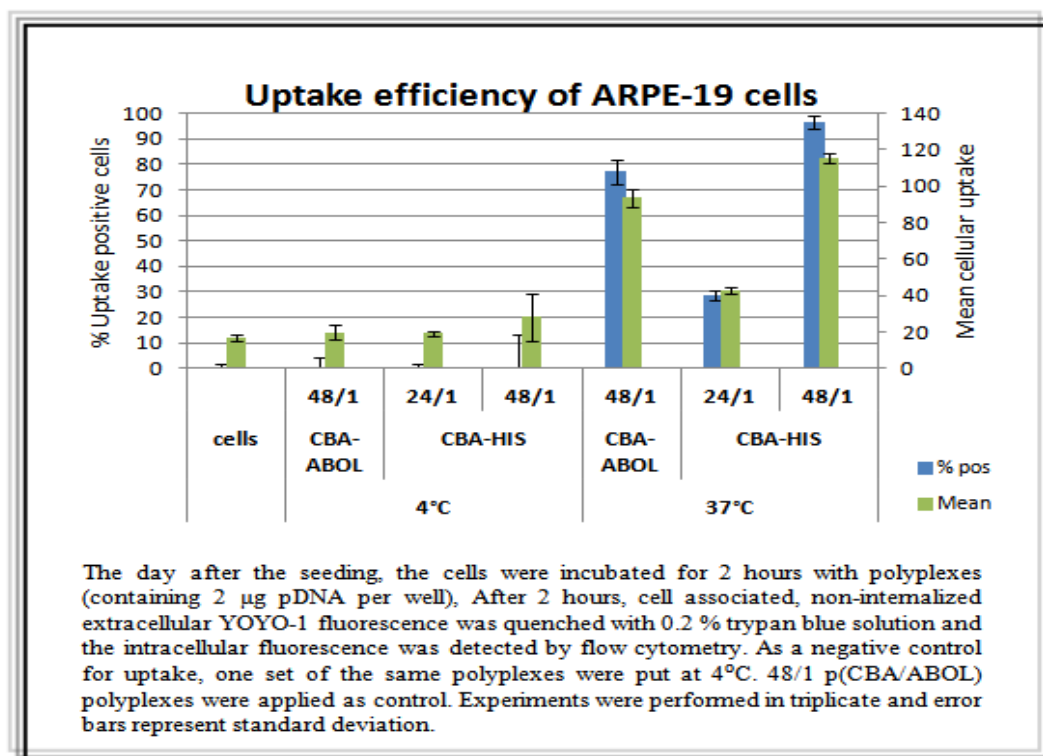


Figure 5.28 : Comparison of internalization of different gene carriers p(CBA-HIS) with different mass ratios, p(CBA-ABOL) and LF in ARPE-19 cells.

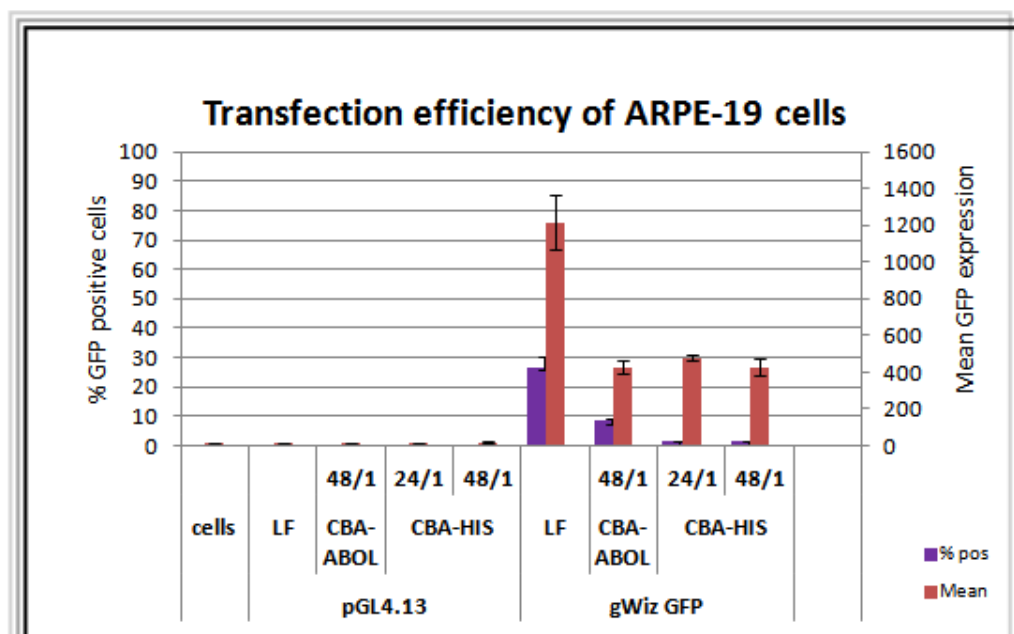


Figure 5.29 : Comparison of transfection efficiencies of different gene carriers p(CBA-HIS) with different mass ratios, p(CBA-ABOL) and LF in ARPE-19 cells.

The cells were transfected with the polyplexes with various mass ratios (2 µg pDNA concentration per well) at the same time with uptake experiment. For transfection experiments, gWiz-GFP plasmid was used. After 24 h the amount of GFP-positive cells (purple bars) and the mean average GFP expression (pink bars) of the total gated population of cells were measured by flow cytometry. Non-treated cells and the cells which were transfected with non-fluorescent pGL4.13 plasmid were negative controls for transfection experiments. As a positive control, three wells were treated with lipoplexes formed by LF. p(CBA-ABOL) polyplexes were used as comparative reference. The measurements were carried out in triplicate and data are shown with standard deviation of three independent samples.

Figure 5.29 (continued) : Comparison of transfection efficiencies of different gene carriers p(CBA-HIS) with different mass ratios, p(CBA-ABOL) and LF in ARPE-19 cells.

Cell viability

The cell viability for p(CBA-HIS) polyplexes on ARPE-19 cells was analyzed with MTT Assay by means of absorbance measurements on Microplate Reader. LF/pDNA and p(CBA-ABOL)/pDNA complexes were applied as controls. It can be seen on the Figure 5.30 that, p(CBA-HIS)/pDNA complexes have significantly favorable cell viability both for 24/1 and 48/1 mass ratios.

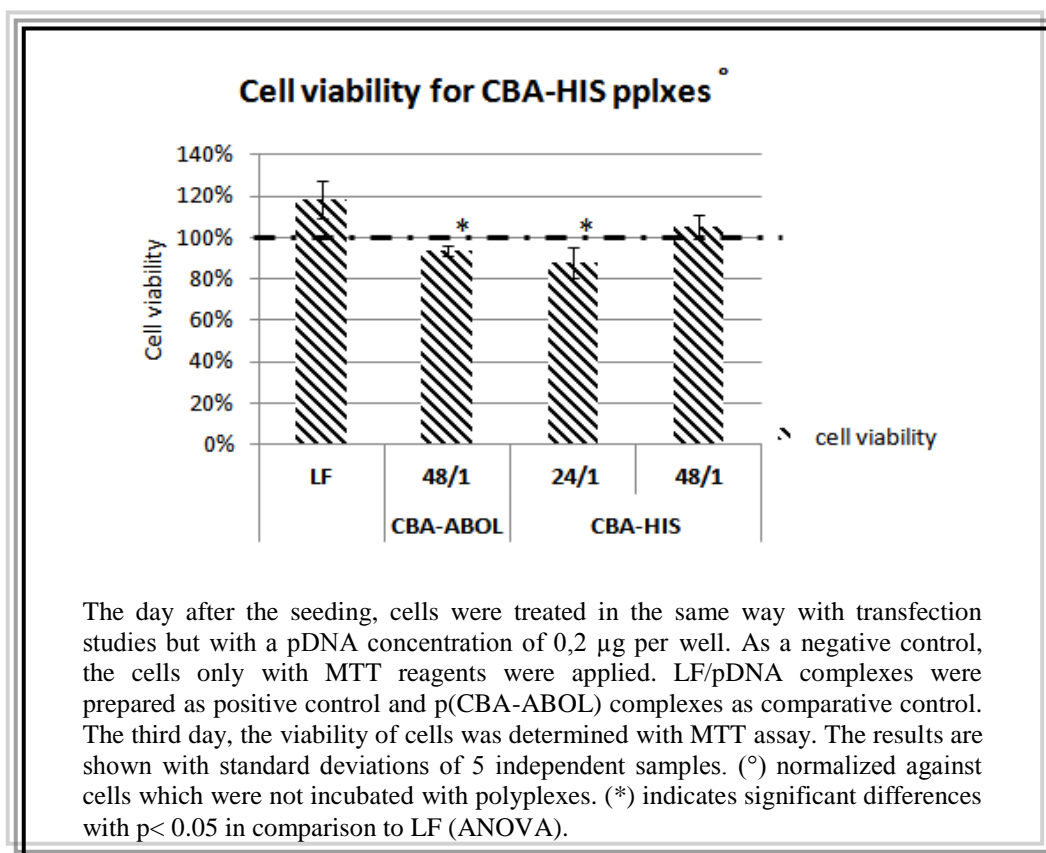


Figure 5.30 : Cell viability results of p(CBA-HIS)/pDNA pplexes with different mass ratios.

5.3.4.3 Discussion

p(CBA-HIS) is a homopolymer with imidazole side groups that was synthesized by Michael type polyaddition of CBA monomer with repetitive disulfide linkages to histamine (HIS) molecule. p(CBA-HIS) homopolymer has a buffering capacity of 58% due to the imidazole groups ($pK_a \sim 6.5$) present in the side chain (Lin et al, 2007b). The same 4 mass ratios as p(CBA-ABOL) polyplexes were applied for both physicochemical and biological evaluation of p(CBA-HIS) by this way, it was possible to compare the effect of buffer capacity of the polymer. First of all, the particle size and surface charge of the polyplexes was analyzed by DLS. According to the data obtained by DLS for the same mass ratios, p(CBA-HIS) polyplexes formed smaller complexes in HEPES buffer than p(CBA-ABOL) polyplexes which may be because of the imidazole groups in p(CBA-HIS) giving rise to stronger interactions with DNA by the means of increased cationic charge (Coue and Engbersen, 2011). Nevertheless, the same aggregation problem in OptiMEM conditions was also observed for p(CBA-ABOL) polyplexes (See Figure 5.26). Secondly, agarose gel electrophoresis was employed to investigate the pDNA binding ability of p(CBA-HIS) polyplexes with various mass ratios. As it is shown in Figure 5.27, the DNA release bands become less clear starting from 24/1 ratio, indicating a stronger condensation. Moreover, p(CBA-HIS) polyplexes were able to condense the pDNA more efficiently in comparison to the bands of p(CBA-ABOL) polyplexes with the same mass ratio of 48/1.

The uptake and transfection efficiency of p(CBA-HIS) polyplexes on ARPE-19 cells was studied with 2 stable mass ratios of 24/1 and 48/1. Furthermore, cell viability of ARPE-19 cells that are incubated with p(CBA-HIS) polyplexes was analyzed by MTT assay. The uptake efficiency results clearly showed that, p(CBA-HIS) polyplexes are taken up with a higher percentage. Especially at 48/1 polymer/pDNA mass ratios where pDNA is condensed into smaller and more positively-charged nanoparticles, the cellular uptake is much increased with comparison to p(CBA-ABOL) polyplexes. The transfection efficiency results of p(CBA-HIS) polyplexes were quite unexpected. The pK_a of imidazole groups present in histamine side chains is in the range of endosomal acidification (pH 7.4–5.1) (Coue and Engbersen, 2011). By this way, these polyplexes were supposed have an advantage of extra pH-responsiveness during endosomal escape which would result in higher transfection

efficiency. However, as it is illustrated in Figure 5.29 that p(CBA-HIS) polyplexes have very low GFP expression where the LF control and p(CBA-ABOL) complexes show an acceptable efficiency. This may be explained by the stronger pDNA binding ability of p(CBA-HIS). Finally, the cell viability experiment indicated that p(CBA-HIS) polyplexes have a negligible cytotoxicity relative to LF complexes and as well as p(CBA-ABOL).

All in all, p(CBA-HIS) is stated to form stable complexes in HEPES but not in the extracellular environment, have high uptake efficiency and good cell viability. The same strategies as for p(CBA-ABOL) polyplexes can be used to increase the stability of p(CBA-HIS) complexes in OptiMEM media and facilitate the transfection efficiency.

6. CONCLUSION

Gene therapy is the treatment of human diseases with an underlying genetic cause by delivering therapeutic genetic material (transgene) into the diseased cells of the patient. It has been a promising way to treat genetic diseases over the last decades because it offers a solution to treat the causes of diseases rather than curing the symptoms.

In this project, pDMAEMA polymer/pDNA complexes were evaluated as an example of non-biodegradable polymers. These polyplexes were able to form stable complexes with pDNA and transfect the ARPE-19 cells with a moderate efficiency. Apart from lower gene expression, pDMAEMA polymer had a cytotoxic effect on ARPE-19 cells.

Secondly, SS-PAAAs were evaluated as an example of biodegradable and bioreducible polymer systems. Additionally different coating strategies and side chains were applied to improve the efficiency of these systems. All types of SS-PAA polymer were able to form stable complexes with pDNA. p(CBA-ABOL) was reported to a good transfection agent with relatively high cell viability however, its stability in the physiological mimicking media should be increased. PEGylation strategy was expected to increase the stability of p(CBA-ABOL) complexes and the positive effect was observed. Nevertheless, PEGylated polymers were not able to taken up by the ARPE-19 cells and transfect. HA-coating was an alternative way to increase the stability of particles and facilitate their uptake efficiency. The experiments resulted in expected way however, the effect of HA Mw on the transfection efficiency should be further investigated.

Finally, p(CBA-HIS) was chosen to be evaluated in terms of cellular uptake and transfection. This polymer was supposed to have an increased transfection efficiency due to the buffering capacity and higher pKa of imidazole groups. The expected efficiency for transfection did not observed with p(CBA-HIS) polyplexes which their DNA release profile in the intracellular environment should be further analyzed.

REFERENCES

- Abdelhady, H. G., Allen, S., Davies, M. C., Roberts, C. J., Tendler, S. J., and Williams, P. M.** (2003). Direct real-time molecular scale visualisation of the degradation of condensed DNA complexes exposed to DNase I. [Research Support, Non-U.S. Gov't]. *Nucleic Acids Res*, 31(14), 4001-4005.
- Akinc, A., Thomas, M., Klibanov, A. M., and Langer, R.** (2005). Exploring polyethylenimine-mediated DNA transfection and the proton sponge hypothesis. [Comparative StudyResearch Support, N.I.H., Extramural Research Support, U.S. Gov't, Non-P.H.S. Research Support, U.S. Gov't, P.H.S.]. *J Gene Med*, 7(5), 657-663. doi: 10.1002/jgm.696
- Al-Dosari, M. S., and Gao, X.** (2009). Nonviral Gene Delivery: Principle, Limitations, and Recent Progress. *Aaps Journal*, 11(4), 671-681.
- Apodaca, G.** (2001). Endocytic traffic in polarized epithelial cells: role of the actin and microtubule cytoskeleton. [Research Support, U.S. Gov't, P.H.S. Review]. *Traffic*, 2(3), 149-159.
- Arscott, P. G., and Bloomfield, V. A.** (1990). Scanning tunnelling microscopy of nucleic acids and polynucleotides. [Research Support, U.S. Gov't, Non-P.H.S. Research Support, U.S. Gov't, P.H.S.]. *Ultramicroscopy*, 33(2), 127-131.
- Bao, S., Thrall, B. D., and Miller, D. L.** (1997). Transfection of a reporter plasmid into cultured cells by sonoporation in vitro. [Research Support, U.S. Gov't, P.H.S.]. *Ultrasound Med Biol*, 23(6), 953-959.
- Behr, J. P.** (1993). Synthetic Gene-Transfer Vectors. *Accounts of Chemical Research*, 26(5), 274-278.
- Belting, M., and Petersson, P.** (1999). Protective role for proteoglycans against cationic lipid cytotoxicity allowing optimal transfection efficiency in vitro. [Research Support, Non-U.S. Gov't]. *Biochem J*, 342 (Pt 2), 281-286.
- Bernfield, M., Gotte, M., Park, P. W., Reizes, O., Fitzgerald, M. L., Lincecum, J., and Zako, M.** (1999). Functions of cell surface heparan sulfate proteoglycans. [Research Support, Non-U.S. Gov't Research Support, U.S. Gov't, P.H.S. Review]. *Annual Review of Biochemistry*, 68, 729-777. doi: 0.1146/annurev.biochem.68.1.729
- Blaese, R. M.** (1995). Steps toward gene therapy .1. The initial trials. *Hospital Practice*, 30(11), 33-40.
- Bleiziffer, O., Eriksson, E., Yao, F., Horch, R. E., and Kneser, U.** (2007). Gene transfer strategies in tissue engineering. [Research Support, Non-U.S.

Gov't Review]. *J Cell Mol Med*, 11(2), 206-223. doi: 10.1111/j.1582-4934.2007.00027.x

- Bolsover, S. R.** (2004). *Cell biology : a short course* (2nd ed.). Hoboken, N.J.: Wiley-Liss.
- Boussif, O., Lezoualc'h, F., Zanta, M. A., Mergny, M. D., Scherman, D., Demeneix, B., and Behr, J. P.** (1995). A versatile vector for gene and oligonucleotide transfer into cells in culture and in vivo: polyethylenimine. [In Vitro Research Support, Non-U.S. Gov't]. *Proc Natl Acad Sci U S A*, 92(16), 7297-7301.
- Bright, G. R., Fisher, G. W., Rogowska, J., and Taylor, D. L.** (1987). Fluorescence ratio imaging microscopy: temporal and spatial measurements of cytoplasmic pH. [Research Support, Non-U.S. Gov't Research Support, U.S. Gov't, Non-P.H.S. Research Support, U.S. Gov't, P.H.S.]. *J Cell Biol*, 104(4), 1019-1033.
- Brown, M. D., Schatzlein, A. G., and Uchegbu, I. F.** (2001). Gene delivery with synthetic (non viral) carriers. *Int J Pharm*, 229(1-2), 1-21.
- Brumbach, J. H., Lin, C., Yockman, J., Kim, W. J., Blevins, K. S., Engbersen, J. F., . . . Kim, S. W.** (2010). Mixtures of poly(triethylenetetramine/cystamine bisacrylamide) and poly(triethylenetetramine/cystamine bisacrylamide)-g-poly(ethylene glycol) for improved gene delivery. [Research Support, N.I.H., Extramural]. *Bioconjug Chem*, 21(10), 1753-1761. doi: 10.1021/bc900522x
- Cavazzana-Calvo, M., Hacein-Bey, S., de Saint Basile, G., Gross, F., Yvon, E., Nusbaum, P., . . . Fischer, A.** (2000). Gene therapy of human severe combined immunodeficiency (SCID)-X1 disease. [Clinical Trial Research Support, Non-U.S. Gov't]. *Science*, 288(5466), 669-672.
- Chen, A., and Moy, V. T.** (2000). Cross-linking of cell surface receptors enhances cooperativity of molecular adhesion. [Research Support, Non-U.S. Gov't Research Support, U.S. Gov't, P.H.S.]. *Biophysical Journal*, 78(6), 2814-2820. doi: 10.1016/S0006-3495(00)76824-X
- Cherng, J. Y., vandeWetering, P., Talsma, H., Crommelin, D. J. A., and Hennink, W. E.** (1996). Effect of size and serum proteins on transfection efficiency of poly((2-dimethylamino)ethyl methacrylate)-plasmid nanoparticles. *Pharm Res*, 13(7), 1038-1042.
- Choi, K. Y., Chung, H., Min, K. H., Yoon, H. Y., Kim, K., Park, J. H., . . . Jeong, S. Y.** (2010). Self-assembled hyaluronic acid nanoparticles for active tumor targeting. [Research Support, Non-U.S. Gov't]. *Biomaterials*, 31(1), 106-114. doi: 10.1016/j.biomaterials.2009.09.030
- Choi, Y. H., Liu, F., Kim, J. S., Choi, Y. K., Park, J. S., and Kim, S. W.** (1998). Polyethylene glycol-grafted poly-L-lysine as polymeric gene carrier. [Research Support, Non-U.S. Gov't]. *J Control Release*, 54(1), 39-48.
- Ciftci, K., and Levy, R. J.** (2001). Enhanced plasmid DNA transfection with lysosomotropic agents in cultured fibroblasts. *Int J Pharm*, 218(1-2), 81-92.

- Condon, C., Watkins, S. C., Celluzzi, C. M., Thompson, K., and Falo, L. D., Jr.** (1996). DNA-based immunization by in vivo transfection of dendritic cells. [Research Support, Non-U.S. Gov't Research Support, U.S. Gov't, P.H.S.]. *Nat Med*, 2(10), 1122-1128.
- Conner, S. D., and Schmid, S. L.** (2003). Regulated portals of entry into the cell. [Review]. *Nature*, 422(6927), 37-44. doi: 10.1038/nature01451
- Coue, G., and Engbersen, J. F. J.** (2011). Functionalized linear poly(amidoamine)s are efficient vectors for intracellular protein delivery. *Journal of Controlled Release*, 152(1), 90-98.
- Dauty, E., and Verkman, A. S.** (2005). Actin cytoskeleton as the principal determinant of size-dependent DNA mobility in cytoplasm: a new barrier for non-viral gene delivery. [Research Support, Non-U.S. Gov't Research Support, U.S. Gov't, P.H.S.]. *J Biol Chem*, 280(9), 7823-7828. doi: 10.1074/jbc.M412374200
- Davis, M. E.** (2002). Non-viral gene delivery systems. *Current Opinion in Biotechnology*, 13(2), 128-131.
- De Smedt, S. C., Demeester, J., and Hennink, W. E.** (2000). Cationic polymer based gene delivery systems. *Pharm Res*, 17(2), 113-126.
- De Smedt, S. C., Remaut, K., Lucas, B., Braeckmans, K., Sanders, N. N., and Demeester, J.** (2005). Studying biophysical barriers to DNA delivery by advanced light microscopy. *Adv Drug Deliv Rev*, 57(1), 191-210.
- Dubruel, P., Christiaens, B., Vanloo, B., Bracke, K., Rosseneu, M., Vandekerckhove, J., and Schacht, E.** (2003). Physicochemical and biological evaluation of cationic polymethacrylates as vectors for gene delivery. *European Journal of Pharmaceutical Sciences*, 18(3-4), 211-220.
- Dubruel, P., Toncheva, V., and Schacht, E. H.** (2000). pH sensitive vinyl copolymers as vectors for gene therapy. *Journal of Bioactive and Compatible Polymers*, 15(3), 191-213.
- Dujardin, N., Van Der Smissen, P., and Preat, V.** (2001). Topical gene transfer into rat skin using electroporation. [Research Support, Non-U.S. Gov't]. *Pharm Res*, 18(1), 61-66.
- Dunn, K. C., Aotaki-Keen, A. E., Putkey, F. R., and Hjelmeland, L. M.** (1996). ARPE-19, a human retinal pigment epithelial cell line with differentiated properties. [Research Support, Non-U.S. Gov't Research Support, U.S. Gov't, P.H.S.]. *Exp Eye Res*, 62(2), 155-169. doi: 10.1006/exer.1996.0020
- Durieux, A. C., Bonnefoy, R., Busso, T., and Freyssen, D.** (2004). In vivo gene electrotransfer into skeletal muscle: effects of plasmid DNA on the occurrence and extent of muscle damage. *J Gene Med*, 6(7), 809-816. doi: 10.1002/jgm.534
- Dworetzky, S. I., and Feldherr, C. M.** (1988). Translocation of RNA-coated gold particles through the nuclear pores of oocytes. [Research Support, U.S. Gov't, P.H.S.]. *J Cell Biol*, 106(3), 575-584.

- Edelstein, M. L., Abedi, M. R., Wixon, J., and Edelstein, R. M.** (2004). Gene therapy clinical trials worldwide 1989-2004 - an overview. *Journal of Gene Medicine*, 6(6), 597-602.
- Edidin, M.** (2003). Lipids on the frontier: a century of cell-membrane bilayers. [Historical Article Review]. *Nat Rev Mol Cell Biol*, 4(5), 414-418. doi: 10.1038/nrm1102
- El-Andaloussi, S., Holm, T., and Langel, U.** (2005). Cell-penetrating peptides: mechanisms and applications. [Review]. *Curr Pharm Des*, 11(28), 3597-3611.
- Endoh, M., Koibuchi, N., Sato, M., Morishita, R., Kanzaki, T., Murata, Y., and Kaneda, Y.** (2002). Fetal gene transfer by intrauterine injection with microbubble-enhanced ultrasound. [Research Support, Non-U.S. Gov't]. *Mol Ther*, 5(5 Pt 1), 501-508. doi: 10.1006/mthe.2002.0577
- Ferruti, P., Marchisio, M. A., and Duncan, R.** (2002). Poly(amido-amine)s: Biomedical applications. *Macromol Rapid Commun*, 23(5-6), 332-355.
- Fuchs, E., and Yang, Y.** (1999). Crossroads on cytoskeletal highways. [Review]. *Cell*, 98(5), 547-550.
- Funhoff, A. M., van Nostrum, C. F., Koning, G. A., Schuurmans-Nieuwenbroek, N. M., Crommelin, D. J., and Hennink, W. E.** (2004). Endosomal escape of polymeric gene delivery complexes is not always enhanced by polymers buffering at low pH. [Research Support, Non-U.S. Gov't]. *Biomacromolecules*, 5(1), 32-39. doi: 10.1021/bm034041+
- Gallagher, J. T., Lyon, M., and Steward, W. P.** (1986). Structure and function of heparan sulphate proteoglycans. [Review]. *Biochem J*, 236(2), 313-325.
- Gao, X., Kim, K. S., and Liu, D. X.** (2007). Nonviral gene delivery: What we know and what is next. *Aaps Journal*, 9(1), E92-E104.
- Gehl, J.** (2003). Electroporation: theory and methods, perspectives for drug delivery, gene therapy and research. [Review]. *Acta Physiol Scand*, 177(4), 437-447.
- Gong, Q., Huntsman, C., and Ma, D.** (2008). Clathrin-independent internalization and recycling. [Review]. *J Cell Mol Med*, 12(1), 126-144. doi: 10.1111/j.1582-4934.2007.00148.x
- Gorlich, D., and Mattaj, I. W.** (1996). Nucleocytoplasmic transport. [Research Support, Non-U.S. Gov't Review]. *Science*, 271(5255), 1513-1518.
- Hajdu, S. I.** (2002). A note from history: Introduction of the cell theory. *Annals of Clinical and Laboratory Science*, 32(1), 98-100.
- Han, S. E., Kang, H., Shim, G. Y., Kim, S. J., Choi, H. G., Kim, J., . . . Oh, Y. K.** (2009). Cationic derivatives of biocompatible hyaluronic acids for delivery of siRNA and antisense oligonucleotides. [Research Support, Non-U.S. Gov't]. *J Drug Target*, 17(2), 123-132. doi: 10.1080/10611860802472461

- Heitz, F., Morris, M. C., and Divita, G.** (2009). Twenty years of cell-penetrating peptides: from molecular mechanisms to therapeutics. [Research Support, Non-U.S. Gov't Review]. *Br J Pharmacol*, 157(2), 195-206. doi: 10.1111/j.1476-5381.2009.00057.x
- Hong, K., Zheng, W., Baker, A., and Papahadjopoulos, D.** (1997). Stabilization of cationic liposome-plasmid DNA complexes by polyamines and poly(ethylene glycol)-phospholipid conjugates for efficient in vivo gene delivery. [Research Support, Non-U.S. Gov't]. *Febs Letters*, 400(2), 233-237.
- Hornof, M., de la Fuente, M., Hallikainen, M., Tammi, R. H., and Urtti, A.** (2008). Low molecular weight hyaluronan shielding of DNA/PEI polyplexes facilitates CD44 receptor mediated uptake in human corneal epithelial cells. [Research Support, Non-U.S. Gov't]. *J Gene Med*, 10(1), 70-80. doi: 10.1002/jgm.1125
- Jang, J. H., Houchin, T. L., and Shea, L. D.** (2004). Gene delivery from polymer scaffolds for tissue engineering. [Review]. *Expert Rev Med Devices*, 1(1), 127-138. doi: 10.1586/17434440.1.1.127
- Jiang, X., van der Horst, A., van Steenberg, M. J., Akeroyd, N., van Nostrum, C. F., Schoenmakers, P. J., and Hennink, W. E.** (2006). Molar-mass characterization of cationic polymers for gene delivery by aqueous size-exclusion chromatography. *Pharm Res*, 23(3), 595-603. doi: 10.1007/s11095-006-9574-4
- Kim, H. J., Greenleaf, J. F., Kinnick, R. R., Bronk, J. T., and Bolander, M. E.** (1996). Ultrasound-mediated transfection of mammalian cells. [Research Support, Non-U.S. Gov't]. *Hum Gene Ther*, 7(11), 1339-1346. doi: 10.1089/hum.1996.7.11-1339
- Knorr, V., Allmendinger, L., Walker, G. F., Paintner, F. F., and Wagner, E.** (2007). An acetal-based PEGylation reagent for pH-sensitive shielding of DNA polyplexes. [Research Support, Non-U.S. Gov't]. *Bioconjug Chem*, 18(4), 1218-1225. doi: 10.1021/bc060327a
- Knudson, W., Chow, G., and Knudson, C. B.** (2002). CD44-mediated uptake and degradation of hyaluronan. [Research Support, Non-U.S. Gov't Research Support, U.S. Gov't, P.H.S. Review]. *Matrix Biol*, 21(1), 15-23.
- Kunath, K., Merdan, T., Hegener, O., Haberlein, H., and Kissel, T.** (2003). Integrin targeting using RGD-PEI conjugates for in vitro gene transfer. [Evaluation Studies]. *J Gene Med*, 5(7), 588-599. doi: 10.1002/jgm.382
- Kursa, M., Walker, G. F., Roessler, V., Ogris, M., Roedl, W., Kircheis, R., and Wagner, E.** (2003). Novel shielded transferrin-polyethylene glycol-polyethylenimine/DNA complexes for systemic tumor-targeted gene transfer. *Bioconjug Chem*, 14(1), 222-231. doi: 10.1021/bc0256087
- Laskey, R. A., Gorlich, D., Madine, M. A., Makkerh, J. P., and Romanowski, P.** (1996). Regulatory roles of the nuclear envelope. [Research Support, Non-U.S. Gov't Review]. *Exp Cell Res*, 229(2), 204-211. doi: 10.1006/excr.1996.0361

- Layman, J. M., Ramirez, S. M., Green, M. D., and Long, T. E.** (2009). Influence of polycation molecular weight on poly(2-dimethylaminoethyl methacrylate)-mediated DNA delivery in vitro. [Research Support, U.S. Gov't, Non-P.H.S.]. *Biomacromolecules*, 10(5), 1244-1252. doi: 10.1021/bm9000124
- Lechardeur, D., and Lukacs, G. L.** (2006). Nucleocytoplasmic transport of plasmid DNA: a perilous journey from the cytoplasm to the nucleus. [Research Support, N.I.H., Extramural Research Support, Non-U.S. Gov't Review]. *Hum Gene Ther*, 17(9), 882-889. doi: 10.1089/hum.2006.17.882
- Lechardeur, D., Sohn, K. J., Haardt, M., Joshi, P. B., Monck, M., Graham, R. W., . . . Lukacs, G. L.** (1999). Metabolic instability of plasmid DNA in the cytosol: a potential barrier to gene transfer. [Research Support, Non-U.S. Gov't Research Support, U.S. Gov't, P.H.S.]. *Gene Ther*, 6(4), 482-497. doi: 10.1038/sj.gt.3300867
- Ledley, F. D.** (1995). Nonviral Gene-Therapy - the Promise of Genes as Pharmaceutical Products. *Hum Gene Ther*, 6(9), 1129-1144.
- Liang, H. D., Lu, Q. L., Xue, S. A., Halliwell, M., Kodama, T., Cosgrove, D. O., . . . Blomley, M. J.** (2004). Optimisation of ultrasound-mediated gene transfer (sonoporation) in skeletal muscle cells. [Research Support, Non-U.S. Gov't]. *Ultrasound Med Biol*, 30(11), 1523-1529. doi: 10.1016/j.ultrasmedbio.2004.08.021
- Lin, C., and Engbersen, J. F. J.** (2009). The role of the disulfide group in disulfide-based polymeric gene carriers. *Expert Opin Drug Deliv*, 6(4), 421-439.
- Lin, C., Zhong, Z., Lok, M. C., Jiang, X., Hennink, W. E., Feijen, J., and Engbersen, J. F.** (2007a). Novel bio reducible poly(amido amine)s for highly efficient gene delivery. *Bioconj Chem*, 18(1), 138-145. doi: 10.1021/bc0602001
- Lin, C., Zhong, Z. Y., Lok, M. C., Jiang, X. J., Hennink, W. E., Feijen, J., and Engbersen, J. F. J.** (2007b). Random and block copolymers of bio reducible poly(amido amine)s with high- and low-basicity amino groups: Study of DNA condensation and buffer capacity on gene transfection. *Journal of Controlled Release*, 123(1), 67-75.
- Liu, M., Chen, J., Cheng, Y. P., Xue, Y. N., Zhuo, R. X., and Huang, S. W.** (2010). Novel poly(amidoamine)s with pendant primary amines as highly efficient gene delivery vectors. [Research Support, Non-U.S. Gov't]. *Macromol Biosci*, 10(4), 384-392. doi: 10.1002/mabi.200900265
- Lodish, H. F.** (2004). *Molecular cell biology* (5th ed.). New York: W.H. Freeman and Co.
- Loser, P., Huser, A., Hillgenberg, M., Kumin, D., Both, G. W., and Hofmann, C.** (2002). Advances in the development of non-human viral DNA-vectors for gene delivery. [Review]. *Curr Gene Ther*, 2(2), 161-171.

- Luby-Phelps, K.** (2000). Cytoarchitecture and physical properties of cytoplasm: Volume, viscosity, diffusion, intracellular surface area. *International Review of Cytology - a Survey of Cell Biology*, Vol 192, 192, 189-221.
- Makrides, S. C.** (2003). *Gene transfer and expression in mammalian cells*. Amsterdam ; Boston: Elsevier.
- Mayor, S., and Pagano, R. E.** (2007). Pathways of clathrin-independent endocytosis. [Research Support, N.I.H., Extramural Research Support, Non-U.S. Gov't Review]. *Nat Rev Mol Cell Biol*, 8(8), 603-612. doi: 10.1038/nrm2216
- Mazzarello, P.** (1999). A unifying concept: the history of cell theory. *Nature Cell Biology*, 1(1), E13-E15.
- Mehier-Humbert, S., and Guy, R. H.** (2005). Physical methods for gene transfer: Improving the kinetics of gene delivery into cells. *Adv Drug Deliv Rev*, 57(5), 733-753.
- Mhashilkar, A., Chada, S., Roth, J. A., and Ramesh, R.** (2001). Gene therapy. Therapeutic approaches and implications. *Biotechnol Adv*, 19(4), 279-297.
- Midoux, P., Breuzard, G., Gomez, J. P., and Pichon, C.** (2008). Polymer-Based Gene Delivery: A Current Review on the Uptake and Intracellular Trafficking of Polyplexes. *Curr Gene Ther*, 8(5), 335-352.
- Mir, L. M., Bureau, M. F., Gehl, J., Rangara, R., Rouy, D., Caillaud, J. M., . . . Scherman, D.** (1999). High-efficiency gene transfer into skeletal muscle mediated by electric pulses. [Research Support, Non-U.S. Gov't]. *Proc Natl Acad Sci U S A*, 96(8), 4262-4267.
- Mislick, K. A., and Baldeschwieler, J. D.** (1996). Evidence for the role of proteoglycans in cation-mediated gene transfer. *Proc Natl Acad Sci U S A*, 93(22), 12349-12354.
- Mounkes, L. C., Zhong, W., Cipres-Palacin, G., Heath, T. D., and Debs, R. J.** (1998). Proteoglycans mediate cationic liposome-DNA complex-based gene delivery in vitro and in vivo. [Research Support, Non-U.S. Gov't Research Support, U.S. Gov't, P.H.S.]. *J Biol Chem*, 273(40), 26164-26170.
- Mountain, A.** (2000). Gene therapy: the first decade. *Trends in Biotechnology*, 18(3), 119-128.
- Naik, R., Mukhopadhyay, A., and Ganguli, M.** (2009). Gene delivery to the retina: focus on non-viral approaches. *Drug Discov Today*, 14(5-6), 306-315.
- Neumann, E., Kakorin, S., and Toensing, K.** (1999). Fundamentals of electroporative delivery of drugs and genes. [Research Support, Non-U.S. Gov't Review]. *Bioelectrochem Bioenerg*, 48(1), 3-16.
- Nichols, B. J., and Lippincott-Schwartz, J.** (2001). Endocytosis without clathrin coats. [Review]. *Trends in Cell Biology*, 11(10), 406-412.
- Nishi, T., Dev, S. B., Yoshizato, K., Kuratsu, J., and Ushio, Y.** (1997). Treatment of cancer using pulsed electric field in combination with chemotherapeutic agents or genes. *Hum Cell*, 10(1), 81-86.

- Ogris, M., Brunner, S., Schuller, S., Kircheis, R., and Wagner, E.** (1999). PEGylated DNA/transferrin-PEI complexes: reduced interaction with blood components, extended circulation in blood and potential for systemic gene delivery. [Research Support, Non-U.S. Gov't]. *Gene Ther*, 6(4), 595-605. doi: 10.1038/sj.gt.3300900
- Ogris, M., Walker, G., Blessing, T., Kircheis, R., Wolschek, M., and Wagner, E.** (2003). Tumor-targeted gene therapy: strategies for the preparation of ligand-polyethylene glycol-polyethylenimine/DNA complexes. *J Control Release*, 91(1-2), 173-181.
- Oupicky, D., Ogris, M., Howard, K. A., Dash, P. R., Ulbrich, K., and Seymour, L. W.** (2002). Importance of lateral and steric stabilization of polyelectrolyte gene delivery vectors for extended systemic circulation. [Research Support, Non-U.S. Gov't]. *Mol Ther*, 5(4), 463-472. doi: 10.1006/mthe.2002.0568
- Pack, D. W., Hoffman, A. S., Pun, S., and Stayton, P. S.** (2005). Design and development of polymers for gene delivery. *Nature Reviews Drug Discovery*, 4(7), 581-593.
- Perrimon, N., and Bernfield, M.** (2000). Specificities of heparan sulphate proteoglycans in developmental processes. [Research Support, Non-U.S. Gov't Research Support, U.S. Gov't, P.H.S. Review]. *Nature*, 404(6779), 725-728. doi: 10.1038/35008000
- Pichon, C., Billiet, L., and Midoux, P.** (2010). Chemical vectors for gene delivery: uptake and intracellular trafficking. *Current Opinion in Biotechnology*, 21(5), 640-645.
- Poo, M., and Cone, R. A.** (1974). Lateral diffusion of rhodopsin in the photoreceptor membrane. *Nature*, 247(441), 438-441.
- Pouton, C. W.** (1998). Nuclear import of polypeptides, polynucleotides and supramolecular complexes. *Adv Drug Deliv Rev*, 34(1), 51-64.
- Remaut, K., Sanders, N. N., De Geest, B. G., Braeckmans, K., Demeester, J., and De Smedt, S. C.** (2007). Nucleic acid delivery: Where material sciences and bio-sciences meet. *Materials Science & Engineering R-Reports*, 58(3-5), 117-161.
- Ross, G., Erickson, R., Knorr, D., Motulsky, A. G., Parkman, R., Samulski, J., . . . Smith, B. R.** (1996). Gene therapy in the United States: a five-year status report. *Hum Gene Ther*, 7(14), 1781-1790. doi: 10.1089/hum.1996.7.14-1781
- Ross, P. C., and Hui, S. W.** (1999). Lipoplex size is a major determinant of in vitro lipofection efficiency. [Research Support, U.S. Gov't, P.H.S.]. *Gene Ther*, 6(4), 651-659. doi: 10.1038/sj.gt.3300863
- Russ, V., and Wagner, E.** (2007). Cell and tissue targeting of nucleic acids for cancer gene therapy. *Pharm Res*, 24(6), 1047-1057.
- Rybak, S. L., and Murphy, R. F.** (1998). Primary cell cultures from murine kidney and heart differ in endosomal pH. [Research Support, Non-U.S. Gov't Research Support, U.S. Gov't, Non-P.H.S.]. *J Cell Physiol*, 176(1),

216-222. doi: 10.1002/(SICI)1097-4652(199807)176:1<216::AID-JCP23>3.0.CO;2-3

- Saito, G., Swanson, J. A., and Lee, K. D.** (2003). Drug delivery strategy utilizing conjugation via reversible disulfide linkages: role and site of cellular reducing activities. [Review]. *Adv Drug Deliv Rev*, 55(2), 199-215.
- Schaffer, D. V., Fidelman, N. A., Dan, N., and Lauffenburger, D. A.** (2000). Vector unpacking as a potential barrier for receptor-mediated polyplex gene delivery. [Research Support, Non-U.S. Gov't Research Support, U.S. Gov't, Non-P.H.S.]. *Biotechnol Bioeng*, 67(5), 598-606.
- Schatzlein, A. G.** (2003). Targeting of Synthetic Gene Delivery Systems. *J Biomed Biotechnol*, 2003(2), 149-158. doi: 10.1155/S1110724303209116
- Scollay, R.** (2001). Gene therapy - A brief overview of the past, present, and future. *New Vistas in Therapeutics, from Drug Design to Gene Therapy: Drug-Resistant Tuberculosis, from Molecules to Macro-Economics*, 953, 26-30.
- Sheikov, N., McDannold, N., Sharma, S., and Hynynen, K.** (2008). Effect of focused ultrasound applied with an ultrasound contrast agent on the tight junctional integrity of the brain microvascular endothelium. [Research Support, N.I.H., Extramural Research Support, Non-U.S. Gov't]. *Ultrasound Med Biol*, 34(7), 1093-1104. doi: 10.1016/j.ultrasmedbio.2007.12.015
- Tacket, C. O., Roy, M. J., Widera, G., Swain, W. F., Broome, S., and Edelman, R.** (1999). Phase 1 safety and immune response studies of a DNA vaccine encoding hepatitis B surface antigen delivered by a gene delivery device. [Clinical Trial Clinical Trial, Phase I]. *Vaccine*, 17(22), 2826-2829.
- ter Haar, G.** (2007). Therapeutic applications of ultrasound. [Review]. *Prog Biophys Mol Biol*, 93(1-3), 111-129. doi: 10.1016/j.pbiomolbio.2006.07.005
- Thomas, C. E., Ehrhardt, A., and Kay, M. A.** (2003). Progress and problems with the use of viral vectors for gene therapy. [Research Support, U.S. Gov't, P.H.S. Review]. *Nat Rev Genet*, 4(5), 346-358. doi: 10.1038/nrg1066
- Unger, E. C., Hersh, E., Vannan, M., Matsunaga, T. O., and McCreery, T.** (2001). Local drug and gene delivery through microbubbles. [Review]. *Prog Cardiovasc Dis*, 44(1), 45-54. doi: 10.1053/pcad.2001.26443
- Url-1** <<http://micro.magnet.fsu.edu/cells/animals/nucleus.html>>, date retrieved 29.05.2012.
- Url-2** <http://www.vcbio.science.ru.nl/images/cellcycle/mcell-transcription-translation_eng_zoom.gif>, date retrieved 23.03.2012.
- Url-3** <<http://www.wiley.com/legacy/wileychi/genmed/clinical/>>, date retrieved 26.04.2012.
- Url-4** <<http://www.molecularinfo.com/MTM/K/K2/K2-1/pGL4.pdf>>, date retrieved 06.02.2012.

- Url-5** <<http://www.aldevron.com/products/dnas/gwiz/>>, date retrieved 16.05.2012.
- Url-6** <<http://www.malvern.com/common/downloads/campaign/MRK656-01.pdf>>, date retrieved 16.05.2012.
- Url-7** <http://www.malvern.com/labeng/products/iwtm/zeta_potential.htm>, date retrieved 16.05.2012.
- Url-8** <http://probes.invitrogen.com/resources/education/tutorials/4Intro_Flow/player.html>, date retrieved 28.03.2012.
- Vader, P., van der Aa, L. J., Engbersen, J. F. J., Storm, G., and Schiffelers, R. M.** (2011). Disulfide-Based Poly(amido amine)s for siRNA Delivery: Effects of Structure on siRNA Complexation, Cellular Uptake, Gene Silencing and Toxicity. *Pharm Res*, 28(5), 1013-1022.
- Vader, P., van der Aa, L. J., Engbersen, J. F. J., Storm, G., and Schiffelers, R. M.** (2012). Physicochemical and Biological Evaluation of siRNA Polyplexes Based on PEGylated Poly(amido amine)s. *Pharm Res*, 29(2), 352-361.
- van de Wetering, P., Cherng, J. Y., Talsma, H., Crommelin, D. J., and Hennink, W. E.** (1998). 2-(Dimethylamino)ethyl methacrylate based (co)polymers as gene transfer agents. *J Control Release*, 53(1-3), 145-153.
- van de Wetering, P., Cherng, J. Y., Talsma, H., and Hennink, W. E.** (1997). Relation between transfection efficiency and cytotoxicity of poly(2-(dimethylamino)ethyl methacrylate)/plasmid complexes. *Journal of Controlled Release*, 49(1), 59-69.
- Vercauteren, D., Piest, M., van der Aa, L. J., Al Soraj, M., Jones, A. T., Engbersen, J. F. J., . . . Braeckmans, K.** (2011). Flotillin-dependent endocytosis and a phagocytosis-like mechanism for cellular internalization of disulfide-based poly(amido amine)/DNA polyplexes. *Biomaterials*, 32(11), 3072-3084.
- Wagner, E., and Kloeckner, J.** (2005). Gene delivery using polymer therapeutics. *Polymer Therapeutics I: Polymers as Drugs, Conjugates and Gene Delivery Systems*, 192, 135-173.
- Wang, Y., Xu, Z., Zhang, R., Li, W., Yang, L., and Hu, Q.** (2011). A facile approach to construct hyaluronic acid shielding polyplexes with improved stability and reduced cytotoxicity. [Research Support, Non-U.S. Gov't]. *Colloids Surf B Biointerfaces*, 84(1), 259-266. doi: 10.1016/j.colsurfb.2011.01.007
- Wente, S. R., and Rout, M. P.** (2010). The nuclear pore complex and nuclear transport. [Research Support, N.I.H., Extramural Review]. *Cold Spring Harb Perspect Biol*, 2(10), a000562. doi: 10.1101/cshperspect.a000562
- Wiethoff, C. M., and Middaugh, C. R.** (2003). Barriers to nonviral gene delivery. *Journal of Pharmaceutical Sciences*, 92(2), 203-217.
- Wilke, M., Fortunati, E., van den Broek, M., Hoogeveen, A. T., and Scholte, B. J.** (1996). Efficacy of a peptide-based gene delivery system depends

- on mitotic activity. [Research Support, Non-U.S. Gov't]. *Gene Ther*, 3(12), 1133-1142.
- Wong, S. Y., Pelet, J. M., and Putnam, D.** (2007). Polymer systems for gene delivery-past, present, and future. *Progress in Polymer Science*, 32(8-9), 799-837.
- Xu, Y., and Szoka, F. C., Jr.** (1996). Mechanism of DNA release from cationic liposome/DNA complexes used in cell transfection. [In Vitro Research Support, U.S. Gov't, P.H.S.]. *Biochemistry*, 35(18), 5616-5623. doi: 10.1021/bi9602019
- Zanta, M. A., Belguise-Valladier, P., and Behr, J. P.** (1999). Gene delivery: a single nuclear localization signal peptide is sufficient to carry DNA to the cell nucleus. [Research Support, Non-U.S. Gov't]. *Proc Natl Acad Sci U S A*, 96(1), 91-96.
- Zanta, M. A., Boussif, O., Adib, A., and Behr, J. P.** (1997). In vitro gene delivery to hepatocytes with galactosylated polyethylenimine. [Research Support, Non-U.S. Gov't]. *Bioconjug Chem*, 8(6), 839-844. doi: 10.1021/bc970098f
- Zauner, W., Ogris, M., and Wagner, E.** (1998). Polylysine-based transfection systems utilizing receptor mediated delivery. *Advanced Drug Delivery Reviews*, 30 (1-3), pp.97-113.
- Zhang, Z. Y., and Smith, B. D.** (2000). High-generation polycationic dendrimers are unusually effective at disrupting anionic vesicles: membrane bending model. [Research Support, U.S. Gov't, P.H.S.]. *Bioconjug Chem*, 11(6), 805-814.
- Zintchenko, A., van der Aa, L. J., and Engbersen, J. F. J.** (2011). Improved Synthesis Strategy of Poly(amidoamine)s for Biomedical Applications: Catalysis by "Green" Biocompatible Earth Alkaline Metal Salts. *Macromol Rapid Commun*, 32(3), 321-325.

APPENDICES

APPENDIX A: Preliminary study with HA

APPENDIX A

Preliminary Study for HA-coated p(CBA-ABOL) Polyplexes

Prior to the studies that were performed by research grade HA obtained from Life Core, the enzymatically degraded HA was evaluated. For this purpose the HA powder with unknown Mw was dissolved in water. Then the hyaluronan degradation enzyme hyaluronidase was dissolved in gelatin hydrolyzed and this enzyme solution was used to digest the HA by stirring overnight. Afterwards, the digested HA solution was filtered by ultrafilters with 30 kDa and 50 kDa molecular weight cut-off (MWCO) and centrifuged. Finally obtained HA was assumed to have a Mw of 30-50 kDa.

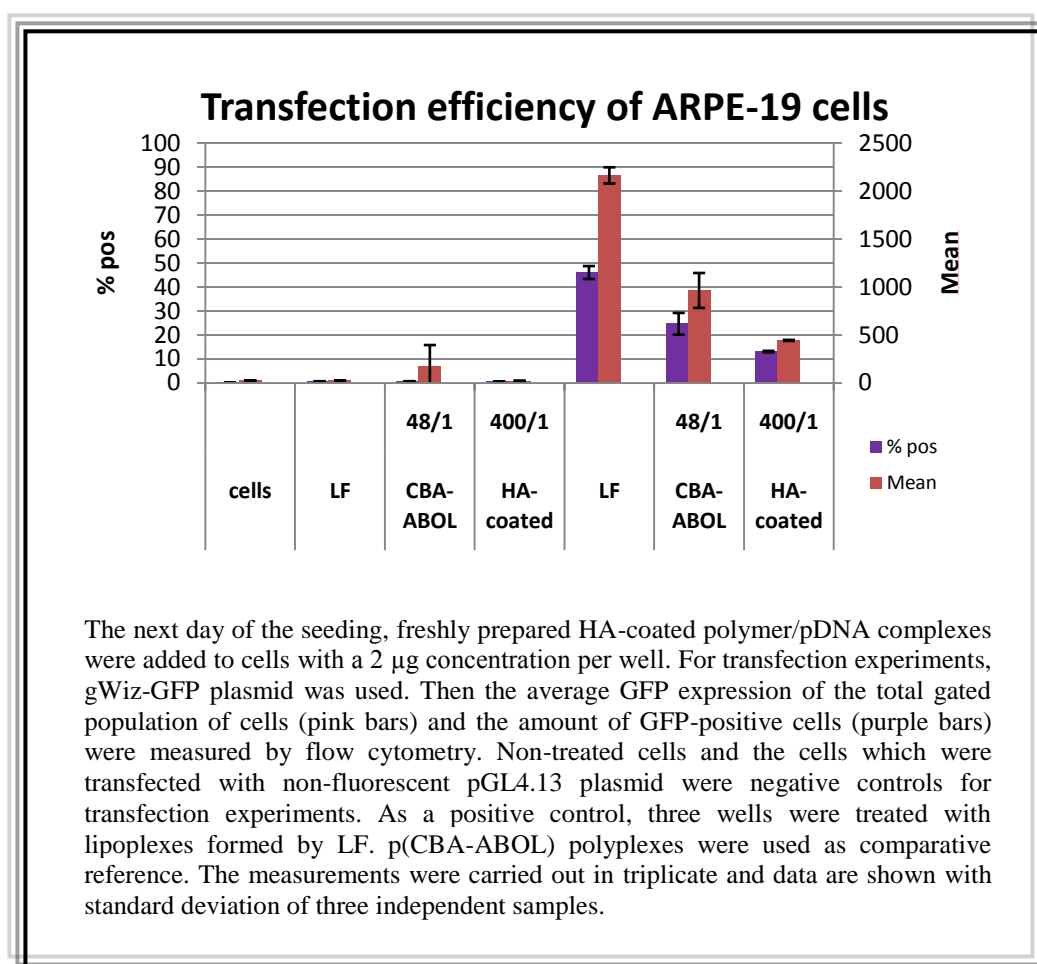


Figure A.1 : Comparison of transfection efficiency of enzymatically degraded HA-coated p(CBA-ABOL) polyplexes on ARPE-19 cells with LF and non-coated p(CBA-ABOL) complexes.

CURRICULUM VITAE

Name Surname: Hatice İmran Güngördü
Place and Date of Birth: Istanbul, 1989
E-Mail: imrangungordu@gmail.com
B.Sc. : Istanbul Technical University, Chemistry (2010)
M.Sc. : Istanbul Technical University, Chemistry (2012)

